CELL DEVELOPMENT IN THE ANTHER, THE OVULE, AND THE YOUNG SEED OF *TRITICUM AESTIVUM* L. VAR. CHINESE SPRING

By M. D. BENNETT, M. K. RAO, J. B. SMITH and M. W. BAYLISS
Plant Breeding Institute, Cambridge, England

(*Communicated by R. Riley, F.R.S. – Received 8 February* 1973)

[Plates 7–25]

CONTENTS

The developmental behaviour of reproductive cells was studied during premeiotic mitotic activity, premeiotic interphase, meiosis in anthers and ovaries, microsporogenesis, megasporogenesis and embryo and endosperm growth in *Triticum aestivum* L. var. Chinese Spring. Particular attention was paid *first* to the timing and rate of cell development in the anthers and the ovary within a floret and *secondly*, to the timing and rate of nuclear and cell development in the young embryo and endosperm. At 20 °C the development studied lasted in each floret about 21 days starting 7 days prior to meiosis in anthers and ending 5 days after anther dehiscence and pollination. The durations of up to twenty successive cell cycles were estimated.

In anthers of plants grown at 20 °C the durations of the three successive cell cycles immediately prior to the cycle which ends at first anaphase of meiosis were about 25, 35 and 55 h respectively. The increase in cell cycle time was correlated with an increase in the size of archesporial cells and their nuclei. A progressive increase in the durations of successive cell cycles as meiosis is approached has not been measured previously in a higher plant species, although it has been noted in the germ line cells of male mice.

The pollen mother cells (p.m.cs) within an anther were synchronized prior to meiosis by having their development blocked somewhere in G_1 of premeiotic interphase. The developmental hold began to operate about 103 h prior to the synchronous onset of meiosis in all the p.m.cs within an anther at 20 °C. About 55 h later, when the last archesporial cell completed its final premeiotic mitosis, all the p.m.cs had accumulated in G_1 of premeiotic interphase and synchrony was complete. Premeiotic interphase after all the p.m.cs were first synchronized in G_1 until the synchronous onset of meiosis lasted about 48 h. During this period the G_1 developmental hold was released and p.m.cs initiated DNA synthesis synchronously about 12 to 15 h prior to the start of leptotene.

Meiosis in p.m.cs lasted 24 h at 20 °C. Within each floret, meiosis in p.m.cs was almost or quite synchronous with, and had the same duration as, meiosis in the embryo sac mother cell. The Q_{10} for meiosis in p.m.cs over the temperature range 15 to 25 °C was about 2.3.

Microsporogenesis from tetrad stage until anther dehiscence lasted about 7.5 days at 20 °C. The first pollen grain mitosis (p.g.m. 1) occurred 2.5 days and second pollen grain mitosis (p.g.m. 2) 5.0 days after the end of meiosis. Concurrent with p.g.m. 1 the functional megaspore in the ovule of the same floret divided. This division was rapidly followed by two more synchronous division cycles (also concurrent with p.g.m. 1) which produced an 8-nucleate embryo sac. By p.g.m. 2 the embryo sac contained 20 to 30 antipodal cells at its chalazal end. The antipodal cells subsequently became highly polyploid and some eventually contained up to 200 times as much DNA as haploid egg nuclei.

At 20 °C the sperm nuclei reached the egg and polar nuclei about 40 min after pollination. The primary endosperm nucleus divided about 6 h after pollination while the zygote did not divide until about 22 h after pollination. The endosperm often contained 16 mitotic nuclei 24 h after pollination. The nuclear division cycle during the first five division cycles was about 4.5 h. Until the tenth division cycle when the endosperm became a cellular tissue, development of endosperm nuclei was synchronous, but thereafter synchrony was progressively lost. Early embryo development was marked by a gradual decrease in the durations of successive cell cycles. This decrease was apparently correlated with a decrease in the size of embryo cells and their nuclei.

Nuclear and cellular developmental rates at 20 °C were very variable. Estimates of nuclear cycle times ranged from about 60 h in the microspore to about 4.5 h in some endosperm nuclei. Nuclear volume was also very variable and ranged from about 240 μm^3 for sperm nuclei in mature microspores to about 160000 μm^3 in some polyploid antipodal cells. Both the wide range of nuclear types described, and the

speed with which nuclear characters changed, illustrates the remarkable plasticity of the wheat nucleus which may occur in several very different forms.

A comprehensive and integrated study of development at the cellular level in reproductive tissues of a higher plant species is presented. The importance of this study is twofold. First, it allows the comparison of reproductive cell behaviour in a higher plant species and in those animal species which have been intensively examined. Secondly the availability of a description of 'normal' development under controlled conditions in euploid plants of Chinese Spring opens the way for comparative studies using the wide range of available mutant or chromosomally different genotypes of Chinese Spring which are known to vary in their reproductive development.

1. Introduction

Although there have been numerous investigations of the wheat spike and good reviews of the work exist (Percival 1921; Bonnett 1966; De Vries 1971), no comprehensive study of development at the cellular level throughout the period from a week before the onset of meiosis in anthers until several days after fertilization, has been made using a single genotype. In particular, little attention has been paid to the rates of cell division and the duration of developmental stages in the anther, the ovary and the young seed, and furthermore, little is known about the timing and inter-relation of developmental events occurring in different organs within the wheat floret. Consequently, it was decided to conduct such an investigation using the variety Chinese Spring.

Because of its economic importance the cytogenetics of hexaploid wheat (*Triticum aestivum* L.) has been extensively studied. Following the development of lines nullisomic, monosomic, and tetrasomic for particular chromosomes in Chinese Spring (Sears 1954) intensive studies of this variety have been made. Such studies have led not only to the accumulation of much data with practical significance for wheat breeding (Riley, Chapman & Johnson 1968; Law 1968), but also to discoveries of more general scientific interest and application. For example, the description of the genetic control of diploid pairing in a polyploid, controlled by the (*Ph*) locus on the long arm of chromosome 5B, made by Riley (1960). The stocks have also proved useful for experiments to investigate somatic association (Feldman, Mello-Sampayo & Sears 1966; Avivi, Feldman & Bushuk 1970). Recent studies on the duration of meiosis in wheat (Bennett, Chapman & Riley 1971) have led to increased understanding of the factors which determine the rate of meiotic development (Bennett 1971; Bennett & Smith 1972). It seems reasonable to hope, therefore, that a detailed study of late floral development in Chinese Spring will provide a useful addition to all that has already been learnt about this plant, and a meaningful reference point for future work.

2. Premeiotic anther development

Our observations were made using Chinese Spring plants grown at 20 ± 1 °C and given continuous illumination. Spikes estimated to be between 1 and 7 days before the onset of meiosis were fixed in 1:3 acetic alcohol. The least developed spikes examined had a length of about 1 cm. Using a binocular microscope, fixed spikelets were subdivided into their constituent first, second and third florets. The three anthers were then carefully dissected out of each floret and transferred to drops of aceto-carmine on separate slides. Each anther has four loculi and each loculus contains a column of archesporial cells (hereafter, the archesporium from a single loculus is referred to as a 'column'). Anther length (taken as the length of the

longest loculus) was measured using a Vickers moving scale micrometer eyepiece. A coverslip was then applied. Sometimes, especially with very young anthers, the weight of the coverslip was sufficient to rupture the anther and extrude intact columns of archesporial cells. Often, however, it was necessary to tap the coverslip gently to extrude the columns. Whenever the complete column was located, its length was measured and the number of cells it contained was counted. In each column the number of cells at mitosis was counted and the mitotic index (m.i.), that is the percentage of archesporial cells at mitosis, was calculated.

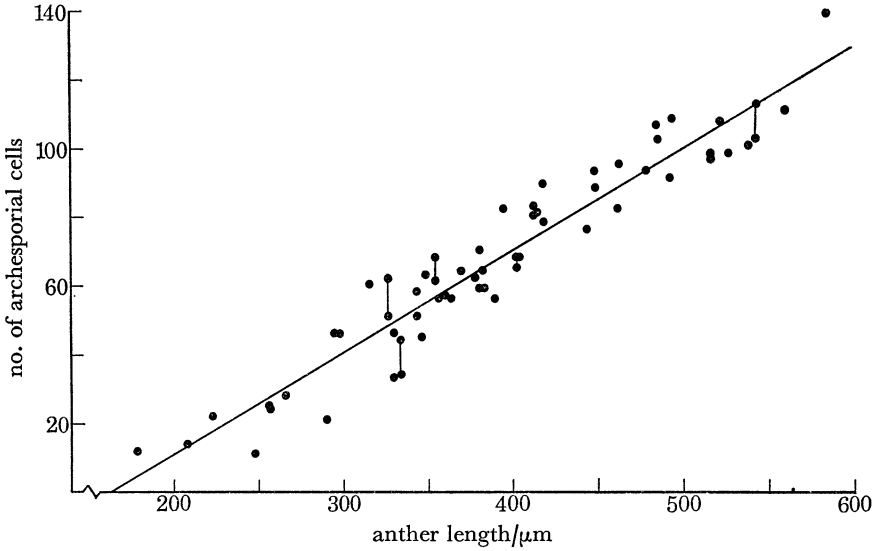

FIGURE 1. The relationship between anther length and the number of archesporial cells per loculus during premeiotic development in Chinese Spring wheat grown at 20 °C.

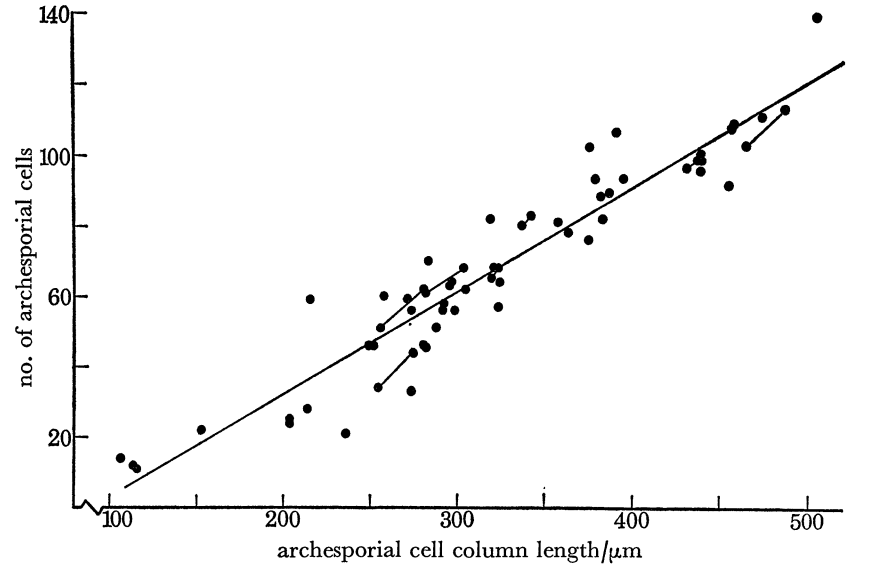

FIGURE 2. The relationship between the length of the archesporial column and the number of archesporial cells per loculus during premeiotic development in Chinese Spring wheat grown at 20 °C.

(a) The relationships between anther length, column length and archesporial cell number

Figure 1 shows the relationship ($P < 0.001$) between anther length and the number of cells per column. Figure 2 shows the highly significant ($P < 0.001$) relationship between column length and the number of cells per column. Only columns containing cells either at, or younger than, the first stage of premeiotic interphase (see §5) were used for these comparisons.

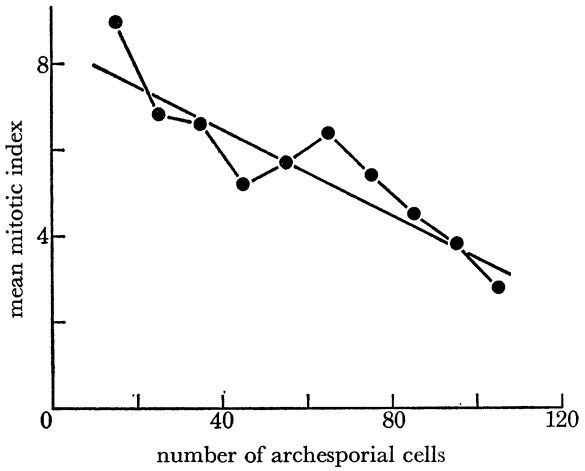

FIGURE 3. The relationship between the number of archesporial cells per loculus and the mitotic index (m.i.) of archesporial cells during premeiotic development in Chinese Spring wheat grown at 20 °C ($r = 0.92$, $P < 0.001$).

(b) Mitosis in the archesporium

The spindles of mitosis in the archespore and of the next two mitotic divisions in the archesporium were parallel with the future long axis of the loculus, and so very young archesporial columns consisted of a single-cell filament. The first mitosis whose spindle was at right angles to the long axis of the column occurred when the column contained about 10 cells. Thereafter, the mitotic spindles were either parallel, or at right angles, to the long axis of the loculus. All spindles were orientated so that every archesporial cell or pollen mother cell (p.m.c.) had one wall forming part of the tangential face of the column. Consequently all p.m.cs were in contact with the tapetum. Anthers containing columns with 10 cells were about 0.2 mm long. Premeiotic mitosis ceased in anthers between 0.5 and 0.6 mm long containing between 90 and 140 p.m.cs. At this time the average number of p.m.cs per loculus was about 104. Columns with fewer than 96 or more than 108 p.m.cs were uncommon.

The m.i. for individual columns ranged from 0 to 37 %, however, the m.i. exceeded 15 % only in columns containing very few cells but several mitotic figures. The mean m.i. was calculated for columns with increments of 10 cells from 10 to 110. Plotting mean m.i. against the number of archesporial cells per column (figure 3) shows that the mean m.i. decreased from about 9 % to about 3 % while the number of archesporial cells per loculus increased from 10 to 100. The mean mitotic index for columns with more than 109 p.m.cs was very close to zero.

Out of 227 archesporial mitoses observed, 111 were at prophase (49 %), 42 were at metaphase (18.5 %), 20 were at anaphase (9 %) and 54 were at telophase (24 %). These proportions are roughly similar to those previously noted for the stages of mitosis at first pollen grain mitosis and in root-tip meristem cells of Chinese Spring (table 1).

TABLE 1. THE PERCENTAGE FREQUENCY OF OCCURRENCE OF NUCLEI AT THE VARIOUS STAGES OF MITOSIS FROM CELLS OF DIFFERENT TISSUES OF *T. AESTIVUM*

cell type	genotype	temperature (°C)	prophase	metaphase	anaphase	telophase	no. of mitoses scored
root-tip meristem 1	Chinese Spring	20	52.7	34.3	6.3	6.3	300
root-tip meristem 2	Chinese Spring	20	40.0	33.0	27.0		100
male archesporium	Chinese Spring	20	49.0	18.5	8.8	23.8	227
tapetum	Chinese Spring and Holdfast (lumped data)	20	42.6	22.7	17.6	17.1	176
microspores at first pollen grain mitosis	Chinese Spring	20	50.0	30.0	6.0	14.0	100
	Holdfast	15	47.0	22.0	9.0	23.0	400

(*c*) *The durations of premeiotic cell cycles*

The mean durations of the three successive mitotic cycles in archesporial cells prior to premeiotic interphase were estimated using the whole spikelet sampling method previously described (Bennett & Smith 1972). At a known time (sampling time), one or two whole spikelets were carefully excised from the spike through either a vertical split or a small 'window' cut in the leaf sheaths surrounding the young spike. After sampling, the incision was sealed with a small piece of transparent adhesive tape to prevent desiccation of the spike. The technique involved very little damage to the sampled spike or the leaf sheaths surrounding it. Each sampled spikelet was fixed in a separate tube of 1:3 acetic alcohol. After fixing, the three anthers were carefully dissected out from the first, second and third floret of each spikelet and their lengths measured. Individual anthers were then placed in a drop of aceto-carmine and squashed gently by tapping the coverslip to extrude the columns of archesporial cells. The stage of archesporial development, the length of the column, the number of cells it contained, and the m.i. were scored for each undamaged extruded column.

Up to 5 days later (at fixing time), the spikelets immediately above and below the position of the spikelet taken at sampling time were excised and fixed in separate tubes of 1:3 acetic alcohol. The spikelets taken at fixing time were then treated in exactly the same way as those taken at sampling time and the length, m.i. and number of cells in each undamaged extruded column was determined.

The increase in the number of archesporial cells per loculus in a known time period was found by comparing the estimates of cell numbers in columns from adjacent corresponding florets excised at sampling time and fixing time. These data were used to estimate cell cycle times for archesporial cells at different stages of premeiotic development. If it is assumed, *first*, that all the archesporial cells in a loculus are capable of dividing, and *secondly*, that all the cells are developing at the same rate at any given time, then, the archesporial cell cycle time must be the interval between sampling time and fixing time during which the number of archesporial cells per loculus doubles.

Throughout the period in which the number of archesporial cells per loculus increases from 10 to 100, mitotic figures were randomly scattered along the length of the column. Furthermore, by early premeiotic interphase the archesporial cells were arranged regularly in eight longitudinal rows with similar numbers of cells in each row. The assumptions on which the

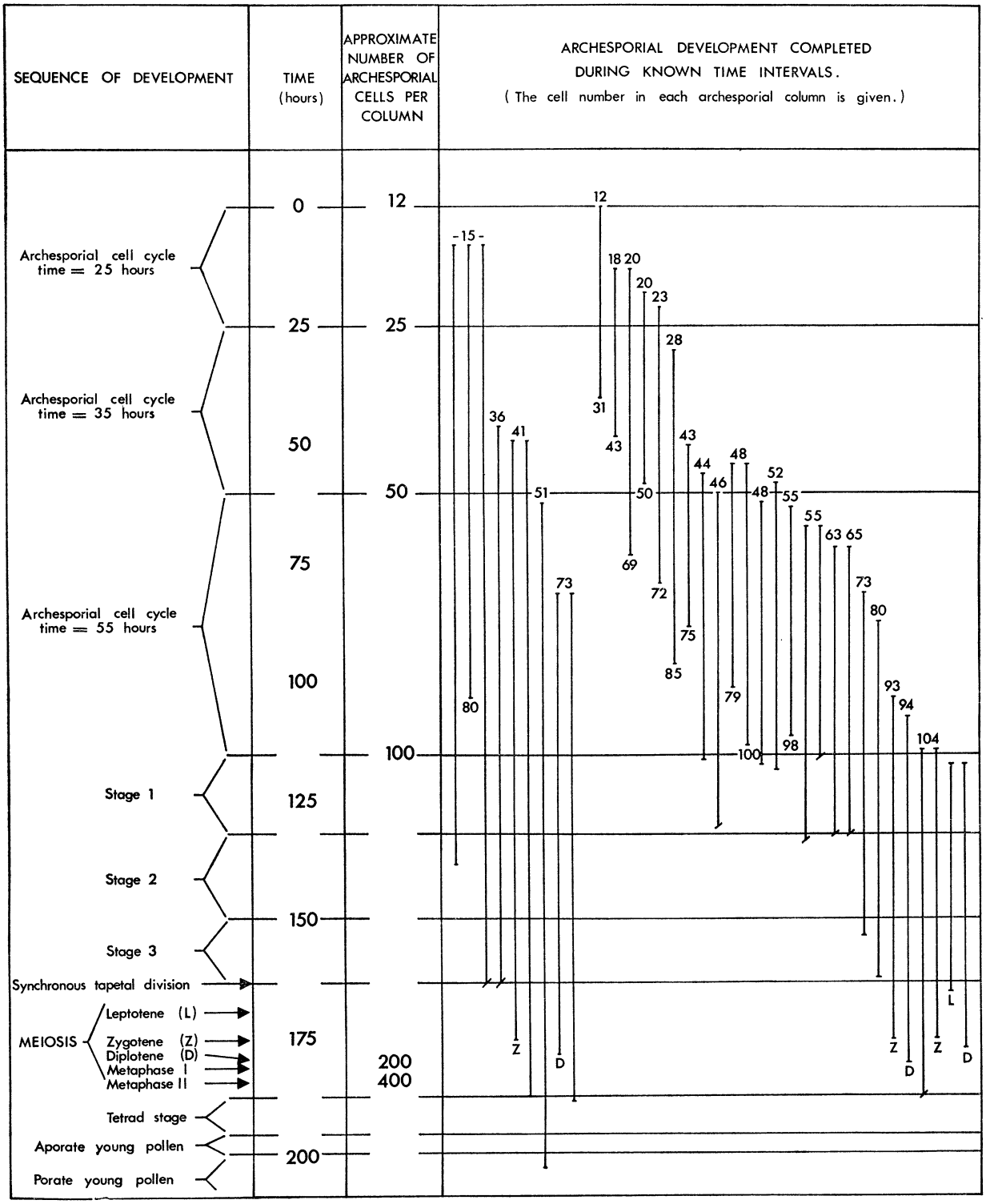

FIGURE 4. Archesporial development completed during known time intervals. The number of archesporial cells per loculus or the stage of premeiotic development are plotted at either end of bars whose lengths are proportional to the developmental interval between anthers in corresponding florets in adjacent spikelets fixed at the beginning and ending of known time periods.

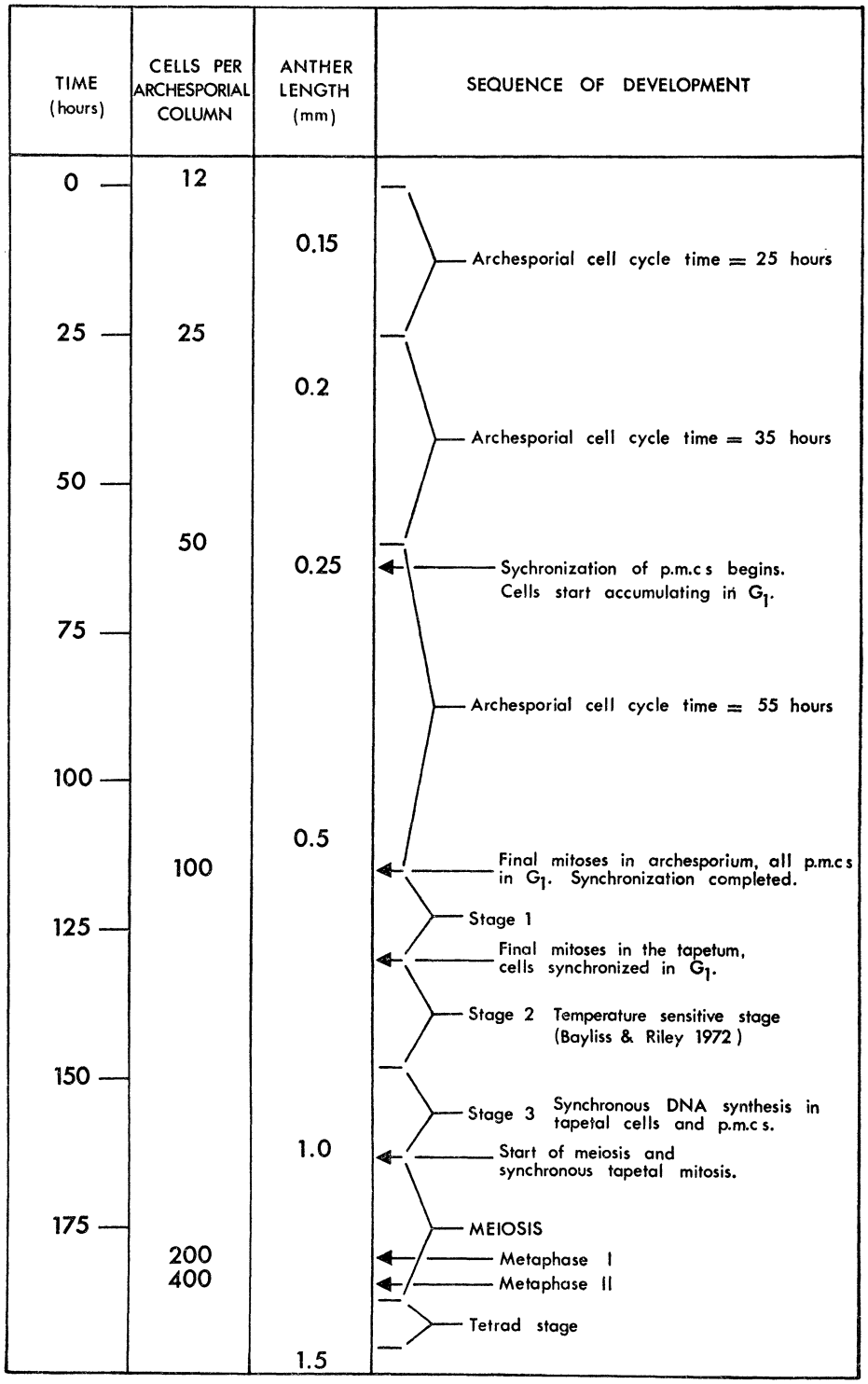

FIGURE 5. The timing and sequence of premeiotic development in male archesporial cells of Chinese Spring wheat grown at 20 °C.

method is based for estimating the duration of premeiotic cell cycles seem, therefore, to be valid.

Figure 4 illustrates some of the results obtained using the method outlined above. For instance, columns from anthers in a third floret excised at sampling time contained 48, 48 and 52 cells respectively, but 51 h later an anther excised at fixing time from an adjacent third floret contained a column with 100 cells, including three at mitosis. Since most anthers contained about 104 p.m.cs per loculus at the onset of meiosis it is concluded, therefore, that the final premeiotic cell cycle lasted about 51 h. The durations of the stages of meiosis and of the stages of premeiotic interphase after the final premeiotic mitosis have been determined (Bennett *et al.* 1971; Bennett & Smith 1972). If anthers taken at 'fixing time' contained these stages, then the duration of archesporial development completed prior to final premeiotic mitosis was estimated by deducting the inclusive durations of the stages after the final premeiotic mitosis from the total time period between sampling time and fixing time. For instance, the onset of meiosis concurrent with a synchronous division of nuclei in cells of the tapetal layer occurs about 48 h after the final premeiotic mitosis in the archesporium (Bennett & Smith 1972). A column with 16 cells was found in a third floret and 140 h later an anther from an adjacent third floret contained p.m.cs at the onset of leptotene with a concurrent synchronous division of the tapetal nuclei. It was concluded, therefore, that the archesporial development between the 16-cell stage and the final premeiotic mitosis lasted about 92 h (that is, 140 – 48 h). Whenever anthers taken at fixing time contained p.m.cs at a meiotic stage of short duration (for instance, diakinesis which lasts only about 24 min), then the time spent in development after the final premeiotic mitosis was precisely known. Consequently, the duration of development completed before the final premeiotic mitosis was estimated by subtracting the duration of development completed after the final premeiotic mitosis from the interval between sampling and fixing times. When plotting the data illustrated in figure 4, allowance was made for the fact that during the premeiotic interphase and meiosis the time difference between the stages in adjacent corresponding spikelets corresponds to development lasting 5 to 6 h (Bennett & Smith 1972). Premeiotic cell cycle times were estimated from the best fit of these data.

The three cell cycles preceding meiosis which commenced when the number of archesporial cells per loculus was 12, 25 and 50 were estimated to last about 25, 35 and 55 h respectively (figure 5). Thus, the durations of successive premeiotic cell cycles were increased.

(*d*) *The duration of mitosis in archesporial cells*

The duration of mitosis was estimated by multiplying the archesporial cell cycle time (T) by the fraction of archesporial cells at mitosis, using the equation

$$\text{duration of mitosis} = \frac{T \times \text{m.i.}}{100}.$$

Figure 3 shows that the m.i. was about 7.5, 6.5 and 4.7 % when the number of archesporial cells per loculus was 18, 37 and 75 respectively. Consequently, the mean duration of mitosis was about 1.9, 2.3 and 2.6 h for cell cycles commencing when the loculus contained 12, 25 and 50 archesporial cells. It has been previously estimated (Bayliss 1972) that the duration of mitosis in root-tip meristem cells at 20 °C was about 1.2 h when the cell cycle time was about 12.5 h. It seems, therefore, that as total cell cycle time is increased so the duration of mitosis is also increased, but, by a smaller proportion (figure 6).

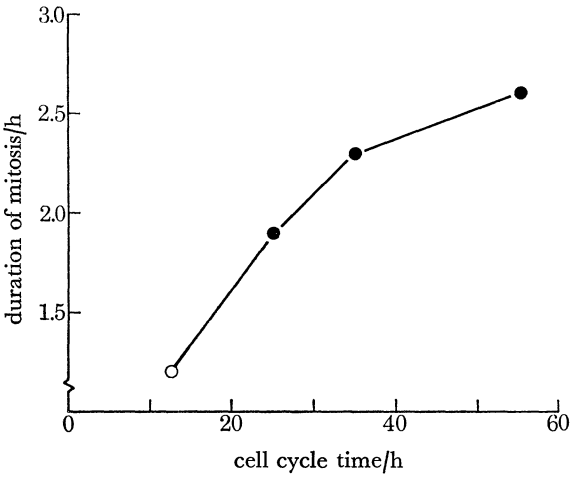

FIGURE 6. The relation between cell cycle time and the duration of mitosis in archesporial cells (●) and root-tip cells (○) of Chinese Spring wheat grown at 20 °C.

(*e*) *Premeiotic interphase*

The duration of the final premeiotic cell cycle was about 55 h and so the first cell to undergo a final premeiotic mitosis did so about 55 h before the last cell to do so. The last cell to undergo premeiotic mitosis did so about 48 h before the almost synchronous onset of leptotene and about 68 h before first telophase of meiosis (Bennett & Smith 1972). Consequently, the maximum and minimum durations of premeiotic interphase were about 103 and 48 h respectively. Furthermore, the trend of increasing durations for successive cell cycles, noted during premeiotic development, was maintained during the cell cycle terminating at the first telophase of meiosis whose maximum and minimum durations were about 123 and 68 h respectively.

As already stated, the duration of the period from the final premeiotic mitosis within a loculus until the synchronous onset of leptotene was about 48 h at 20 °C (Bennett & Smith 1972). Three cytologically distinct stages of p.m.c. development have been recognized within this period and a detailed description of the method used to time the durations of these stages has already been given (Bennett & Smith 1972) and has been outlined above.

The appearance of p.m.cs and tapetal cells in aceto-carmine or Feulgen stained anther squashes (figures 8–11, plates 8 to 11) is described below.

(i) *Stage* 1

Following the final premeiotic mitosis all the p.m.c. nuclei became enlarged and had a diffuse reticulate appearance. Although they were poorly stained parts of individual chromatin threads could be distinguished. During this stage, which persisted for about 18 h after the final premeiotic mitosis, the m.i. of the tapetal layer was about 8–10 %. No callose was seen on p.m.c. walls during stage 1. Microdensitometry of Feulgen-stained nuclei prepared using the method first described by McLeish & Sunderland (1961) showed that while the DNA content of tapetal cells ranged from 2*C* to 4*C*, the p.m.cs all had a 2*C* nuclear DNA content. Figure 8*c*, plate 8 shows p.m.c. nuclei in an unsquashed extruded archesporial column at stage 1 stained in aceto-carmine, and figure 9*a*, plate 9, shows their characteristic appearance after squashing.

It was difficult to see any detail of the structure of stage 1 nuclei stained by the normal aceto-carmine or Feulgen methods. Nuclei became contracted after heating or hydrolysis.

Alternatively, they were either contained in stained cytoplasm or poorly stained. A technique was evolved, therefore, which preserved the structure of the nucleus while allowing improved staining of chromatin alone. This was done by extruding a column of archesporial cells from a freshly fixed anther and transferring it to a drop of 45 % acetic acid on an albumenized slide. After applying a coverslip the column was squashed and warmed gently over a spirit lamp. The coverslip was later removed using the dry ice method (Conger & Fairchild 1953) and slides were washed in distilled water for 5 min, hydrolysed for 12 min in 1 N HCl at 60 °C, stained in leuco-basic fuchsin for 2 h and washed in distilled water for 5 min. After placing a drop of 20 % glycerol over the squash a coverslip was applied and sealed with brown cement. In this method, stage 1 p.m.c. nuclei were stuck to the slide in their extended state and subsequent hot hydrolysis did not cause contraction. A typical stage 1 p.m.c. nucleus prepared by this method is shown in figure 9*c*, plate 9.

(ii) *Stage* 2

About 18 h after the final premeiotic mitosis in the archesporium the m.i. of the tapetal layer decreased abruptly to zero. At the same time the p.m.c. nuclei became contracted, much denser and darker staining than during stage 1. Individual chromosome threads could no longer be distinguished in aceto-carmine stained squashes. The typical appearance of aceto-carmine stage 2 nuclei in unsquashed extruded archesporial columns and in squashed preparations is shown in figures 8*d*, plate 8 and 10*a*, plate 10. Microdensitometry of Feulgen-stained anther squashes showed that during stage 2 all the tapetal and archesporial cell nuclei contained the 2*C* DNA amount. The callose wall which completely enclosed each p.m.c. during meiosis became visible during stage 2. Callose first appeared on those p.m.c. walls at the centre of the archesporial column, and so, in extruded columns, it was frequently seen as a 'backbone' running along the long axis of the archesporium (figure 11*a*, plate 11). During stages 1 and 2, p.m.c. nuclei usually contained three nucleoli of various sizes and these were invariably enclosed within the nucleus.

Bayliss & Riley (1972) have demonstrated the existence of a premeiotic stage at which temperature changes affect chromosome pairing at first metaphase of meiosis. They showed that Chinese Spring plants nullisomic for chromosome 5D but tetrasomic for 5B exhibited normal chromosome pairing when grown at 20 °C but were asynaptic when grown at 15 °C. Using temperature switch experiments they showed that the temperature sensitive stage was about 39 h prior to first metaphase at 20 °C. Chiasma formation in euploid Chinese Spring is also sensitive to a high temperature treatment at a similar time. The rate of meiotic development is the same in both euploid and nulli5D-tetra5B stocks of Chinese Spring. Consequently, temperature sensitivity is identified with stage 2 of premeiotic interphase.

(iii) *Stage* 3

There were no mitotic divisions in either p.m.c. or tapetal nuclei during stage 3 which lasted about 15 h before the start of meiosis in p.m.cs. During this phase the p.m.c. and tapetal nuclei became larger but remained densely staining in aceto-carmine stained squash preparations. Microdensitometry of Feulgen stained anther squashes showed that during stage 3 both p.m.c. and tapetal nuclei underwent synchronous DNA synthesis and that their DNA contents increased from 2*C* to 4*C* in about 12 to 15 h. The onset of stage 3 was marked by the migration of nucleoli to, and their projection from, the surface of the nucleus (figures 10*b*, plate 10 and 11*a*,

plate 10). P.m.cs usually contained three nucleoli at the start of stage 3 but only one by the onset of leptotene. It is not known whether the three nucleoli fuse or whether two regress during stage 3. Throughout stage 3 callose continued to be laid down on p.m.c. walls. By the end of stage 3 it covered the whole wall, nevertheless, the callose layer was much thinner on the p.m.c. walls in contact with tapetal cells than on p.m.c. walls at the centre of the column. During stage 3 protochromosomes gradually appeared and were visible in both acetocarmine and Feulgen stained p.m.cs. The typical appearance of aceto-carmine stained stage 3 nuclei is illustrated in figure 11*a*.

Since p.m.c. nuclei in stages 1 and 2 all have the 2*C* DNA content, these stages are together equivalent to G_1 stage in a normal somatic cell cycle. Stage 3 is the DNA synthesis phase (*S*). It seems doubtful whether p.m.cs undergo a G_2 phase after *S* and before the onset of leptotene, since chromatin threads were clearly visible at the time when p.m.cs first reached the 4*C* DNA amount. If there is a G_2 phase in p.m.cs it cannot last longer than about 1 h because all the p.m.cs in a loculus were clearly well into leptotene stage 2 h after reaching the 4*C* nuclear DNA amount.

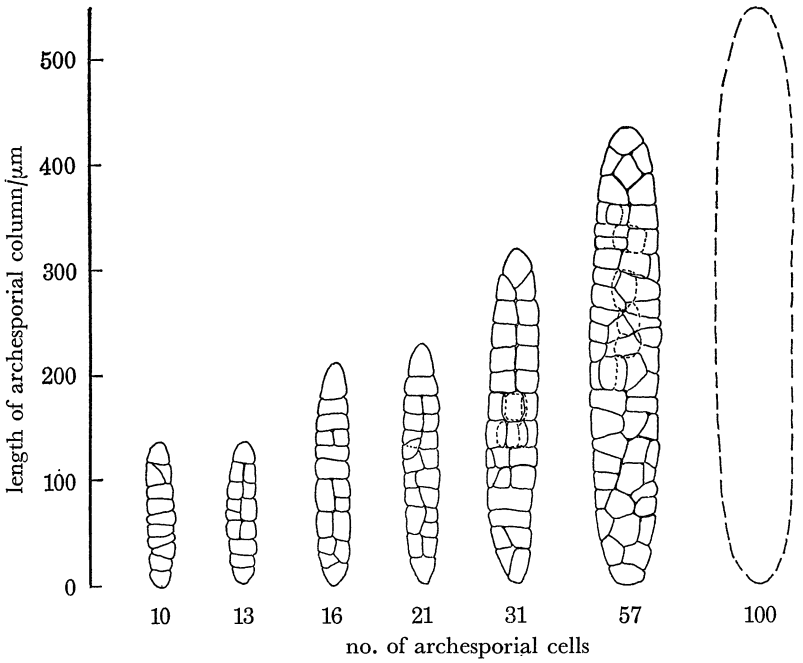

FIGURE 12. Diagrammatic illustration of the relative sizes of columns of archesporial cells extruded from anthers containing different numbers of archesporial cells per loculus.

(*f*) *Archesporial cell size*

Figure 12 illustrates diagrammatically the relative sizes of archesporial columns at several stages during the period when the number of cells per archesporial column increased from 10 to 100. The approximate archesporial cell volume for development during this period was estimated using the equation:

$$\text{volume} = \frac{\pi \times \text{column radius}^2 \times \text{column length}}{\text{number of cells in the column}}.$$

Since the column radius was taken at the widest point, and the archesporial column tapers toward the ends, the cell volume was slightly overestimated. After the final premeiotic mitosis

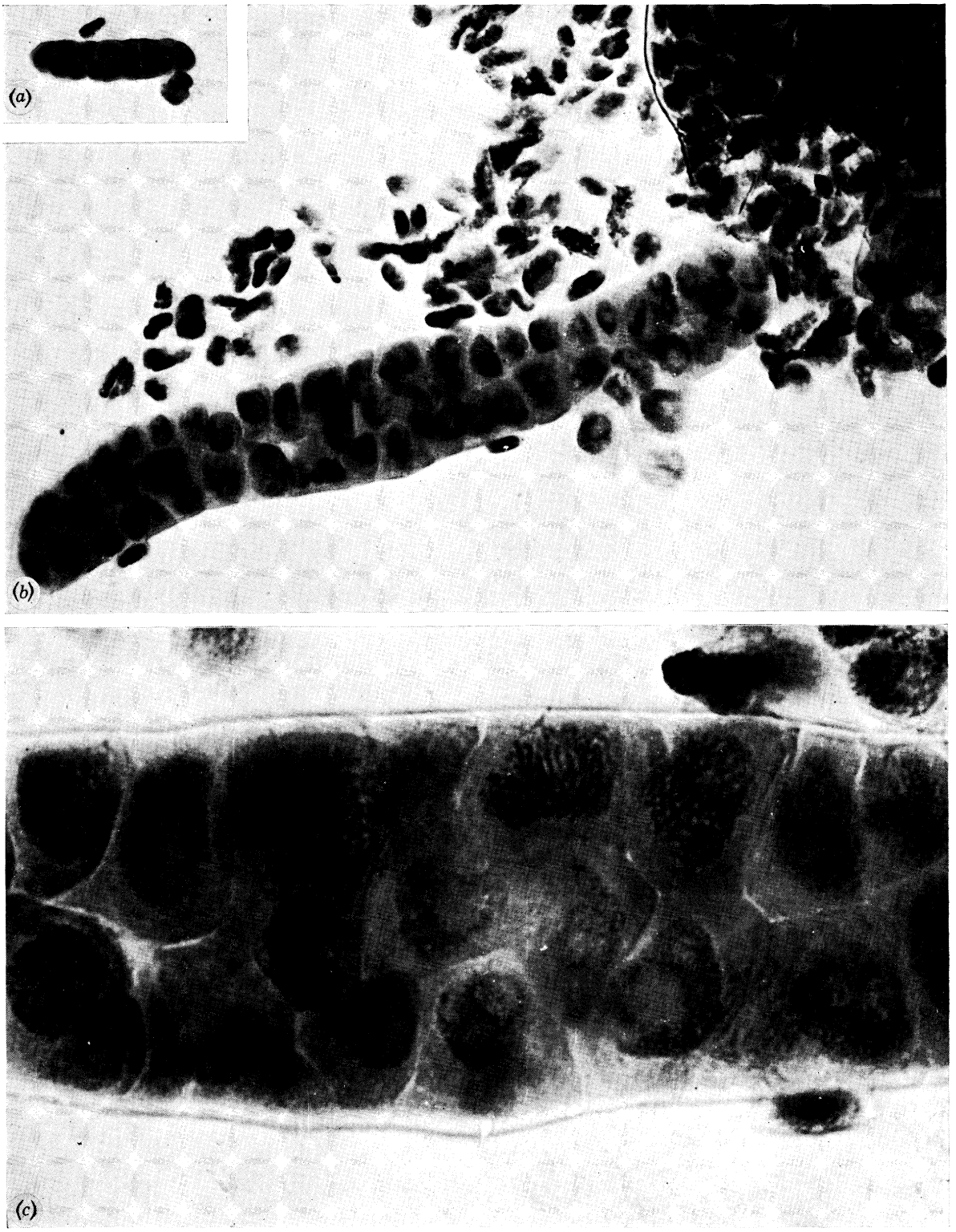

FIGURE 7. Complete archesporial columns extruded from loculi of anthers containing (*a*) 12 archesporial cells and (*b*) about 70 cells. (Magn. × 375.) In (*c*), which is a detailed view of part of the column in (*b*), premeiotic archesporial cells including several at prophase are seen. (Magn. × 1230.)

(*Facing p.* 50)

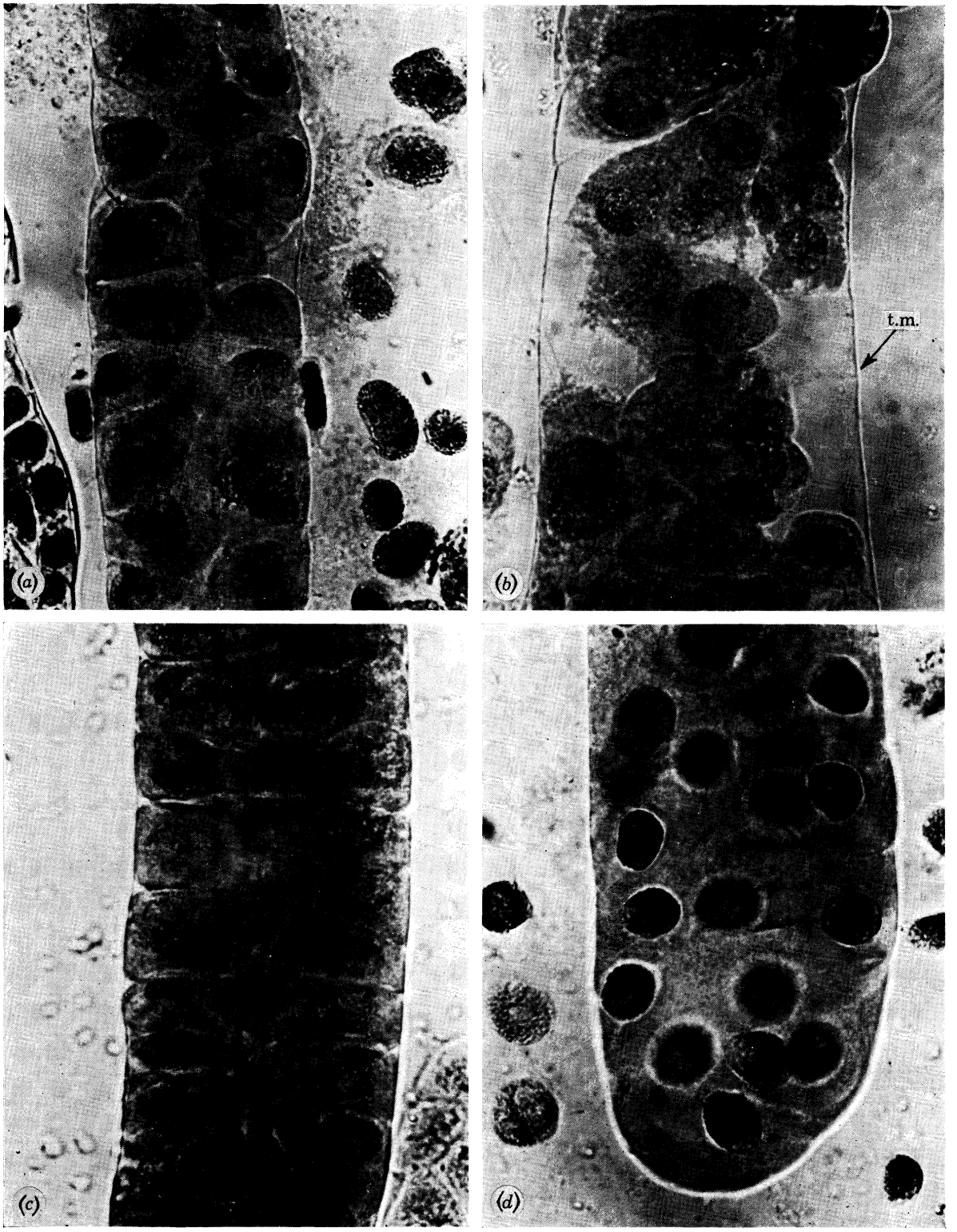

FIGURE 8. Detailed views of parts of extruded columns of archesporial cells containing aceto-carmine stained nuclei at premeiotic mitosis (*a*, *b*), stage 1 of premeiotic interphase (*c*) and stage 2 or premeiotic interphase (*d*). In (*b*), which shows the effect of gentle heating, the tapetal membrane (t.m.) is clearly visible. (Magn. × 815.)

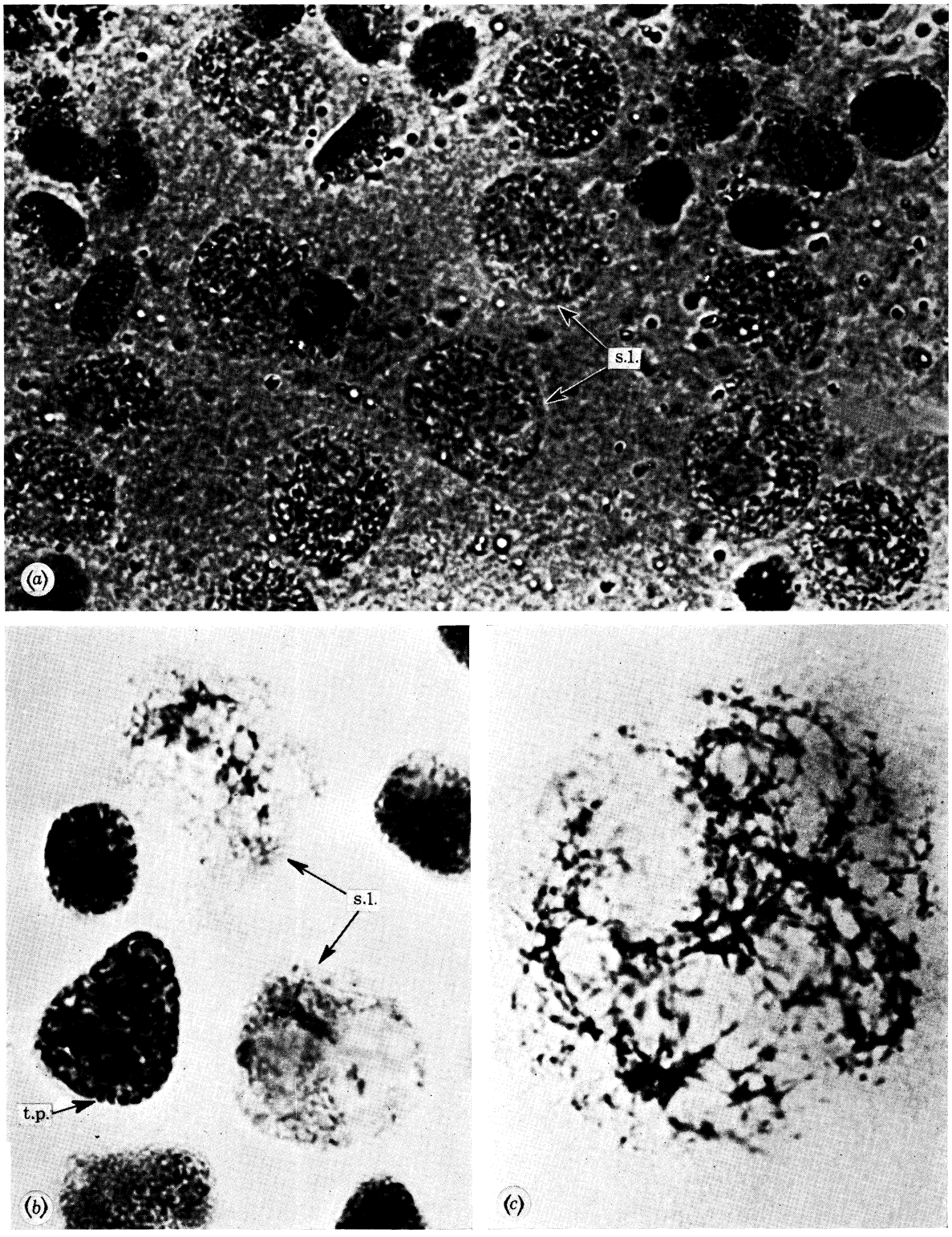

FIGURE 9. Nuclei at stage 1 (s.1) of premeiotic interphase stained using (*a*) aceto-carmine (× 1055), (*b*) the normal Feulgen method (× 825) and (*c*) the modified Feulgen method (× 3190). A tapetal nucleus at prophase (t.p.) is also included for comparison in (*b*).

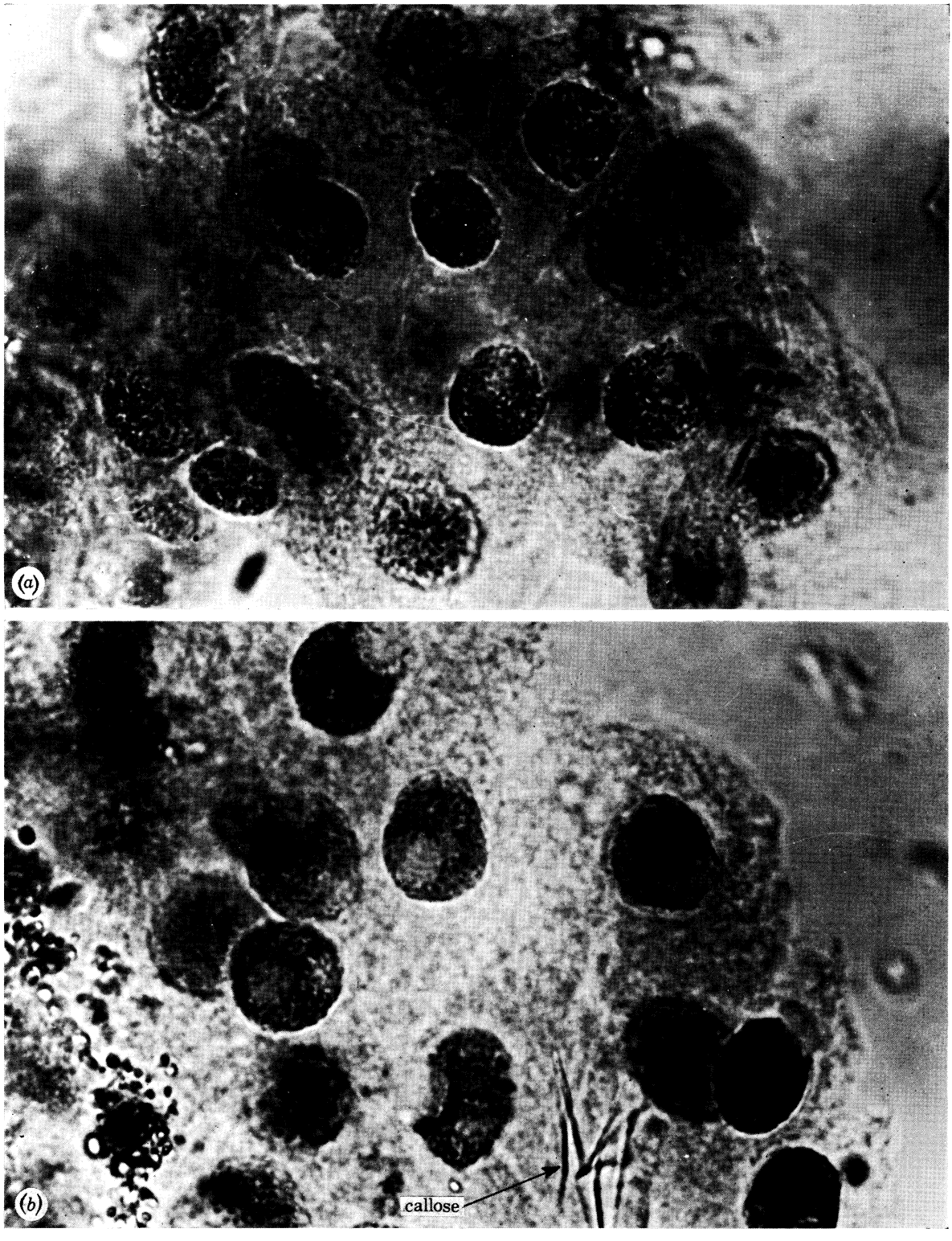

FIGURE 10. Nuclei at stage 2 (*a*) and early stage 3 (*b*) of premeiotic interphase seen in aceto-carmine stained anther squashes. (Magn. × 1145.) Note the migration of the nucleolus to the nuclear periphery and the presence of callose in (*b*).

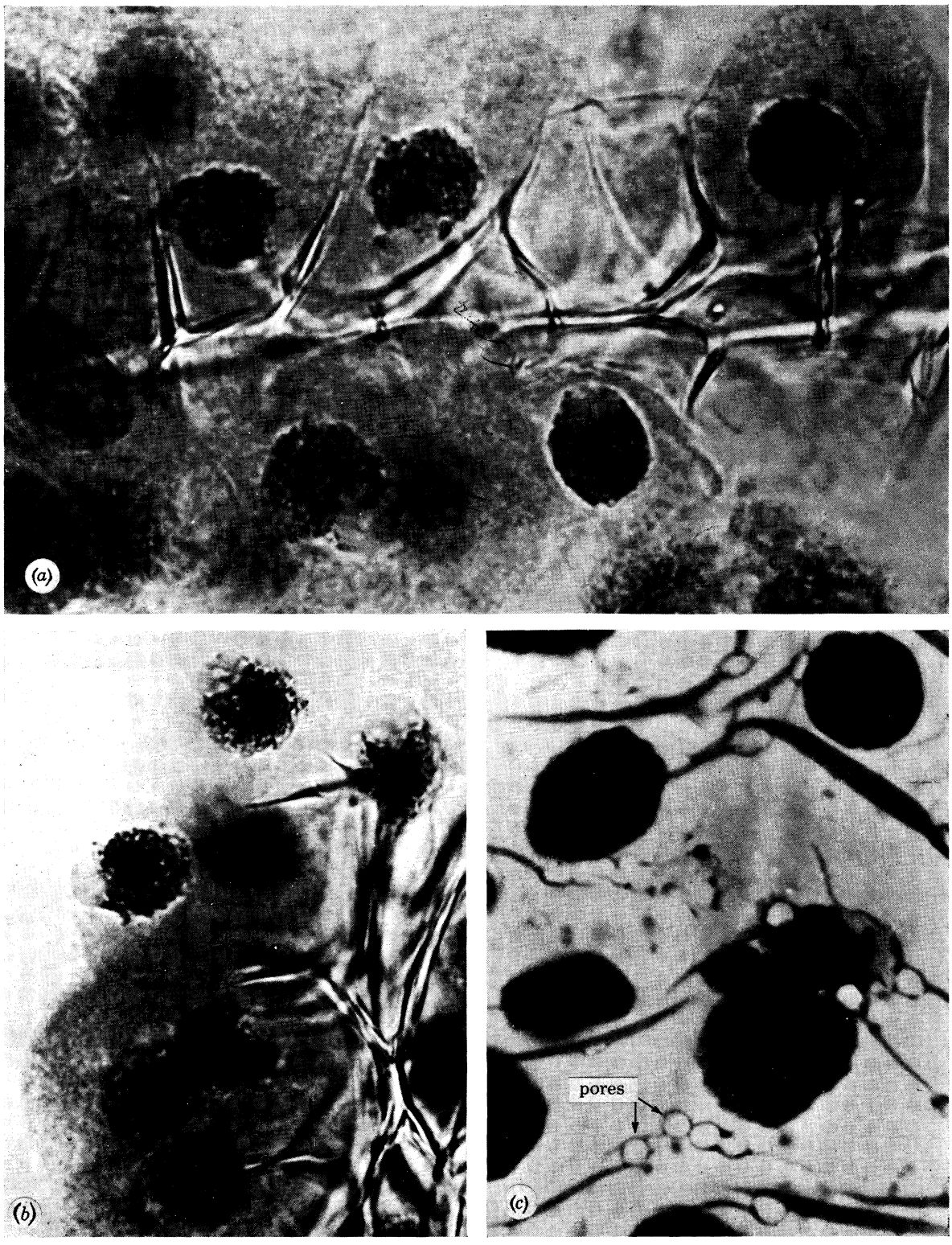

FIGURE 11. (*a*) Nuclei at midstage 3 of premeiotic interphase seen in part of an extruded column of archesporial cells stained in aceto-carmine. Note the central spine of callose within the column and the characteristic position of the nucleolus (× 1145). (*b*) Very early leptotene nuclei in part of an extruded column of archesporial cells from an anther stained in aceto-carmine (× 1145). (*c*) Surface view of the tapetal membrane showing pores of up to 2 μm in diameter in a Feulgen stained anther containing p.m.cs at leptotene (× 2200).

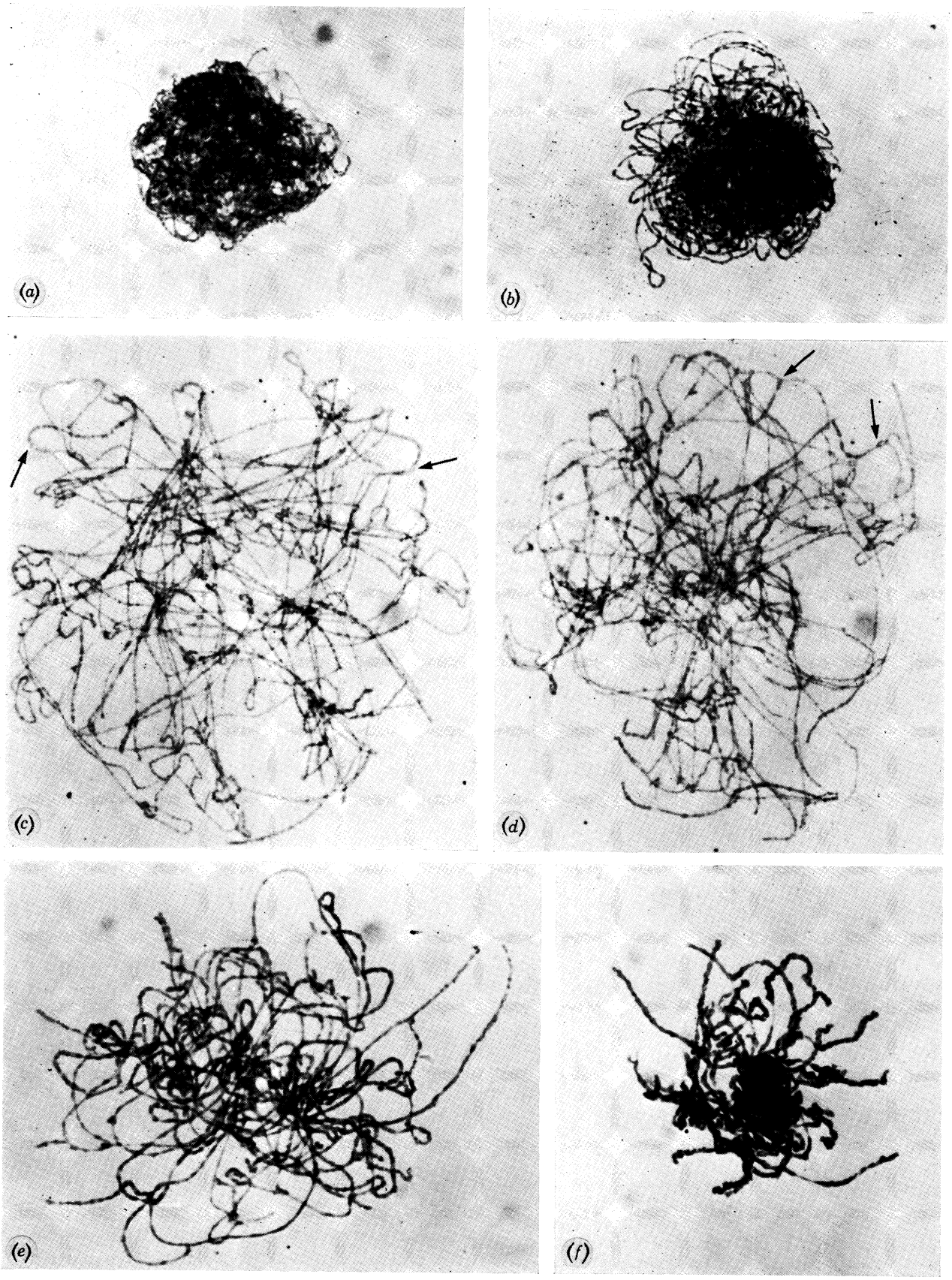

FIGURE 15. Nuclei of pollen mother cells at: (*a*) early leptotene, (*b*) late leptotene, (*c*) early zygotene, (*d*) late zygotene, (*e*) early pachytene; and (*f*) late pachytene. (Magn. × 2000.) (N.B. Some junctions between regions of paired and unpaired chromosomes are indicated by arrows in (*c*) and (*d*).)

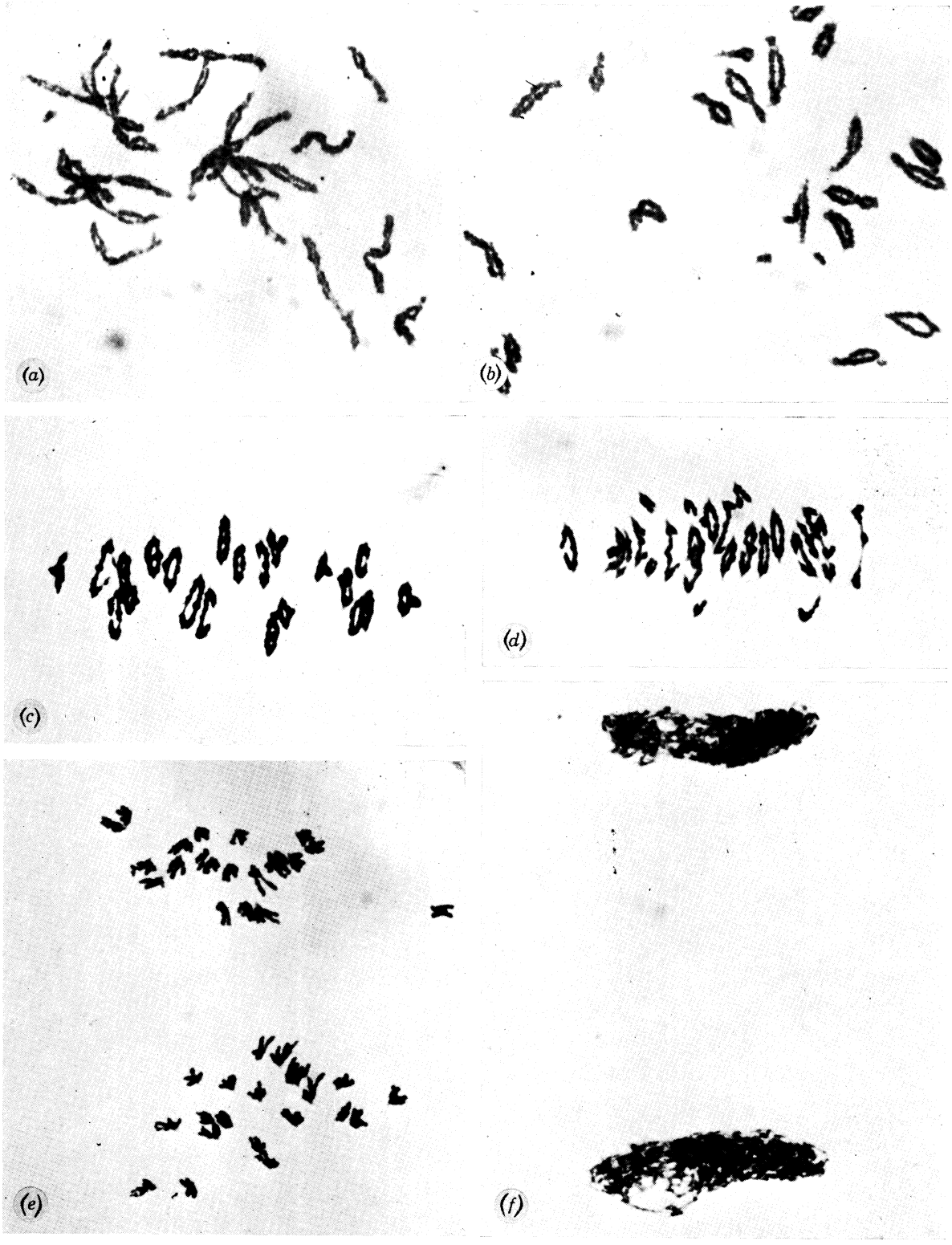

FIGURE 16. Nuclei of pollen mother cells at: (*a*) diplotene, (*b*) diakinesis, (*c*) first metaphase, (*d*) first anaphase (early), (*e*) first anaphase (late), (*f*) first telophase. (Magn. × 2200.)

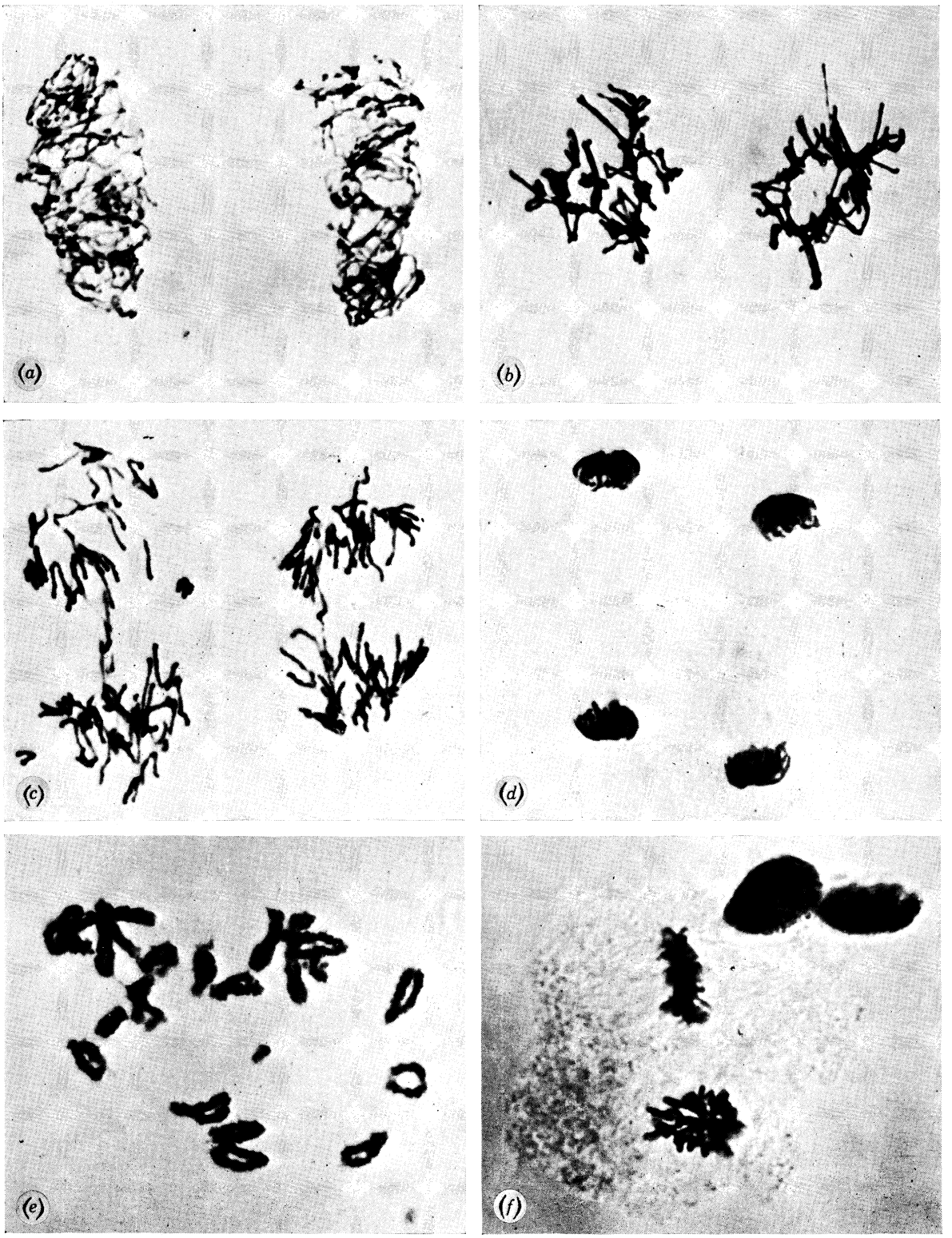

FIGURE 17. Nuclei of pollen mother cells at: (*a*) second prophase, (*b*) second metaphase, (*c*) second anaphase, (*d*) second telophase, (Magn. × 2200.) Nuclei of embryo sac mother cells at: (*e*) diakinesis, (*f*) second metaphase. (Magn. × 1210.)

p.m.c. volume was estimated from measurements of the diameters of individual cells in unsquashed extruded columns of p.m.cs.

Using these methods archesporial cell volume was estimated to be about 6.2×10^3 μm^3 when the archesporial column contained 12 cells, about 9.1×10^3 μm^3 when it contained 50 cells, about 13.6×10^3 μm^3 when it contained 100 cells, and about 31.1×10^3 μm^3 at the onset of leptotene. Comparison of these data with the duration of the cell cycle in archesporial columns with 12, 50 and 100 cells shows that cell cycle time increased while the archesporial cell volume increased. It seems reasonable to suggest that these two characters may be causally related.

(*g*) *The tapetum and tapetal membrane*

The tapetum in wheat is of the secretory or non-invasive type. Throughout the period of anther development studied the tapetum consisted of a single layer of cells completely surrounding the archesporium. The tapetal cells continued to divide until the onset of stage 2 in p.m.cs at premeiotic interphase at which time mitosis ceased. By this time the tapetal cells were much smaller than the p.m.cs but considerably outnumbered them. Microdensitometry of Feulgen-stained anther squashes showed that the tapetal nuclei had a 2*C* DNA content when p.m.cs were at stage 2 of premeiotic interphase and completed DNA synthesis concomitant with stage 3 in p.m.cs. Almost immediately after completing *S* the nuclei of all the tapetal cells underwent a synchronous mitosis which yielded binucleate cells concomitant with the onset of leptotene in p.m.cs.

Throughout the period of premeiotic anther development studied, and throughout meiosis there was an acetolysis resistant membrane between the tapetal cells and the archesporial column. The tapetal membrane was particularly well seen if undamaged columns of archesporial cells at premeiotic mitosis were heated gently in aceto-carmine (figure 8*b*, plate 8). In Feulgen-stained anther squashes the membrane was often seen to be faintly Feulgen positive and when seen in surface view frequently appeared to have pores in it of about 2 μm diameter (figure 11*c*, plate 11). The existence of similar tapetal membranes, in other grasses and in species of the Compositae, is well known (Banerjee 1967; Heslop-Harrison 1969).

(*h*) *Developmental difference within and between spikelets*

Comparisons of the three anthers within individual florets showed that their development was usually very similar. They had similar lengths and contained similar numbers of archesporial cells throughout the period of premeiotic development studied. In a spikelet with late meiotic stages in the most developed floret (first floret), the difference between the stages found in anthers from the first and second florets corresponded to development lasting about 12 ± 2 h at 20 °C. For example, when the first floret contained second telophase, the second floret usually contained zygotene or pachytene (see figure 13). The developmental interval between anthers from the second and third florets corresponded to development lasting about 26 ± 6 h. It has already been shown (Bennett & Smith 1972) that the time difference between the development of first and second florets within the spikelet remained constant from the start of premeiotic interphase (stage 1) until the end of meiosis (second telophase). Comparison of the number of archesporial cells in extruded loculi from first, second and third florets within the same spikelet showed that the developmental intervals seen at meiosis are similar to those found during early premeiotic development. For instance, the mean number of archesporial cells per loculus for first, second and third florets in one spikelet was, 52.5, 42, and 17 respec-

tively, and in another spikelet 93, 82.5 and 46 respectively. The archesporial cell cycle times for loculi with various cell numbers are known, and so the developmental interval between florets can be expressed in hours of corresponding archesporial development.

It has already been shown that the time difference between the development of first or second florets in adjacent corresponding spikelets remained constant during the period from early premeiotic interphase until the end of meiosis (Bennett & Smith 1972) and equalled about 5 to 6 h. No evidence was found indicating that this changed significantly during the period of premeiotic archesporial development studied.

(i) *Discussion*

It is now possible to state with certainty when in premeiotic development synchrony between p.m.cs within an anther starts to be established, and when it is completed. Figure 4 shows the developmental sequence in Chinese Spring anthers at 20 °C over the period from 7 days before meiosis until its completion. Within each loculus, the first cell to undergo a final premeiotic mitosis did so about 103 h before the start of leptotene. The nuclei produced remained in G_1 phase until about 12 to 15 h before the start of meiosis when they entered *S*-phase. The products of all mitotic divisions in the archesporium between 103 and 48 h prior to the start of leptotene, when premeiotic mitosis ceased, all remained in G_1 phase until they entered *S*-phase synchronously together with the cells produced by the first final premeiotic mitosis. It follows, therefore, that synchrony between p.m.cs is established by some factor(s) which block cell development somewhere in G_1 phase, and that this begins to act no later than at the end of mitosis in the first archesporial cell to complete its final premeiotic mitosis, that is about 103 h prior to the start of leptotene. It is unclear, however, whether the G_1 hold is achieved by blocking the initiation of *S*-phase, or whether it is achieved by blocking development at some earlier stage of G_1. All cells at stages other than the hold-sensitive stage continue to develop until they reach it in G_1. By 48 h prior to the start of leptotene, when the last archesporial cells underwent premeiotic mitosis, all the p.m.cs were in G_1 at stage 1 of premeiotic interphase, and the establishment of synchrony between p.m.cs was completed. During premeiotic interphase, probably during stage 2, p.m.cs must be released from the G_1 hold since they all enter stage 3 (premeiotic DNA synthesis) synchronously before the start of meiosis. It seems as if the factor(s) which blocked p.m.c. development in G_1 also acted on cells of the tapetal layer since they were also synchronized in G_1 by 15 to 18 h after the p.m.cs.

The present results showing that the cell cycles in cells of the germ line are increasingly prolonged as meiosis is approached is interesting because spermatogonial cells in the mouse behave similarly (Monesi 1962). The authors believe, however, that the present work gives the first report of this phenomenon in a higher plant species.

Monesi (1962) also noted that the duration of *S*-phase increased from about 7 to about 14 h during the course of several spermatogonial cell cycles and these results have been confirmed by Kofman-Alfaro & Chandley (1970). Crone, Levy & Peters (1965) have shown that the duration of premeiotic *S*-phase in oocytes is much longer than *S*-phase of normal somatic cells but similar to the duration of *S*-phase in primary spermatocytes, that is, about 14 h. Callan (1972) reported that in male germ line cells of *Triturus*, phases of DNA synthesis take progressively more time as meiosis is approached, and that the final *S*-phase takes 8 to 9 days at 18 °C compared with a typical *S*-phase in somatic cells which lasts only about 24 h. Extended final premeiotic *S*-phases have also been noted in *Xenopus laevis* (Bird & Birnstiel 1971; Coggins

& Gall 1972), in *Triturus* (Wimber & Prensky 1968) and in several mammal species including *Mesocricetus auratus* (Ghosal & Mukherjee 1971). It was previously noted that in the higher plant species *Lilium longiflorum* and *Triticum aestivum* the duration of the final premeiotic *S*-phase is much longer than somatic cells of those species (Bennett & Smith 1972).

On the basis of the evidence listed above it seems reasonable to suggest that a progressively decreasing rate of development in germ line cells may be a constant feature of, and perhaps a necessary prerequisite for, the approach to meiosis. Certainly, in all plant and animal species for which data are available the duration of meiosis is greatly prolonged compared with the durations of normal somatic divisions (for a review see Bennett 1971).

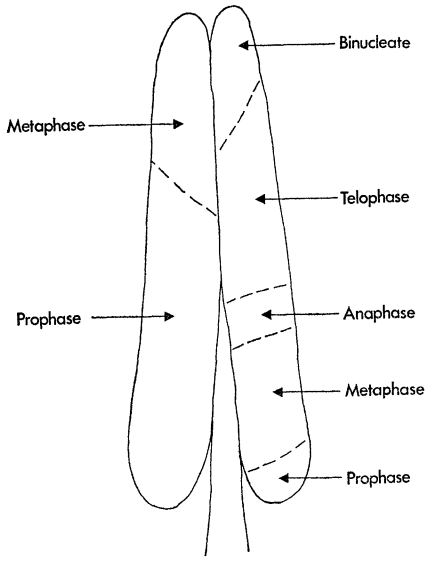

FIGURE 13. Diagrammatic illustration of the developmental gradients in tapetal cells viewed in optical section in two loculi of an anther containing p.m.cs at early leptotene. The tapetum was seen in optical section through the anther epidermis.

3. MEIOSIS

(*a*) *Male meiosis*

In plants grown at 20 °C with continuous light meiosis occurred in the leading tiller about 45 days after germination. At this time the spike was usually still enclosed by two leaf sheaths and about 1–2 cm of the flag leaf sheath showed above the junction of the blade and sheath of the penultimate leaf.

(i) *The anther at meiosis*

The mean anther length increased from about 1.0 mm at the start of leptotene to about 1.2 mm at pachytene, and about 1.3 mm by the start of tetrad stage. The rate of increase in anther length during meiosis was, therefore, fairly constant.

(ii) *Anther gradients*

A developmental gradient along the axis of the anther was seen in both the cells of the tapetum and of the archesporium. In both tissues the anther tip invariably contained the cells most advanced in development and below this there was a gradient with the cells least

advanced at the anther base. Figure 13 shows a typical developmental gradient observed in the tapetal tissue of two loculi of an intact anther. Anther gradients in the archesporium were detected by dividing Feulgen-stained anthers, by transverse cuts, into tip, middle and base segments, and then scoring the frequency of occurrence of p.m.cs at the meiotic stages in each segment. Some results obtained in this manner are given in table 2. They are not typical, however, because in order to demonstrate the direction of the developmental gradient only anthers with pronounced asynchrony between p.m.cs have been included. The asynchrony between p.m.cs within anthers usually does not exceed development that would take 1 to 2 h to complete (Bennett *et al.* 1971).

TABLE 2. THE PERCENTAGE FREQUENCY OF OCCURRENCE OF INDIVIDUAL STAGES OF MEIOSIS IN TIP, MIDDLE AND BOTTOM SEGMENTS OF TEN CHINESE SPRING ANTHERS SHOWING THE BASIPETAL DEVELOPMENTAL GRADIENTS

		stage of meiosis											
anther no.	anther segment	zygotene	pachytene	diplotene	diakinesis	metaphase 1	anaphase 1	telophase 1	dyads	metaphase 2	anaphase 2	telophase 2	tetrads
1	B†	2	98	—	—	—	—	—	—	—	—	—	—
	M	—	40	60	—	—	—	—	—	—	—	—	—
	T	—	—	100	—	—	—	—	—	—	—	—	—
2	B	100	—	—	—	—	—	—	—	—	—	—	—
	M	58	42	—	—	—	—	—	—	—	—	—	—
	T	—	4	96	—	—	—	—	—	—	—	—	—
3	B	100	—	—	—	—	—	—	—	—	—	—	—
	M	64	36	—	—	—	—	—	—	—	—	—	—
	T	—	82	18	—	—	—	—	—	—	—	—	—
4	B	—	40	31	24	4	—	—	—	—	—	—	—
	M	—	—	27	15	58	—	—	—	—	—	—	—
	T	—	—	—	7	93	—	—	—	—	—	—	—
5	B	—	—	—	43	57	—	—	—	—	—	—	—
	M	—	—	—	35	65	—	—	—	—	—	—	—
	T	—	—	—	—	96	4	—	—	—	—	—	—
6	B	—	—	—	44	56	—	—	—	—	—	—	—
	M	—	—	—	—	100	—	—	—	—	—	—	—
	T	—	—	—	—	87	12	—	—	—	—	—	—
7	B	—	—	—	—	12	6	12	59	12	—	—	—
	M	—	—	—	—	—	—	—	65	27	8	—	—
	T	—	—	—	—	—	—	—	—	22	45	33	—
8	B	—	—	—	—	—	—	22	76	2	—	—	—
	M	—	—	—	—	—	—	7	50	43	—	—	—
	T	—	—	—	—	—	—	—	—	78	17	56	—
9	B	—	—	—	—	—	—	—	85	15	—	—	—
	M	—	—	—	—	—	—	—	17	50	33	—	—
	T	—	—	—	—	—	—	—	—	62	38	—	—
10	B	—	—	—	—	—	—	—	—	—	12	29	58
	M	—	—	—	—	—	—	—	—	—	—	—	100
	T	—	—	—	—	—	—	—	—	—	—	—	100

† B, base; M, middle; T, tip.

(iii) *The tapetum*

In Chinese Spring the nuclei of the tapetal cells all undergo a synchronous mitotic division concomitant with the start of leptotene in p.m.cs. Prior to this division the tapetal cells are mononucleate but subsequently they remain binucleate until the time of anther dehiscence.

Consequently, the stage of the tapetal cells may be used as a cytological marker for the start of meiosis in p.m.cs of Chinese Spring. It should be noted, however, that the synchronous mitotic division in tapetal cell nuclei does not occur concomitant with the start of meiosis in p.m.cs of all hexaploid wheat varieties. For instance in Holdfast, it occurred at the start of zygotene stage (Bennett & Smith 1972). Microdensitometry of Feulgen stained anther squashes showed that during meiosis the DNA content of each of the two tapetal nuclei remained constant at the 2*C* amount. It is clear, therefore, that the tapetal cells were in G_1 during meiosis since they did not commence DNA synthesis phase (*S*). Since, the number of tapetal cells did not increase during meiosis but the size of the anther did increase it follows that the tapetal cells increased in volume during meiosis.

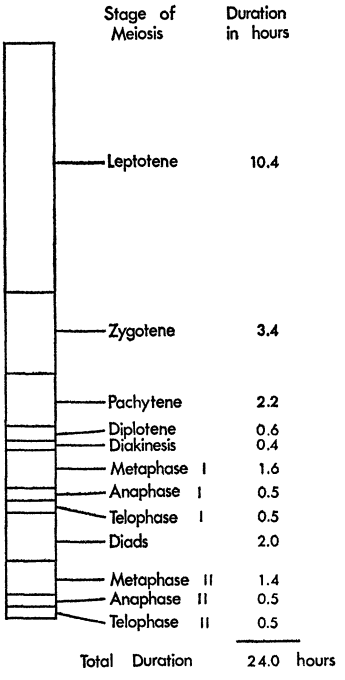

FIGURE 14. The durations of the stages of meiosis in Chinese Spring wheat grown at 20 °C.

(iv) *Meiosis in p.m.cs*

At the onset of leptotene the mean p.m.c. volume was about 3×10^4 μm^3 and this increased to about 3.6×10^4 μm^3 by second telophase. The duration of meiosis in Chinese Spring has been estimated using both autoradiographic and anther sampling methods (Bennett *et al.* 1971). Both methods yielded similar results and figure 14 shows the durations of the meiotic stages at 20 °C. Lasting 24 h at 20 °C, *T. aestivum* has one of the shortest meiotic divisions known in higher plants (figure 14). The duration of first prophase is about 17 h and occupies about 70 % of the total meiotic division time, while the stages from first metaphase to second telophase together last about 7 h and only occupy about 30 % of the meiotic duration. The lengths of individual stages range from about 10.4 h (leptotene) to 0.4 h (diakinesis).

The appearance of each of the stages of male meiosis in Chinese Spring is illustrated in figures 15 to 17, plates 12–14.

Leptotene (*figures* 15*a*, *b*, *plate* 12). In the variety Chinese Spring, leptotene began at about the time of the synchronous tapetal division. Prior to this time, it was virtually impossible to distinguish p.m.c. and tapetal nuclei in normal squash preparations of Feulgen stained anthers.

Early leptotene nuclei were more expanded than stage 3 interphase nuclei but chromosome threads were only visible as occasional peripheral loops or by careful focusing on the body of the nucleus. As leptotene proceeded and more chromosome contraction occurred, it became easier to squash the nuclei and more peripheral strands became visible.

Zygotene (*figures* 15*c*, *d*, *plate* 12). The start of zygotene was characterized by the initiation of chromosome pairing. At or slightly before this, chromosome contraction became sufficient for squashing to reveal a characteristic looping of chromosome threads around the nuclear periphery. This, and the tendency for chromosome ends to lie around the periphery of squashed nuclei, was reminiscent of the 'bouquet' arrangement of chromosomes seen in insects (John & Lewis 1965). As regions where pairing had occurred always included chromosome ends, and these ends were near the nuclear periphery, it would seem that pairing is initiated at the telomeres as in barley (Kasha & Burnham 1963). The occurrence of the chromosome ends near the nuclear periphery correlates with the ultrastructural observations of Wollam, Ford & Millen (1966), Wettstein & Sotelo (1967) and Gillies (1972) who found the pachytene synaptonemal complexes of various organizers to be attached to the nuclear membrane only at chromosome ends.

Pachytene (*figures* 15*c*, *f*, *plate* 12). By the completion of zygotene pairing, some chromosome contraction had occurred, and this process was accelerated during pachytene. Throughout pachytene, the general looping of chromosomes was retained, and though pairing remained complete, it was possible to distinguish the two homologues at various points along their length. As the chiasmata and also presumably points of crossing over are largely terminal in wheat, the pachytene appearance may indicate only a small terminal region of 'effective pairing' as envisaged by Henderson (1969).

Diplotene and diakinesis (*figures* 16*a*, *b*, *plate* 13). The start of diplotene was evidenced by active repulsion between paired homologues though their component chromatids remained indistinguishable. Further chromosome contraction occurred in both diplotene and diakinesis and, associated with presumed breakdown of the nuclear membrane, the looped structure of the nucleus broke up to yield bivalents scattered within the cell.

First metaphase, anaphase and telophase (*figures* 16*c–f*, *plate* 13). At first metaphase, the bivalents became alined on the equatorial plate and showed their maximum contraction. At 20 °C there was a mean of between 43 and 44 chiasmata per cell producing 21 ring bivalents. The chiasmata were usually terminal, though additional chiasmata were accommodated in more proximal positions. Separation of homologues occurred regularly during anaphase and telophase and during these stages the chromatids of each homologue became visible.

Dyads. Following the first division there was a brief interphase accompanying the formation of a cell wall between the two nuclei of the dyad. The dyad nuclei, however, typically remained elongated or crescent shaped, retaining the form of the telophase nuclei.

Second division (figures 17*a–d*, *plate* 14). The dyad nuclei expanded to give a characteristic net-like appearance in prophase of the second division. Both second metaphase plates and spindle axes then showed a similar orientation such that anaphase separation produced a planar ring of second telophase nuclei.

(v) *The effect of temperature on meiotic behaviour*

There is a pronounced temperature effect on meiosis so that its duration decreases with increasing temperature over the range 15–25 °C. The duration of meiosis is about 42 h at 15 °C,

about 24 h at 20 °C, and about 18 h at 25 °C (Bennett, Smith & Kemble 1972). Thus, the Q_{10} for meiosis over the temperature range 15 to 25 °C is about 2.3. Over this temperature range, the mean chiasma frequency per cell (figure 18) was almost constant (Bayliss & Riley 1972*b*) even though the durations of zygotene and pachytene, the stages when pairing and crossing-over occur, varied considerably. In fact the mean chiasma frequency per cell did not vary much between 12 and 23 °C but decreased considerably at temperatures below 12 °C and above 23 °C (figure 18).

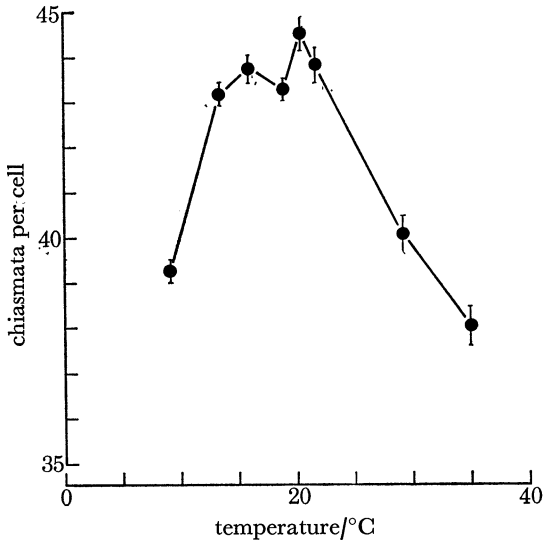

FIGURE 18. The relationship of chiasma frequency to temperature in Chinese Spring euploid. The vertical bars indicate the standard errors of the mean chiasma frequency of three or four plants measured at each temperature. The mean value at 35 °C was derived from plants given a short exposure to this temperature at an appropriate time in the premeiotic interphase (see Bayliss & Riley 1972). Continuous exposure to 35 °C caused chromosome stickiness and prevented measurement of chiasma frequency.

(*b*) *Female meiosis*

In *T. aestivum* each floret contains one ovary with a single bitegmic ovule which contains a single archesporial cell. There is, therefore, only a single embryo sac mother cell (e.m.c.) per floret. The e.m.c. is located immediately below the epidermis of the nucellar dome apex. The large e.m.c. has a distinctive shape, being greatly elongated and having its micropylar end much wider than its chalazal end so that it is pear-shaped. In this respect the e.m.c. differs from p.m.cs which are roughly spherical. Meiosis in e.m.cs is successive and the appearance of the chromosomes at each stage of meiosis was the same as at the corresponding stage in p.m.cs. The plane of the first meiotic division is at right angles to the long axis of the nucellus and the e.m.c. so that at first anaphase the chromosomes move to poles at either end of the e.m.c. The planes of the second meiotic division differ in the two cells of the dyad (figure 18*f*). In the micropylar cell it is at right angles to the plane of the first meiotic division, while in the chalazal cell it is in the same plane as the first meiotic division. Consequently, the product of female meiosis was a T-shaped tetrad (figure 26*a*, plate 19).

Microdensitometry of Feulgen-stained ovule squashes shows the nuclear DNA content decreased from 4*C* in first meiotic prophase, to 2*C* during first anaphase, and to 1*C* during second telophase.

Like p.m.cs, the e.m.c. is surrounded by a callose wall during meiosis, and this becomes thickened during the later stages.

Each floret contains only a single e.m.c., and within a floret meiosis occurs in the e.m.c. at approximately the same time as in the p.m.cs. Consequently, it is possible to make precise comparisons between the stages of male and female development within individual florets.

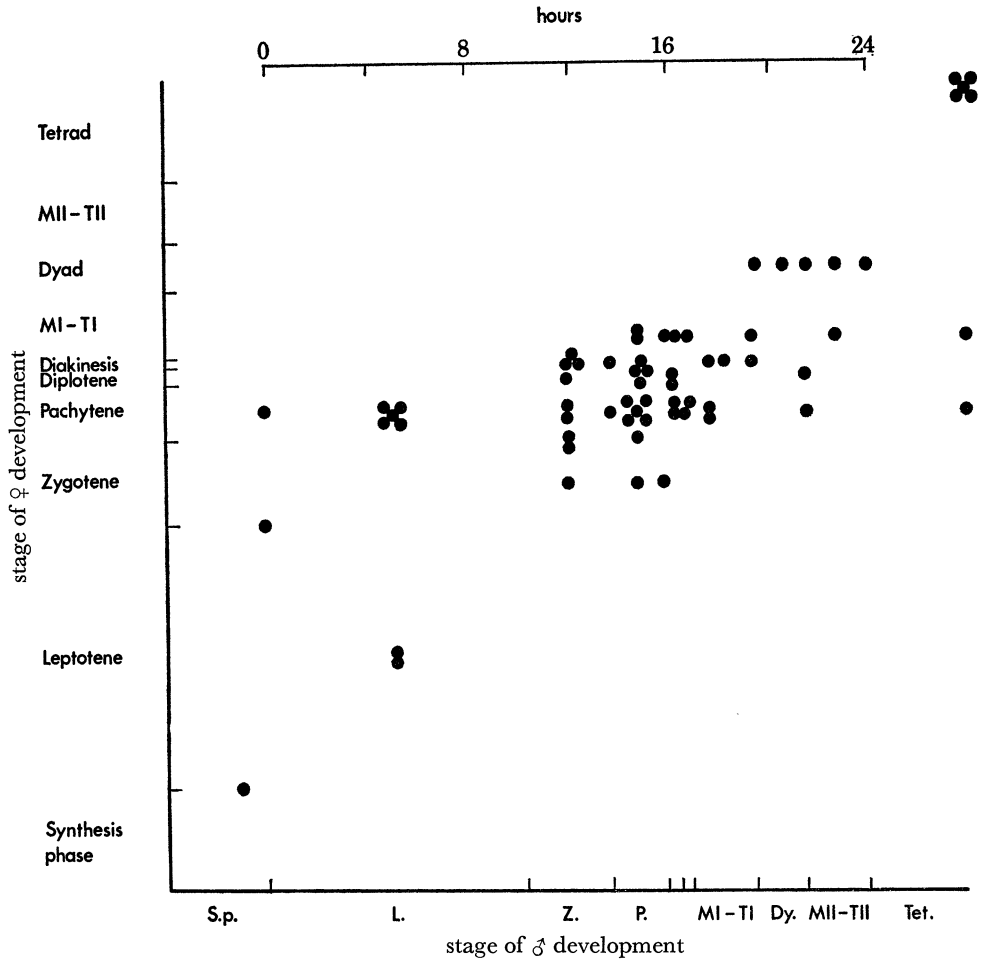

FIGURE 19. The relationship between the stages of meiotic development in embryo sac mother cells and pollen mother cells from individual florets of Chinese Spring wheat grown at 20 °C. The stages are given their relative durations, previously determined for male meiosis (Bennett *et al.* 1971), and a time scale corresponding to the known duration of male meiosis in Chinese Spring grown at 20 °C is also given.

Since the duration of the stages of male development at 20 °C is known it is possible to express differences between development of e.m.c. and p.m.cs in terms of hours of corresponding male development at 20 °C. It was shown (Bennett, Finch, Smith & Rao 1973), first, that male and female meiosis occur almost synchronously within each floret in plants grown at 20 °C, and second, that the duration of female meiosis at 20 °C is very similar to that of male meiosis at the same temperature. Thus, out of 31 florets with female meiosis, 28 contained some stage of male meiosis, and three contained identical meiotic stages in both the e.m.c. and p.m.cs. Furthermore, the greatest asynchrony between male and female development within a single floret corresponded to male development lasting about 11 h, which is less than half the duration

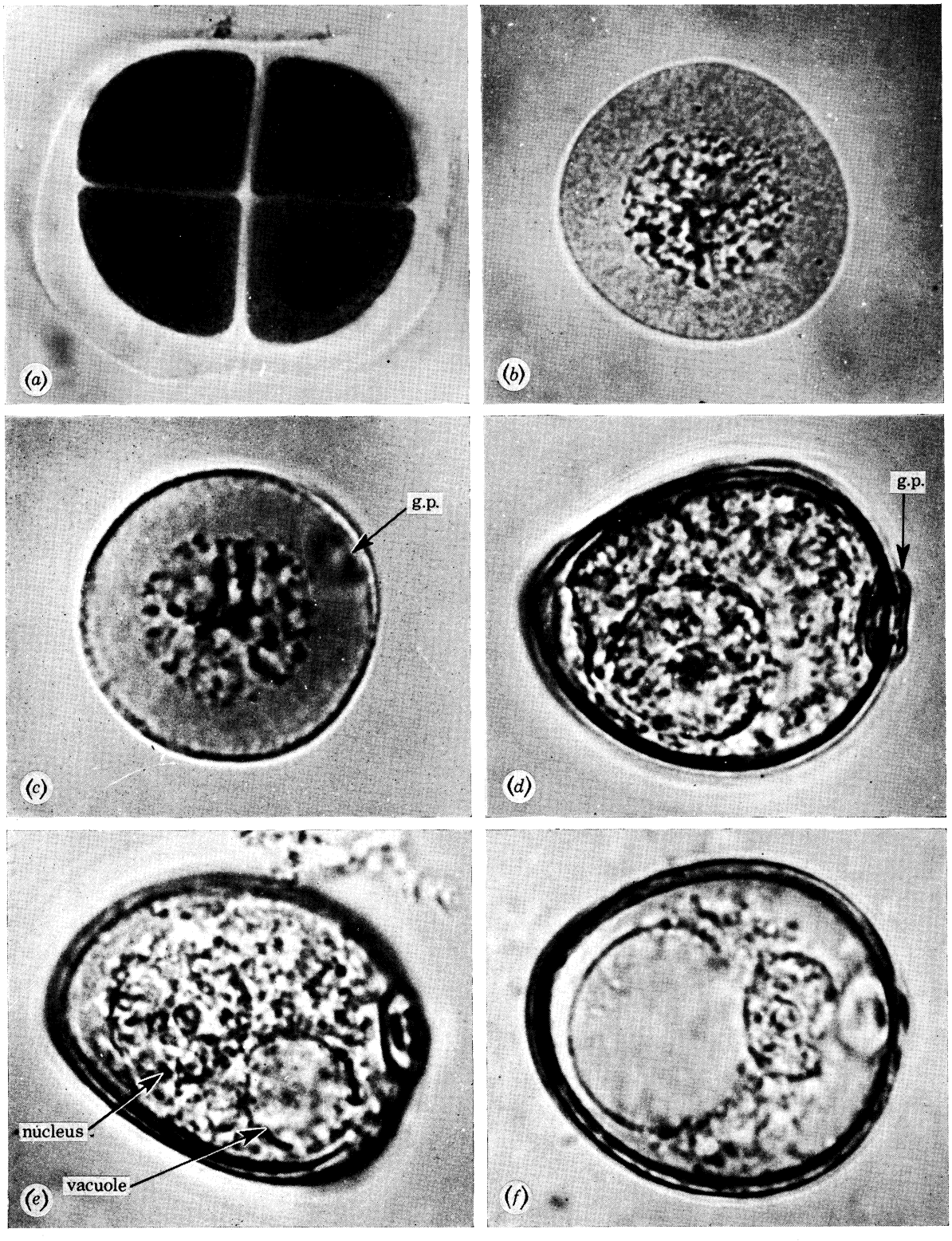

FIGURE 20. Pollen development in Chinese Spring wheat grown at 20 °C showing: (*a*) late tetrad stage (× 1375); (*b*) young pollen without a germ pore (× 1650); (*c*) young pollen with germ pore (g.p.) just visible; (*d*) young pollen with well formed germ pore but no single obvious vacuole; (*e*) young pollen soon after the appearance of a single obvious vacuole; (*f*) young pollen about 18 h after breakdown of the tetrad wall. (*c* to *f*, magn. × 2255.)

(*Facing p.* 58)

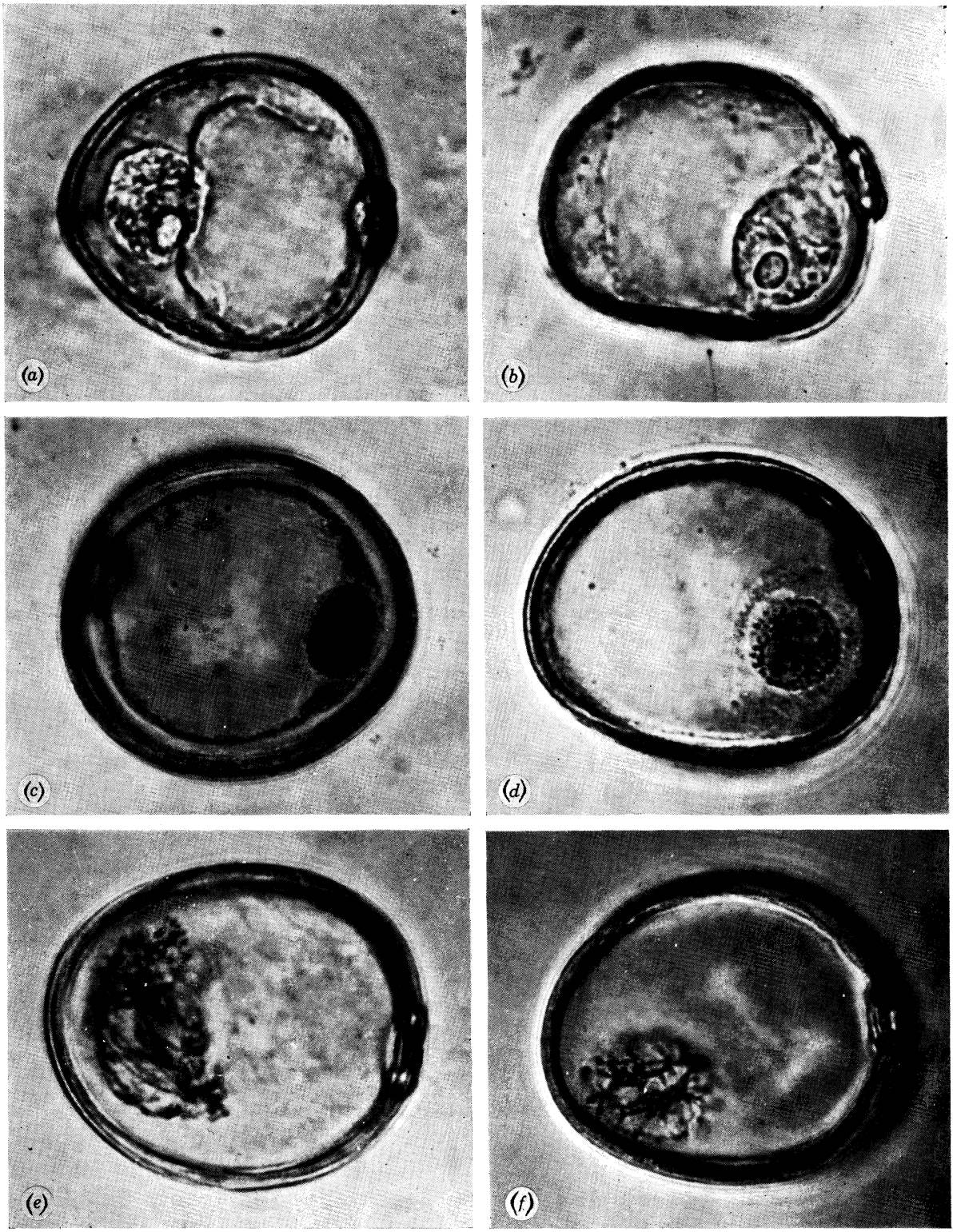

FIGURE 21. Pollen development in Chinese Spring wheat grown at 20 °C showing: (*a* to *c*) The increasing size of the microspore and the vacuole. Note the nucleus may be at either pole; either under the pore (*b*) and (*d*) or at the other end of the spore (*a*) and (*c*). (*c, d*) Nuclear contraction before first pollen grain mitosis probably concurrent with DNA synthesis phase. (*e, f*) Early and late stages of prophase of first pollen grain mitosis. (Magn. × 1430.)

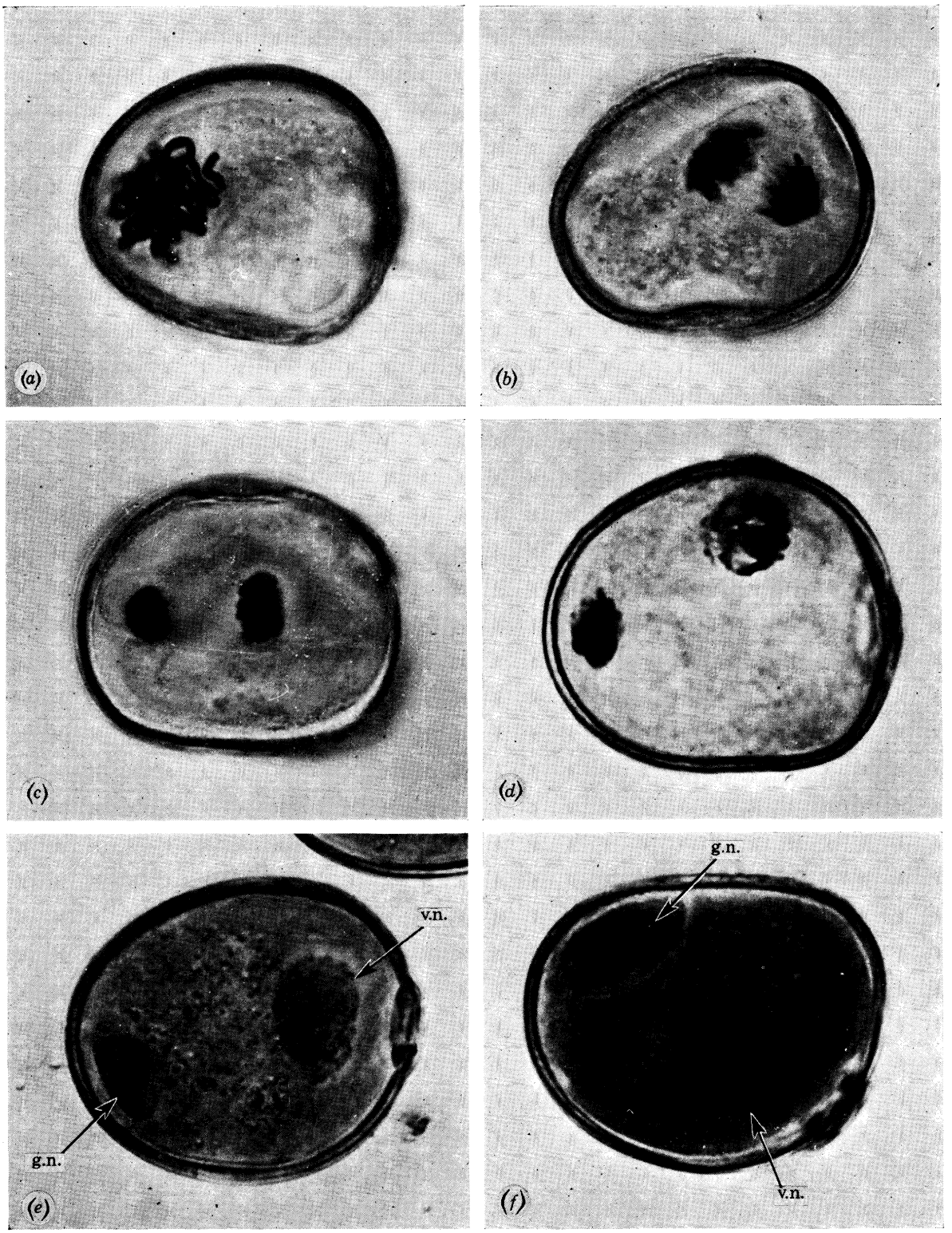

FIGURE 22. Pollen development in Chinese Spring wheat grown at 20 °C showing: (*a*) metaphase of p.g.m.1; (*b*) anaphase of p.g.m.1; (*c*) telophase of p.g.m.1; (*d*) migration of the nuclei to opposite poles of the microspore after p.g.m.1; (*e*) differentiation of the generative nucleus (g.n.) and vegetative nucleus (v.n.) (note the first appearance of starch granules); (*f*) pollen grain half way between p.g.m.1 and p.g.m.2 showing the organization of a separate cell around the generative nucleus, and numerous starch granules around the vegetative nucleus. (Magn. × 1430.)

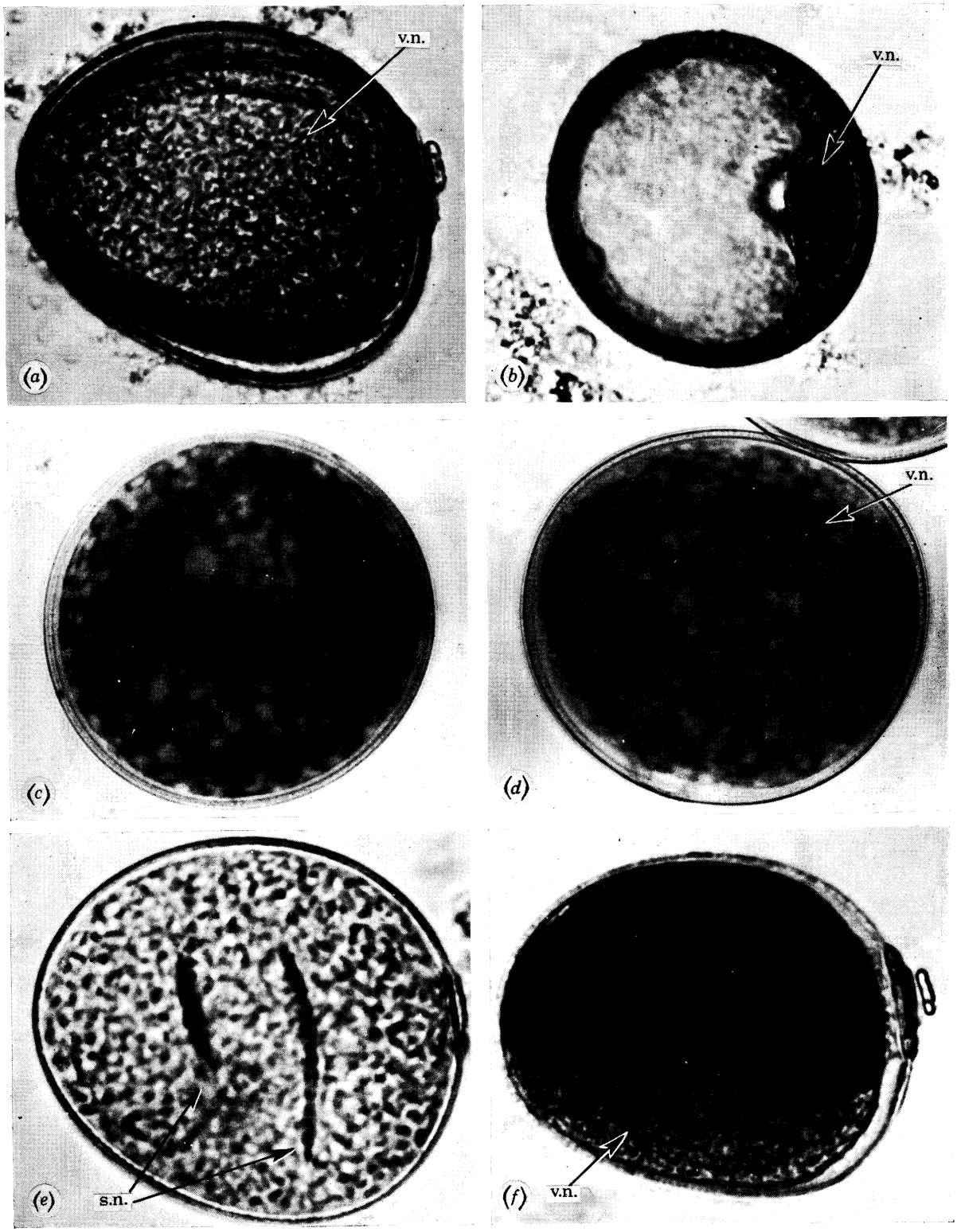

FIGURE 23. (*a*, *b*) Pollen grains later in the interval between p.g.m.1 and p.g.m.2 showing the size of the vacuole and the position and shape of the vegetative nucleus (v.n.); (*c*) late prophase of p.g.m.2; (*d*) metaphase of p.g.m.2; (*e*) almost mature pollen grain showing elongated sperm nuclei (s.n.); (*f*) Pollen at anther dehiscence stained in iodine solution showing the presence of starch granules on one side of the spore only away from the vegetative nucleus. (Magn. × 1320.)

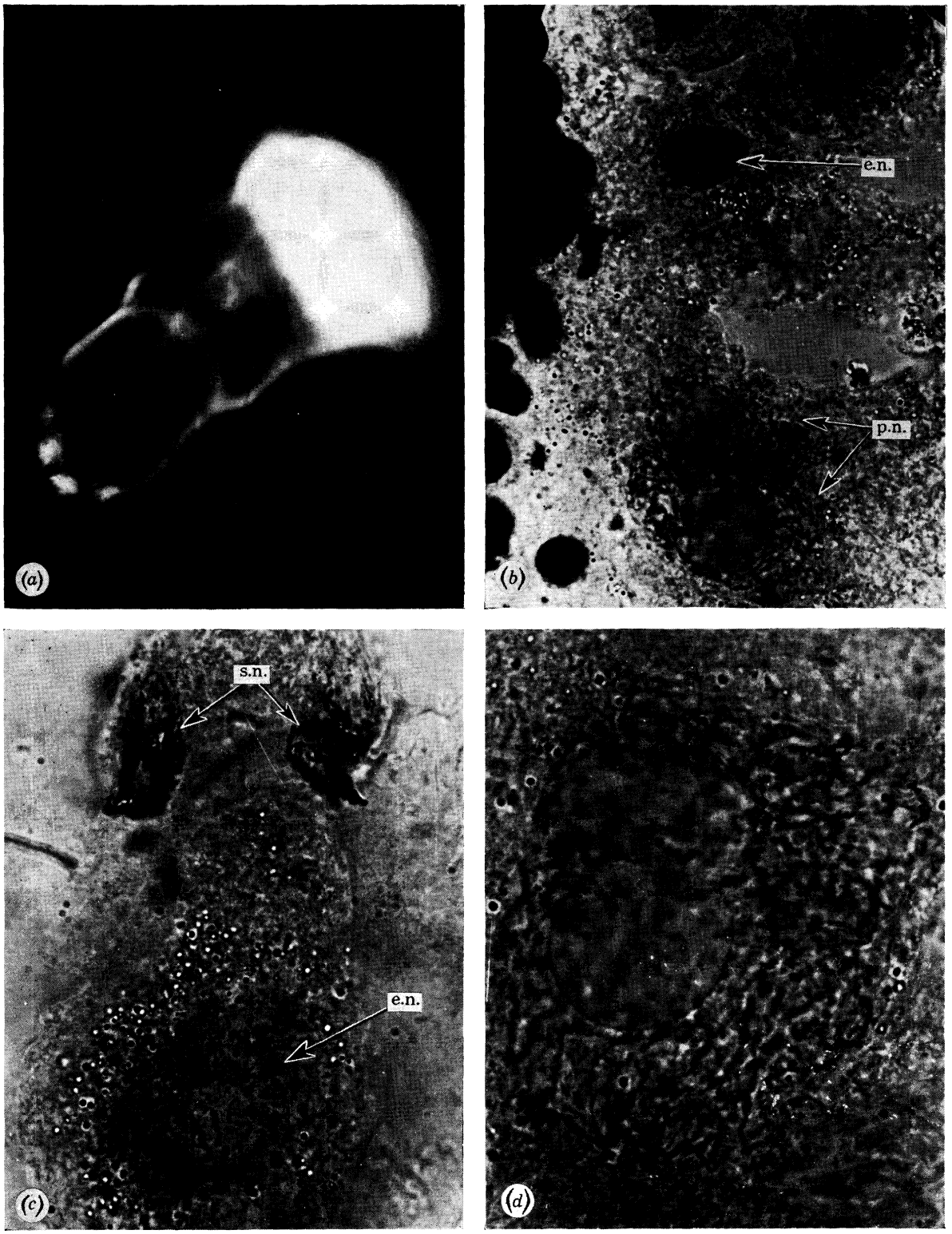

FIGURE 26. Embryo sac development in Chinese Spring wheat showing: (*a*) fluorescing callose around the female tetrad soon after the end of meiosis – the functional megaspore is at the bottom left-hand corner (× 1055); (*b*) part of an embryo sac about 4 days after meiosis showing the polar nuclei (p.n.), and the undifferentiated egg nucleus (e.n.) (× 1320); (*c*) part of an almost mature embryo sac prior to fertilisation showing the two degenerating synergid nuclei (s.n.) and the differentiated egg nucleus surrounded by refractile globules (bottom) (× 1045); (*d*) another part of the embryo sac in (*c*) showing the polar nuclei (× 1320).

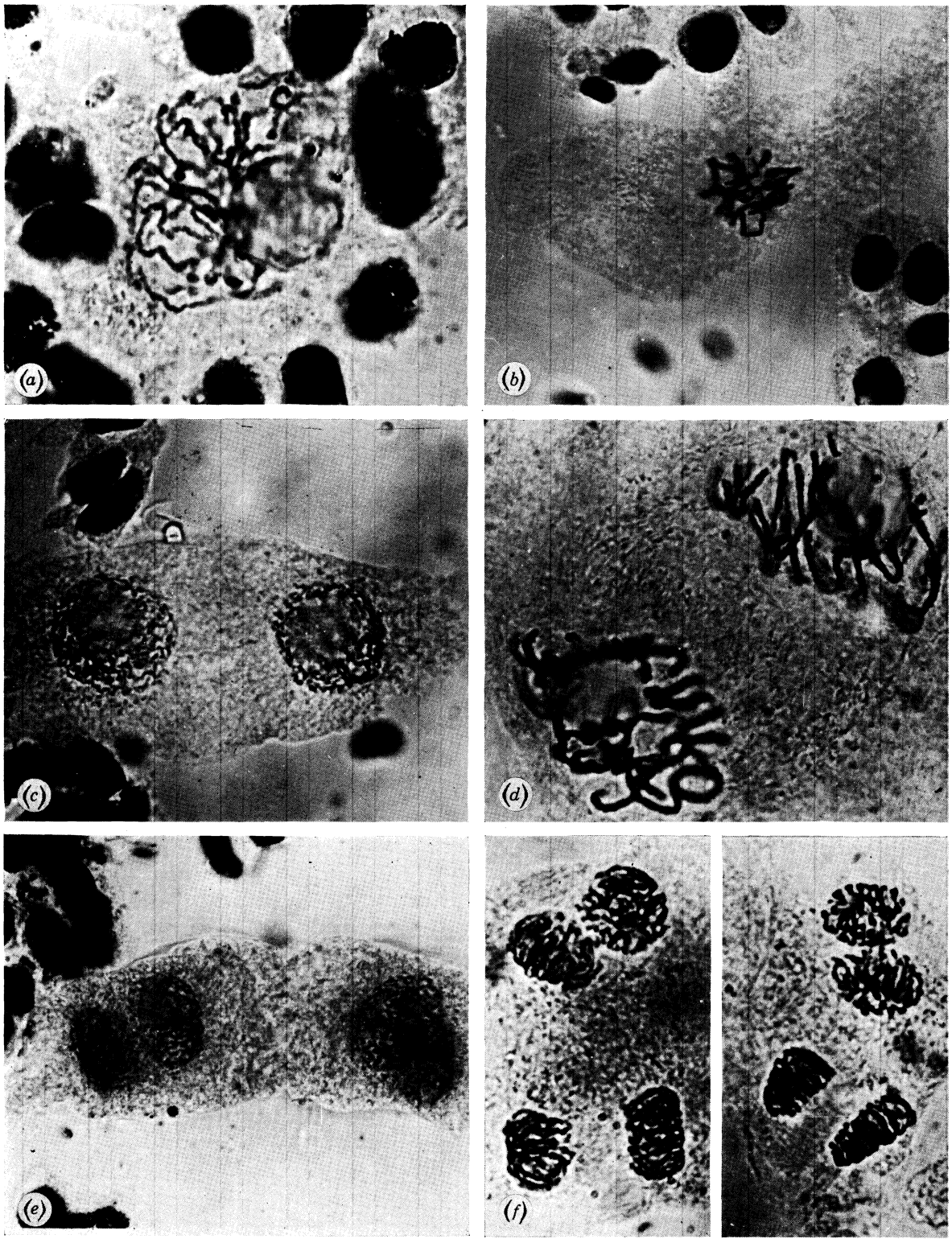

FIGURE 27. Embryo sac development in Chinese Spring wheat at 20 °C showing: (*a*) prophase of mitosis in the functional megaspore (× 1375); (*b*) metaphase of mitosis in the functional megaspore (× 725); (*c*) a two-celled embryo sac at interphase (× 880); (*d*) synchronous mitosis in the two-celled embryo sac (× 1320); (*e*) a four-celled embryo sac at interphase (× 965); (*f*) synchronous mitosis in the four-celled embryo sac (× 945). (N.B. only the four pairs of dividing nuclei are included.)

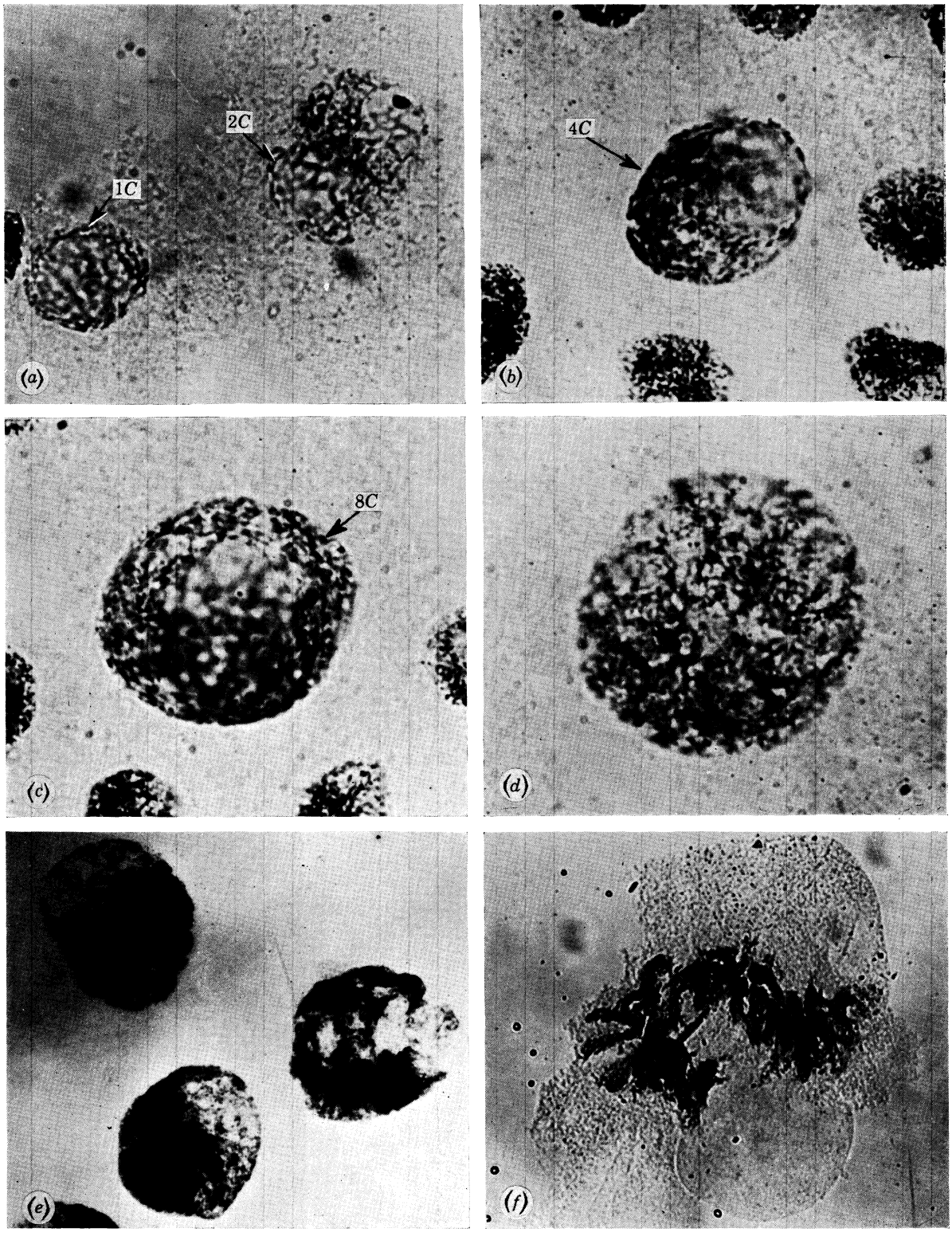

FIGURE 29. Antipodal nuclei in Chinese Spring wheat grown at 20 °C showing: (*a*) 1*C* and 2*C* nuclei; (*b*) a 4*C* nucleus; (*c*) an 8*C* nucleus; (*d*) a 16*C* nucleus; (*a–d* magn. × 1320); (*e*) 50–100*C* nuclei (× 285); (*f*) nucleus with more than 100*C* DNA content showing individual polyneme chromosomes and a very large nucleolus (× 275).

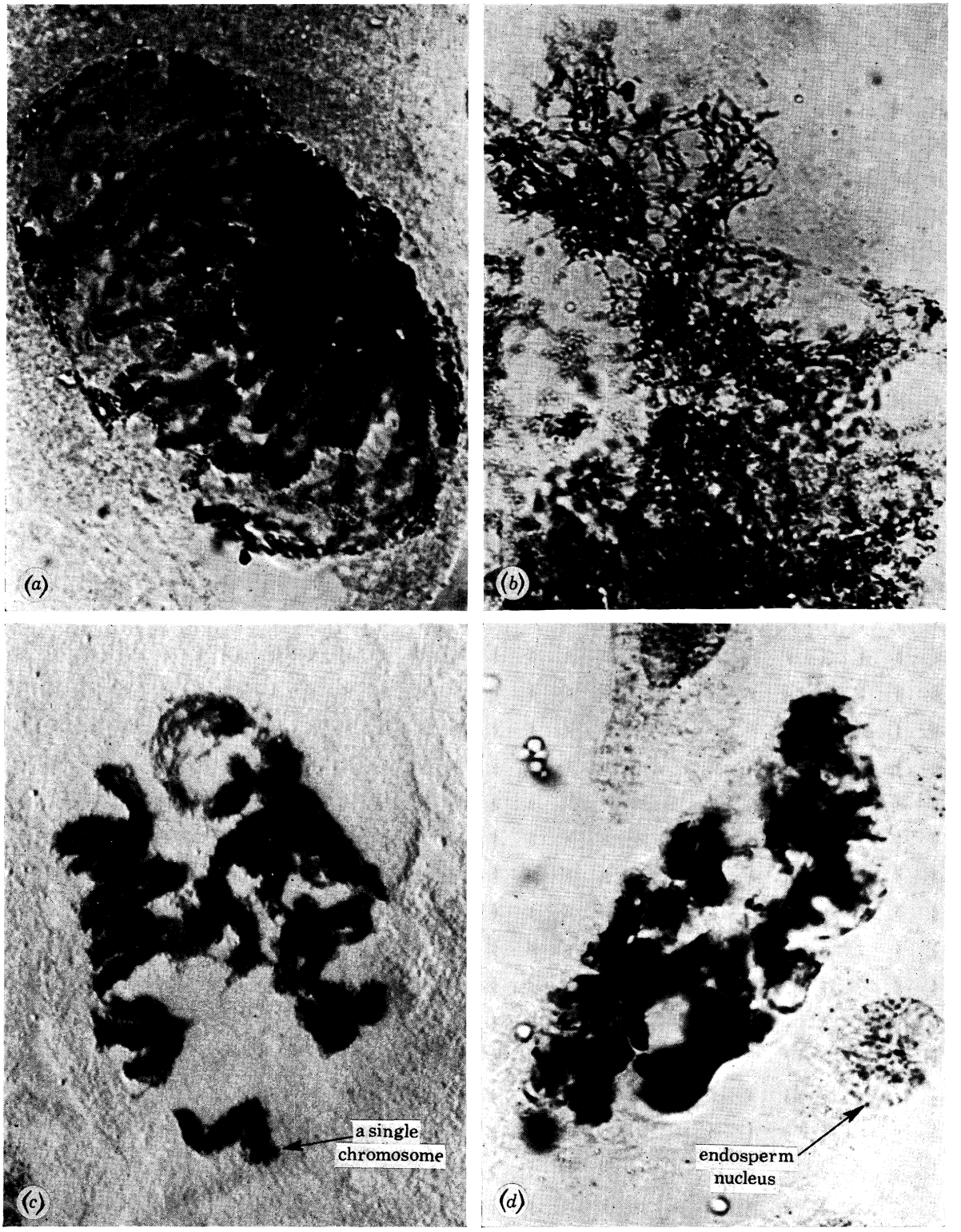

FIGURE 30. Antipodal nuclei in Chinese Spring wheat grown at 20 °C showing: (*a*) a single nucleus with about 100*C* DNA amount showing the arrangement of chromosomes with their centromeres all at one side of the nucleus (× 1045); (*b*) detail of polynemic chromosomes (× 2420); (*c*) a nucleus 3 days after pollination showing individual highly polynemic chromosomes (× 495); (*d*) degenerating antipodal nucleus with a triploid endosperm nucleus for comparison (× 750).

of male meiosis (24 h). Figure 19 is a scatter diagram of stages of development in the male and female germ lines from 65 florets from Chinese Spring plants grown at 20 ± 1 °C in continuous light. The data, modified and extended from (Bennett *et al.* 1973), corroborate the previous findings. In the previous instances, out of 60 florets containing female meiosis, 58 florets also contained some stage of male meiosis, and in nine florets both the e.m.c. and p.m.cs contained identical meiotic stages.

The high degree of synchrony between male and female development in individual florets may be an adaptive feature associated with inbreeding. Asynchrony between male and female meiotic development within the floret may be induced by environmental stresses (Bennett *et al.* 1973).

4. Pollen development

At the tetrad stage the spike was still enclosed within one or two leaf sheaths, but by first pollen grain mitosis the spike had usually completely emerged from the sheath. The observations of pollen development described below were made using anthers fixed in 1:3 acetic alcohol. Anther length and pollen size were measured using a moving scale micrometer eyepiece. Anther length measurements are the mean of not less than 10 observations and pollen size estimates are the mean of measurements made using samples of 100 microspores at each stage. Various staining methods were used to show up individual features of pollen development. Most features could be seen in aceto-carmine stained grains. The best results were obtained by macerating the anther with a glass rod in a drop of stain, removing the anther debris, applying a coverslip, gently warming the slide for about 3 to 4 s and leaving the slide for a few minutes to allow the nuclei to take up the stain. It is important to prevent the microspores becoming squashed between the slide and the coverslip as this distorts the pollen wall. Up until the formation of starch grains the vacuole was seen best in unfixed grains stained in dilute iodine solution. Thereafter, this method was good for staining starch grains but these made observations of the vacuole almost impossible. Generally, Feulgen stain did not give good results, although it was useful for staining the elongated sperm nuclei in nearly mature pollen. Aceto-carmine stained both the starch grains and the nuclei while Feulgen stained only chromatin.

In *T. aestivum* the normal product of male meiosis is an isobilateral tetrad (figure 20*a*, plate 15). Microdensitometry of Feulgen-stained anther squashes has shown that each of the four constituent microspores, which contain the haploid complement of 21 chromosomes, had a 1*C* nuclear DNA content of about 18 pg. The maximum diameter of the whole tetrad was about 50 μm, measured for mid-tetrads.

The microspores within a tetrad are bounded by a callose wall. This fact was verified by fluorescence microscopy for callose using unfixed tetrads treated with 0.1 % aniline blue in 0.1 M K_3PO_4 (cf. Ramanna & Mutsaerts 1971). The callose tetrad wall can be digested with helicase to release naked microspore protoplasts (Professor Cocking, personal communication).

Timing experiments using an anther sampling method have shown that the tetrad stage lasts about 10 h at 20 °C. Tetrad stage can be subdivided into early, mid and late periods from the appearance of aceto-carmine stained tetrads in anther squashes. In early tetrads, the chromosomes retained their appearance as at second telophase for up to 2 h after the appearance of cross-walls separating the products of second meiotic division. Thereafter the microspore nuclei lost the appearance of telophase and became more rounded. During this stage, which

lasted 4 to 5 h and which may be termed mid-tetrad stage, the callose wall was closely bound to the microspore cell boundary. The onset of late-tetrad stage was characterized by a loosening of the callose wall which became detached from the outer microspore wall. The breakdown of the callose wall did not take very long so that late-tetrad stage did not last more than 1 to 2 h (figure 20*a*, plate 15). Presumably the callose tetrad wall was degraded by callase produced either by the microspores or the tapetal cells.

At the time of their release from the tetrad wall the microspores are aporate and appear to possess almost no cell-wall material. After release the individual microspores soon lost their irregular shape within the tetrad and rounded off to become almost spherical. The haploid nucleus was centrally located within the cell and had no obvious nucleolus. At this stage the nucleus occupied a relatively greater part of the total microspore volume than at any other time during pollen development, having a diameter of about one half that of the microspore (figure 20*b*, plate 15). The microspore volume at tetrad break-up was about 1.14×10^4 μm^3.

About 4 h after their release from the tetrad, germ pore rudiments were just visible on some microspores (figure 20*c*, plate 15) and by 6 h after tetrad break-up these were clearly distinguished on all microspores. Once begun, deposition of pollen wall material and formation of the germ pore were rapid as illustrated by figure 20*d*, plate 15 which shows a typical microspore about 6 h after the first appearance of the germ pore rudiment.

During the first 12 h after the break-up of tetrads the microspore increased in size and the nucleus became more compact. Towards the end of this period a small nucleolus was first visible within the nucleus. There was no single obvious vacuole in the microspore cytoplasm during this period, although several small vacuoles became visible. About 12 h after the break-up of tetrads these coalesced to give a single obvious vacuole (figure 20*e*, plate 15). Thereafter, the vacuole increased rapidly in size (figures 20*e*, plate 15 to 21*c*, plate 16) until 12 h later it occupied the greater part of the microspore volume. The nucleus, which became increasingly condensed, occupied a progressively smaller percentage of the microspore and usually lay just beneath the germ pore. In a few grains, however, the nucleus was located at the end farthest from the germ pore (figure 21*d*, plate 16). During the second day of pollen development both the vacuole and the microspore continued to increase in size. Eventually, the cytoplasm constituted only a thin layer next to the pollen grain wall. Around the nucleus, however, it extended further into the lumen of the microspore. By about 36 h after break-up of tetrads the nucleus occupied its smallest percentage of the total microspore volume; about 3 to 5% (figure 21*c*). Up until this stage the nucleus still contained the haploid 1*C* DNA amount. At the start of, and throughout, DNA synthesis (*S*) the nucleus was darkly staining and had a granular appearance. In many nuclei a second nucleolus could be seen (figure 21*d*). During *S* the nucleus doubled its volume and from this point on it came to occupy a progressively greater fraction of the microspore volume until first pollen grain mitosis. The duration of *S*-phase was not measured accurately, but it was certainly longer than *S*-phase in root-tip meristem cells (about 3.8 h Bayliss 1972) at 20 °C and probably lasted about 12 h.

After *S*-phase the nucleus increased rapidly in size and individual chromosome threads became visible especially where they ran over the nucleolus which was large and distinct (figure 21*f*, plate 16). Nuclei remained at early prophase for about 12 h. By late prophase of first pollen grain mitosis (p.g.m.1) the nucleus and the cytoplasm together occupied a much greater portion of the microspore than previously. The total duration of p.g.m.1 was about 18 to 24 h. An estimate of the relative durations of individual mitotic stages was obtained from their

relative frequencies of occurrence in squashes of anthers at p.g.m.1 (see Bennett & Smith 1972) (table 1). Compared with prophase each of the later mitotic stages was much shorter in duration.

In plants grown at 20 °C with continuous light pollen development to p.g.m.1 was still fairly synchronous between microspores both within and between anthers from a single floret. Thus, in Chinese Spring, anthers were scored in which at least 70 % of the microspores contained mitotic stages, and up to 30 % contained metaphase stage. Even higher proportions of cells at these stages were recorded in the variety Holdfast (Bennett & Smith 1972). At p.g.m.1 the mean anthers length (figure 24) was about 3.1 mm and the mean microspore volume was about 5×10^4 μm^3. As at meiosis, a clear developmental gradient along the anther with progressively more advanced stages from base to tip was seen at p.g.m.1.

The two nuclei produced at p.g.m.1 initially had similar appearances but soon began to differentiate. The vegetative nucleus usually remained near the germ pore and rapidly increased in size becoming at the same time very diffuse and poorly staining both in Feulgen or aceto-carmine (figures 22*c–f*, plate 17). The generative nucleus migrated to the aporate pole of the microspore becoming at the same time highly condensed and darkly staining. Having reached the aporate end of the microspore the generative nucleus organized a separate cell with its own cytoplasm (figure 22*f*). Soon the generative nucleus became a flattened disk lying close to the pollen grain wall while the vegetative nucleus remained less flattened for a time and more centrally located in the cytoplasm beneath the germ pore. The cell organized by the generative nucleus occupied no more than 10 % of the microspore volume, the remaining volume being occupied by the large cell organized by the vegetative nucleus.

No starch grains could be seen at p.g.m.1 but they first became visible about 12 to 24 h later. At first, starch grains were visible only in the centre of the microspore, however, by second pollen grain mitosis (p.g.m.2) the microspore cytoplasm was packed with numerous starch grains which made cytological observations of the nuclei very difficult. The period between p.g.m.1 and p.g.m.2 lasted about 60 h. During this period the size of the vacuole increased once again and the vegetative nucleus, like the generative nucleus, became flattened and located in a thin layer of cytoplasm coating the microspore wall (figure 23*b*, plate 18). The vegetative nucleus remained near the germ pore at the opposite end of the microspore from the generative nucleus. By p.g.m.2 and thereafter, it was not possible to see the vacuole clearly owing to the numerous starch granules.

At p.g.m.2 the anther length was about 3.7 mm and the mean microspore volume was about 8×10^4 μm^3. At p.g.m.2 only the generative nucleus divided giving rise to two sperm nuclei (figures 23*c* to *e*, plate 18). During the division of the generative nucleus the vegetative nucleus was very large, diffuse and weakly staining while by comparison the chromosomes of the generative nucleus were very condensed and darkly stained (figure 23*d*). The duration of p.g.m.2 in individual microspores was not estimated accurately because, owing to the numerous starch grains, early prophase could not be identified. The duration of p.g.m.2 was probably very similar to the duration of p.g.m.1, and was certainly much longer than the duration of mitosis in root-tip meristems at 20 °C (Bayliss 1972). At p.g.m.2, as at p.g.m.1, microspore development within the anther was fairly synchronous. In one Chinese Spring anther the mitotic index was 60 % with 13 % of microspores at metaphase. Even higher mitotic indices and metaphase indices were recorded in the variety Holdfast (Bennett & Smith 1972). The developmental gradient found at p.g.m.1 was maintained at p.g.m.2 so that the most developed microspores were located in the anther tip.

After p.g.m.2 the two sperm nuclei became greatly elongated and finally were about 35 μm long and about 3 μm wide. The sperm nuclei were dense and dark staining. By comparison the vegetative nucleus remained nearly spherical with a diameter of about 15 μm. The duration of the period from p.g.m.2 until dehiscence was about 60 h. At dehiscence the anthers were about 4.1 mm long and the mean microspore volume was 11×10^4 μm^3. Thus, at 20 °C the duration of pollen development from tetrad stage until dehiscence was about 7.5 days (figure 25) and during this time the mean microspore volume increased about 12-fold. Pollen maturation time, like meiotic duration, is temperature sensitive and lasted about 13.5, 7.5 and 5.8 days at 15, 20 and 25° C respectively (Bennett *et al.* 1972).

Immediately prior to dehiscence, the starch granules all disappeared on one side of the microspore nearest to the vegetative nucleus (figure 23*f*, plate 18). This was clearly observed in pollen collected from dehiscing anthers and stained for starch using iodine solution. At dehiscence the vegetative nucleus lay near the equator of the microspore while at p.g.m.2 it lay just below the germ pore. Consequently, at some time between p.g.m.2 and dehiscence the vegetative nucleus must have moved to its final position, however, the timing of this was not observed.

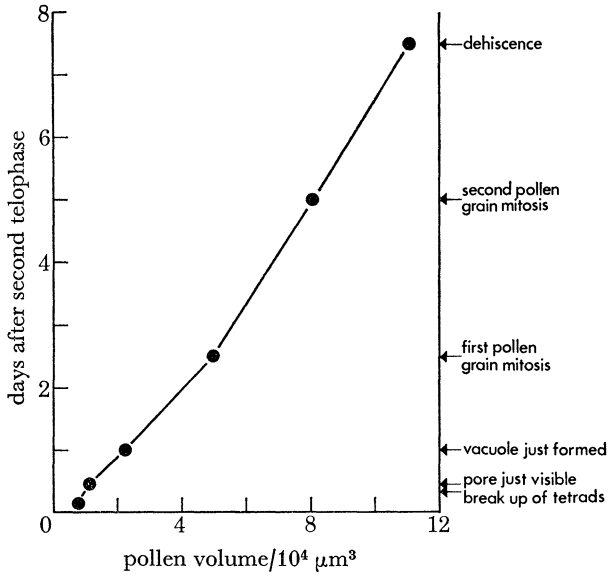

FIGURE 24. The relationship between pollen volume and time after the end of meiosis in Chinese Spring wheat grown at 20 °C.

5. EMBRYO SAC DEVELOPMENT

(*a*) *Description of embryo sac development*

Embryo sac development is of the polygonum type (Maheshwari 1950) in wheat. The first division of the functional megaspore gives rise to two nuclei: the primary micropylar and the primary chalazal. The second division produces one pair of nuclei at the micropylar and one pair of nuclei at the chalazal end of the embryo sac. The third division results in two quartets of haploid nuclei lying at opposite poles of the elongating embryo sac. The micropylar quartet differentiates into a 3-celled egg apparatus (consisting of an egg cell and two synergid cells) and the upper polar nucleus. The chalazal quartet differentiates into the lower polar nucleus

and, after repeated divisions of the remaining three nuclei, a group of 20 to 30 antipodal cells which subsequently enlarge and become highly polynemic. The two haploid polar nuclei move to the centre of the embryo sac and become closely appressed to each other before fusing to give a secondary nucleus: the polar nuclear body which, after fertilization, gives rise to the primary endosperm nucleus.

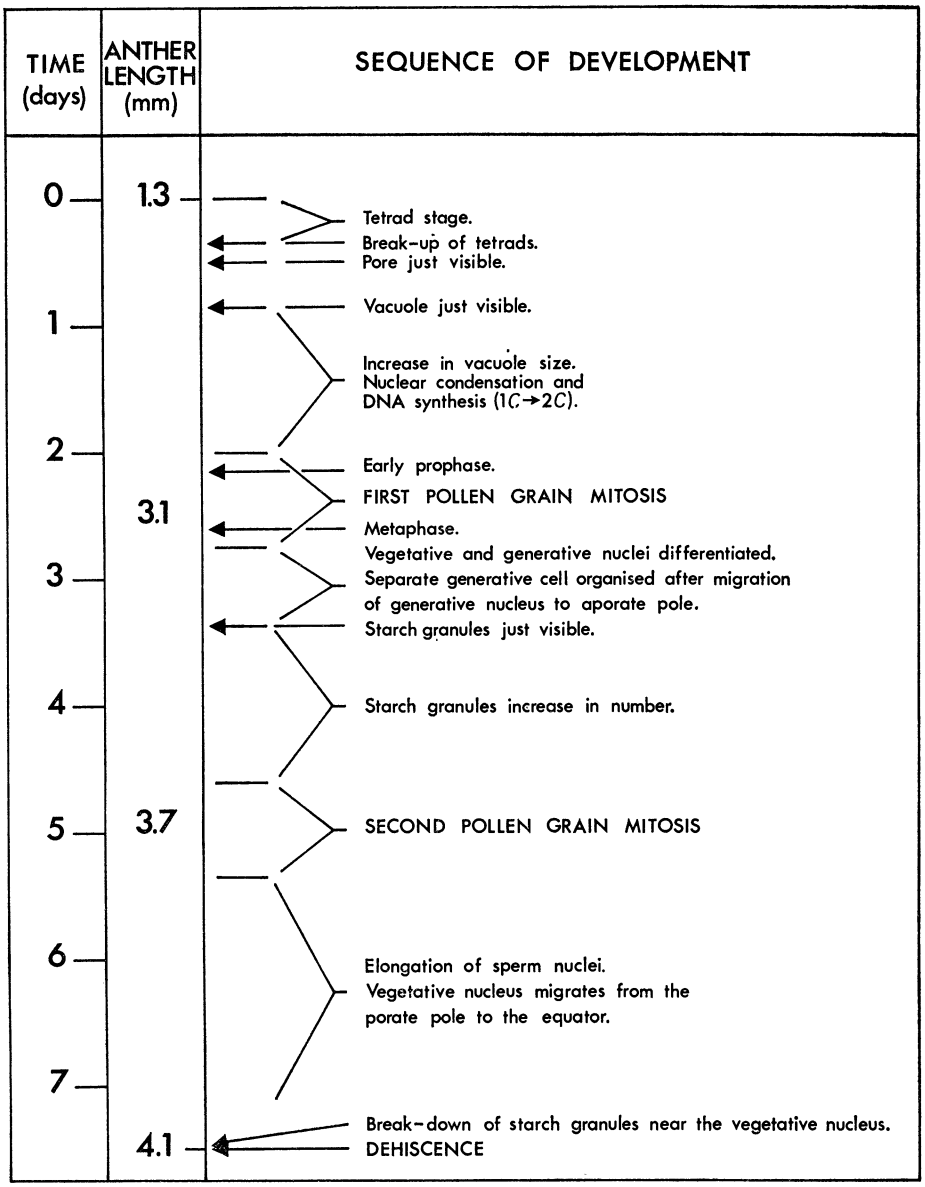

FIGURE 25. The time and sequence of pollen development in anthers of Chinese Spring wheat grown at 20 °C.

Embryo sac development was studied in aceto-carmine or Feulgen-stained ovule squashes as recommended by Morrison (1955). The ovules were dissected from florets together with the anthers and fixed in 1:3 acetic alcohol. The stage of meiotic or pollen development in the p.m.cs was determined so that precise comparisons between the stages of development in the microspores and the embryo sac could be made. In this way some idea could be obtained of the

timing of developmental events in the embryo sac since the timing of pollen development was already known (see §4).

The embryo sac developed from the haploid megaspore at the chalazal end of the female tetrad. This cell was formed at the second meiotic division which usually occurred within a few hours of second meiotic division in p.m.cs from anthers in the same floret. The other three cells of the female tetrad degenerated and played no further part in development. The cells of the female tetrad were enclosed in a layer of callose when they were first formed (figure 26*a*).

The first mitotic division in the functional megaspore sometimes occurred a few hours before the onset of p.g.m.1 in microspores from anthers in the same floret. However, developing embryo sacs were seen with one, two, four and eight nuclei in florets whose anthers contained numerous microspores at p.g.m.1. In florets whose embryo sacs contained either the third mitotic division or eight haploid nuclei, the anthers contained mostly pollen grains with two nuclei and only a small proportion at p.g.m.1. In plants grown at 20 °C, p.g.m.1 occurred in nearly all microspores between 48 and 72 h after the end of meiosis. It is concluded, therefore, that the first cell cycle in embryo sac development lasted between about 40 and 55 h. The mean duration of the second and third cell cycles which occurred concurrent with p.g.m.1 cannot have been more than 12 h and may have been slightly less.

The volume of the newly formed functional megaspore was about 8.5×10^3 μm^3. The callose wall surrounding the functional megaspore was broken down before the first mitotic division in the developing embryo sac. The plane of the first mitotic spindle was parallel to the long axis of the developing embryo sac so that the nuclei produced were located one at the micropylar end and one at the chalazal end. Soon after the first mitotic division a vacuole appeared in the centre of the developing embryo sac between the two nuclei. The second and third mitotic divisions in the developing embryo sac always occurred synchronously (figures 27*d*, *f*, plate 20) in all the embryo sac nuclei. At the second embryo sac division the planes of the spindles of the two mitoses are often at right angles to each other. No cell walls were formed around the individual nuclei in the embryo sac until after the 8-cell stage. The volume of the developing embryo sac continued to increase in size until fertilization.

Pollen development from p.g.m.1 to p.g.m.2 lasted about 60 h at 20 °C. During this period about 20 to 30 antipodal nuclei were formed at the chalazal end of the embryo sac. Soon after p.g.m.1 in anthers from the same floret, three of the four nuclei at the chalazal end of the embryo sac divided. Twenty-two antipodal nuclei were counted in an ovule squash from a floret with microspores estimated to have developed for 40 h after p.g.m.1. No increase in the number of nuclei in the embryo sac occurred, however, after the completion of p.g.m.2.

The two polar nuclei moved towards the centre of the embryo sac soon after p.g.m.1. The two nuclei were observed closely appressed near the centre of the embryo sac in a floret whose pollen development was estimated to be 24 to 36 h post p.g.m.1 because the microspores had starch grains just visible.

At the time of anther dehiscence the egg nucleus and the synergid nuclei from the same floret were contained in distinct cells. The egg cell was very large and centrally located at the micropylar end of the embryo sac. It contained a large subspherical nucleus whose volume was about 14×10^3 μm^3, and which usually contained a single prominent nucleolus. The nucleus was composed of faintly staining chromatin threads (figure 26*c*, plate 19). The cytoplasm of the egg cell was easily distinguished from the rest of the contents of the embryo sac because it con-

tained numerous small highly refractile globules (figures 26*d*, plate 19, 33*a*, plate 23). Morrison (1955) previously noted that neither the synergid nor the polar cells contain similar bodies. The two synergid cells were arranged one on either side of the egg cell. The synergid nuclei were smaller than the egg cell nucleus and somewhat elongated (figure 26*c*). The two polar nuclei were each larger than the egg cell nucleus and each was still enclosed within its own separate nuclear membrane. Each nucleus contained one prominent large nucleolus and several smaller ones. The general appearance of the two polar nuclei together was of bilateral symmetry and this made them easy to find in ovule squashes (figures 26*d*, 33*c*). The timing and sequence of cell development in the embryo sac is summarized in figure 28.

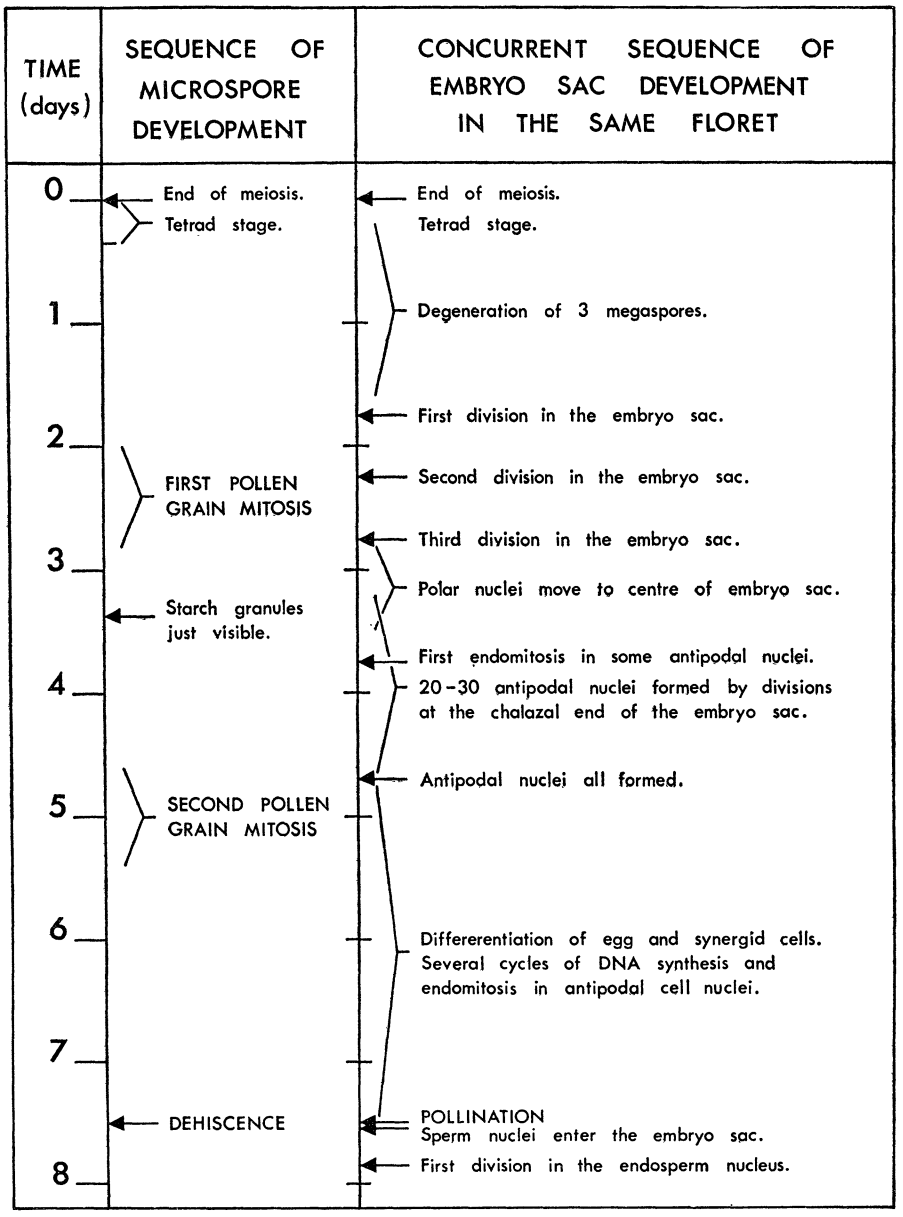

FIGURE 28. The time and sequence of development in the embryo sac of Chinese Spring wheat at 20 °C compared with the concurrent development in anthers from the same floret.

(b) The antipodal cell nuclear DNA content

Morrison (1955) drew attention to the large endopolypoid antipodal nuclei in wheat. We have studied in detail the development of these nuclei during late embryo sac development and also during early embryo and endosperm development. The DNA content of antipodal cells was estimated from Feulgen-stained squashes of ovules. On each slide the 4*C* DNA value was estimated from somatic prophase nuclei.

As mentioned above, the antipodal cells were all produced by repeated divisions of cells at the chalazal end of the embryo sac within about 60 h of the first appearance of the 8-celled embryo sac. As up to 30 antipodal cells were produced during this time, the maximum mean cell cycle time cannot have been more than 15 h, because the observed number of antipodal cells could not be produced by less than four division cycles starting from three cells. The mean cell cycle time was probably shorter than 15 h since many antipodal cells were already endopolyploid by 60 h after the first appearance of the 8-celled embryo sac. Such cells must have spent some time undergoing DNA synthesis and endo-reduplication. Allowing for this the mean antipodal cell cycle time prior to the onset of endoreduplication was probably about 10 to 12 h and very similar to the durations of the second and third cell cycles in the embryo sac.

Concurrent with late p.g.m.1 in microspores the embryo sac from the same floret contained eight nuclei, each with the 1*C* DNA amount. In a floret estimated to have completed about 40 h of development after p.g.m.1, 22 antipodal nuclei were counted and the DNA contents of 19 of these were measured. They ranged from 2*C* to 8*C* indicating that in some cells DNA synthesis followed by endo-reduplication had already occurred three times. More than half of the antipodal nuclei measured at this stage of development had DNA contents of between 3*C* and 4*C* (figure 29*b*, plate 21).

The antipodal cells were large compared with nucellar cells at all times, but until late embryo sac development they were smaller than the egg, the synergids and the polar nuclei. There was a single nucleus in each antipodal cell. At first the antipodal cell nuclei were diffuse compared with nucellar cell nuclei and, in Feulgen-stained cells, the nucleolus was seen as a large eccentric unstained object.

In a floret estimated to have completed about 21 h of pollen development after p.g.m.2, the DNA contents of antipodal cells ranged from 6*C* to 23*C* with a mean of about 10.6*C*. Thus, some cells were engaged in the fifth cycle of DNA synthesis while others were only engaged in their third *S*-phase.

In florets fixed one day after anthesis and self-pollination, the nuclear DNA contents of antipodal cells ranged from 14*C* to 136*C* with a mean of about 52*C*. The maximum mean and range of DNA values was reached on the third day after anthesis. Estimates at this time ranged from 37*C* to 196*C* with a mean value of about 84*C*. This indicated that some nuclei were engaged in their 8th cycle of DNA synthesis, and that all had completed five DNA synthesis cycles. It should be realized that each chromosome in antipodal nuclei with the highest DNA amounts was represented by about 1.2 times the total 4*C* DNA content of somatic prophase nuclei.

Three days after anthesis the antipodal nuclei were extremely large, some having volumes of up to 16×10^4 μm^3. The volume of these nuclei was larger than the volume of the mature pollen grain in wheat. Each antipodal nucleus contained a single very large nucleolus itself many times larger than the total nuclear volume of somatic cells in the nucellus.

The appearance of developing antipodal nuclei was of two types as reported by Morrison (1955). One, the 'resting stage' type, probably represented DNA synthesis (endo-reduplication), while the second 'prophase' type probably represented endomitosis. In the 'resting stage' the nuclear contents showed no regular pattern of organization. In antipodal nuclei at the 'prophase-like' stage, the chromosomes presented a bouquetlike appearance, particularly in highly endopolyploid nuclei. In these nuclei 21 compact densely staining masses could be seen in a group at one pole of the nucleus. These objects probably represented the centromeric regions of the chromosomes and they increased in size with increasing nuclear DNA content.

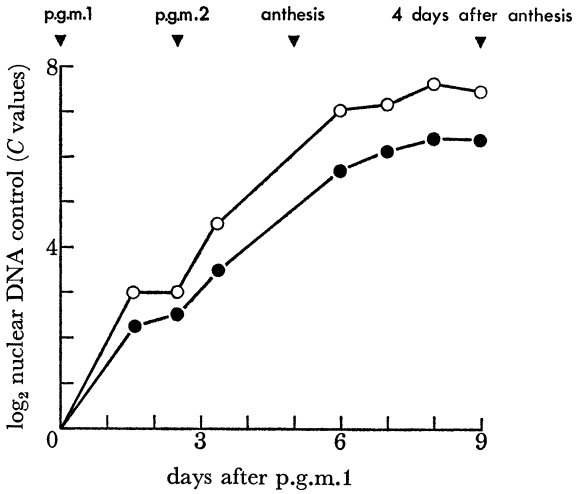

FIGURE 31. The mean (●) and maximum (○) DNA content of antipodal nuclei at different stages of floret development in Chinese Spring grown at 20 °C.

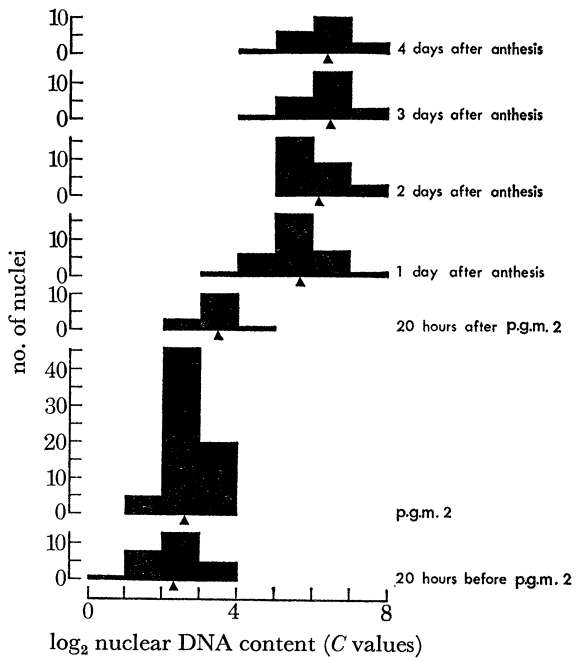

FIGURE 32. The frequency of occurrence of antipodal nuclei with various nuclear DNA contents at seven stages of floret development.

From each of these dense objects more faintly staining chromatin threads ran to the other pole of the nucleus over the surface of and around the centrally located nucleolus and distinct chromomeres were visible on these threads (figure 30*a*, plate 22). The number of fibres visible in each chromosome increased with the increasing DNA content of the nucleus.

TABLE 3. THE MEAN AND RANGE OF NUCLEAR DNA CONTENTS (IN *C* VALUES) IN ANTIPODAL NUCLEI FROM EMBRYO SACS AT SEVEN STAGES OF DEVELOPMENT

stage of development	no. of florets examined	no. of nuclei measured	nuclear DNA content	
			mean	range
40 h after p.m.g.1	2	32	4.7	1–9
p.g.m.2	6	71	5.7	2–9
20 h after p.g.m.2	1	14	10.6	6–24
1 day after anthesis	4	32	51.6	14–136
2 days after anthesis	4	28	69.3	35–144
3 days after anthesis	5	23	86.9	37–196
4 days after anthesis	3	20†	83.6	27–175
		15	100.0	36–175

† This included five degenerating nuclei. Values excluding these nuclei are given in the second row of figures for this stage of development.

In plants grown at 20 °C the first signs of degeneration were seen in some antipodal nuclei 3 to 4 days after anthesis of anthers in the same floret. By 5 to 6 days after anthesis most of the antipodal nuclei had completely degenerated. Regression commenced with individual chromosome bundles becoming increasingly compact, so that individual chromosomes became increasingly separated and easy to see (figure 30*c*, plate 22). In some nuclei the 21 chromosomes could easily be counted. As degeneration proceeded the faintly staining chromatin threads were seldom seen until, eventually, only 21 densely staining masses of various sizes remained. Microdensitometry of degenerating antipodal nuclei showed that there was a fall in their DNA contents at this time. The chromatin in degenerating antipodal nuclei became highly vacuolated (figure 30*d*, plate 22). As the antipodal cells degenerated and disappeared they were replaced by the developing endosperm cells. The means and ranges of DNA contents of antipodal cell nuclei (table 3) at different stages of embryo sac and early seed development are shown in figures 31 and 32.

6. FERTILIZATION AND EARLY SEED DEVELOPMENT

(*a*) *Fertilization*

Fertilization was studied in plants kept at 20 ± 1 °C with continuous light in a growth cabinet. About 2 days before normal anther dehiscence, spikes were emasculated and covered with cellophane bags to prevent out-pollination. Two days after emasculation, stigmas were pollinated with pollen collected from other tillers on the same plant. Pollination was carried out in a laboratory at 20 ± 1 °C but individual plants were only removed from the growth cabinet for less than 5 min. Pollinated florets were fixed in 1:3 acetic alcohol at intervals of between 30 min and 5 days after pollination. The ovaries were dissected out from fixed florets, hydrolysed for 12 min in 1 M HCl at 60 °C and stained in leuco-basic fuchsin for 4 h. The ovules were then dissected out from stained ovaries in a drop of 45 % acetic acid on a microscope slide.

After carefully applying a coverslip the ovules were squashed gently and examined to see how far post-pollination development had proceeded.

The structure and appearance of the unfertilized embryo sac and the various cells it contained was essentially as previously described for *T. aestivum* (Percival 1921; Morrison 1955). Until fusion with the sperm nucleus, when their individual nuclear membranes disappeared, the polar nuclear mass was easily recognized by its large size, spherical shape and bilateral symmetry. The latter resulted from the equal arrangement of the polar nuclei and the nucleoli within the two hemispheres of the polar nuclear mass (figures 26*b*, *d*, plate 19). The egg cell, and after fertilization the first embryo cells, were identified by the numerous small refractile bodies which they contained (figures 26*c*, 33*a*, *d*, plate 23). As Morrison (1955) noted, these bodies are not destroyed by acid hydrolysis. They were not found in the synergids, around the polar nuclei or in the antipodal cells. After their arrival in the embryo sac, the sperm nuclei were easily recognized by their characteristic elongated shape and high staining density (figure 33*a*).

The time taken by growth of the pollen tube down the style, and the discharge of sperm nuclei into the embryo sac, was very short but varied somewhat. No sperm nuclei were detected in ovules fixed 30 min after pollination and various situations were observed in ovules fixed 41 min after pollination. In one ovule both the egg nucleus and the polar nuclei were already accompanied by sperm nuclei. In another instance, the egg cell contained a sperm nucleus but no sperm nucleus was seen near the polar nuclei. Elsewhere, one sperm nucleus was observed still within the pollen tube and neither the egg nor the polar nuclei were accompanied by a male gamete. We conclude, therefore, that at 20 °C the pollen tube can grow down the style and discharge both sperm nuclei into the embryo sac within 41 min of pollination. In ovules from plants grown at about 25 °C in a glasshouse, both male nuclei were seen in the cytoplasm of the egg cell 30 min after pollination.

The pollen tube discharged the sperm nuclei either into the egg cell or close to it and, while one sperm nucleus became appressed to the egg cell nucleus, the other sperm nucleus migrated to and became appressed to the polar nucleus. The male gamete going to the egg nucleus apparently reached its destination before the male nucleus going to the polar nucleus, though the interval between their arrivals must have been very short, since both were observed near their destinations 41 min after pollination.

Development between the time of the arrival of the male gamete near to the egg and the polar nuclei and division of the primary endosperm nucleus was studied using plants grown at 23 ± 0.5 °C in a glasshouse. At 2 and 3 h after pollination the chromosomes of the two polar nuclei and the sperm nucleus were in prophase but still formed three separate groups (figure 33*c*, plate 23). Each nucleus still had, apparently, a separate nuclear membrane. No changes were detected between samples at these two times. The sperm nucleus in the egg cell became increasingly diffuse but did not fuse with the egg cell nucleus. Four primary endosperm nuclei at metaphase, and one at anaphase, were found in five ovules fixed 5 h after pollination. In one primary endosperm nuclei at metaphase a group of chromosomes, probably derived from the male gamete, was clearly separate from the rest, however, these could not be counted. It seems, therefore, that the chromosomes from the male gamete remained distinct throughout prophase and merged with the female chromosomes only as increasing contraction and congression occurred at the later stage of metaphase.

Our observations differ, therefore, from Morrison's (1955), who stated that the two types of chromosomes were not visible as separate groups at primary division of the endosperm nucleus.

At 2, 3, 6 and 11 h after pollination, the sperm nucleus in the egg cell still had not fused with the egg cell nucleus, but had become increasingly diffuse. No trace of a distinct sperm in the egg cell was seen in ovules fixed 19 h after pollination. At this time the Feulgen stained zygote showed no sign of dividing. A dense area of chromatin, probably representing the male chromosomes, was observed in the same ovules, after orcein staining.

Fusion of the male and female nuclei in the zygote probably occurred about 18 to 20 h after pollination. The first division in the zygote was seen in ovules fixed 22 h after pollination. At this time zygotes were observed with nuclei at metaphase, late anaphase and late telophase but no cytokinesis was seen. The embryo consisted of two nuclei in some ovules fixed 24 h after pollination.

While division in the primary endosperm nucleus occurred 5 h after pollination in plants grown at about 23 °C in a glasshouse, it occurred slightly later in plants grown at 20 °C in a controlled environment cabinet. Thus, in six ovules from plants grown at 20 °C fixed 6 h after pollination, primary endosperm nuclei were seen at metaphase in four ovules and at anaphase in the other two ovules.

In plants grown at 20 °C the second division in the endosperm occurred about 11 h after pollination. The division was synchronous in both endosperm nuclei. Endosperm nuclei, all at stages from metaphase to early interphase, were observed in ovules fixed 11 h after pollination.

Twenty-four hours after pollination the endosperm consisted of 16 nuclei (table 3). Sometimes they were seen all in mitosis, and often all at the same stage of division, although occasionally some nuclei were found to be one stage of division ahead of the others.

(*b*) *The endosperm*

The endosperm in wheat, formed by the fusion of two haploid embryo sac nuclei and one haploid sperm nucleus, is therefore triploid and so each nucleus contains 63 chromosomes. Unlike in the embryo, where divisions occurred asynchronously, the endosperm continued to exhibit synchronous mitoses until it contained several hundred nuclei. Figure 35*c*, plate 25, illustrates typical interphase endosperm nuclei. During interphase the nuclei were large and quite darkly staining and had maximum and minimum diameters of about 50 and 24 μm respectively. Each nucleus contained several, often three, nucleoli whose diameters ranged up to about 20 μm. The arrangement of the chromosomes within the nucleus was clearly seen at prophase. All the centromeres were located together at one side of the nucleus and all the chromosome arms ran almost parallel to the opposite side of the nucleus. This was especially clear where the chromosomes ran over and around the surface of the nucleoli (figure 34*a*, b, plate 24). Endosperm nuclei at the other stages of mitosis are also shown (figure 34*c*, *d*, plate 24; figure 35*a*, *b*, plate 25). At all stages of the cell cycle endosperm nuclei were larger than somatic nuclei.

After endosperm development became asynchronous, adjacent groups of nuclei were still seen to be all at a similar developmental stage (figure 34*d*). Observations of the endosperm and microdensitometry of Feulgen-stained endosperm nuclei in ovule squashes showed that waves of mitotic divisions were initiated at the suspensor and then passed down through the endosperm to its chalazal end. For instance, DNA measurements on endosperm nuclei along a transect from the suspensor to the chalazal end of the endosperm showed that nuclei at mitosis next to the suspensor of the embryo had either 3*C* or 6*C* amounts. These were followed by nuclei

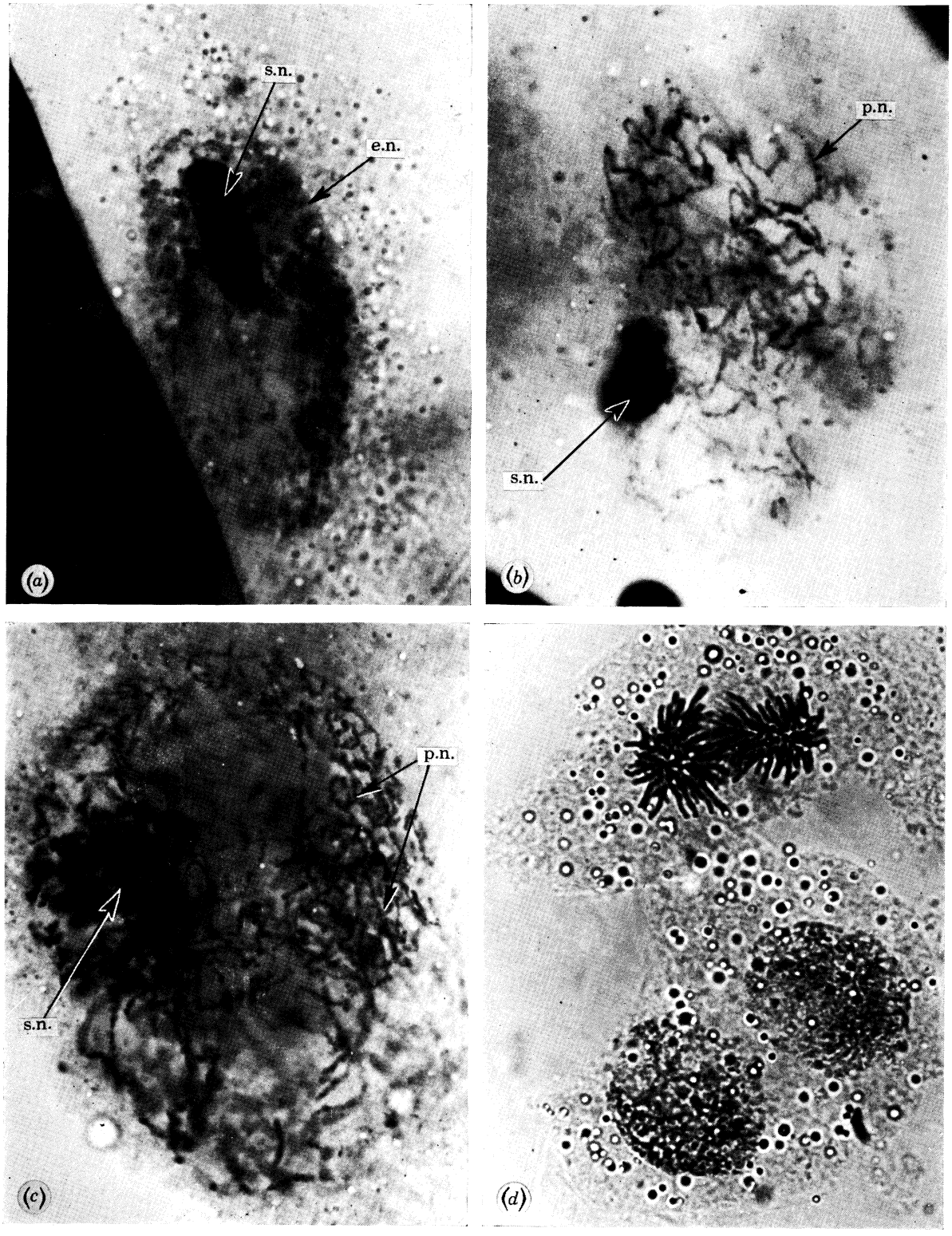

FIGURE 33. (*a*) An egg nucleus (e.n.) and a sperm nucleus (s.n.) about 3 h after pollination at 20 °C in Chinese Spring wheat (× 1320); (*b*) a polar nuclei (p.n.) and a sperm nucleus about 1 h after pollination at 20 °C in Chinese Spring wheat (× 1100); (*c*) a polar nuclei and a differentiating sperm nucleus about 3 h after pollination at 20 °C in Chinese Spring (× 1485); (*d*) typical young embryo cells from a five-celled embryo showing characteristic refractile globules in the cytoplasm (× 1210).

(*Facing p.* 70)

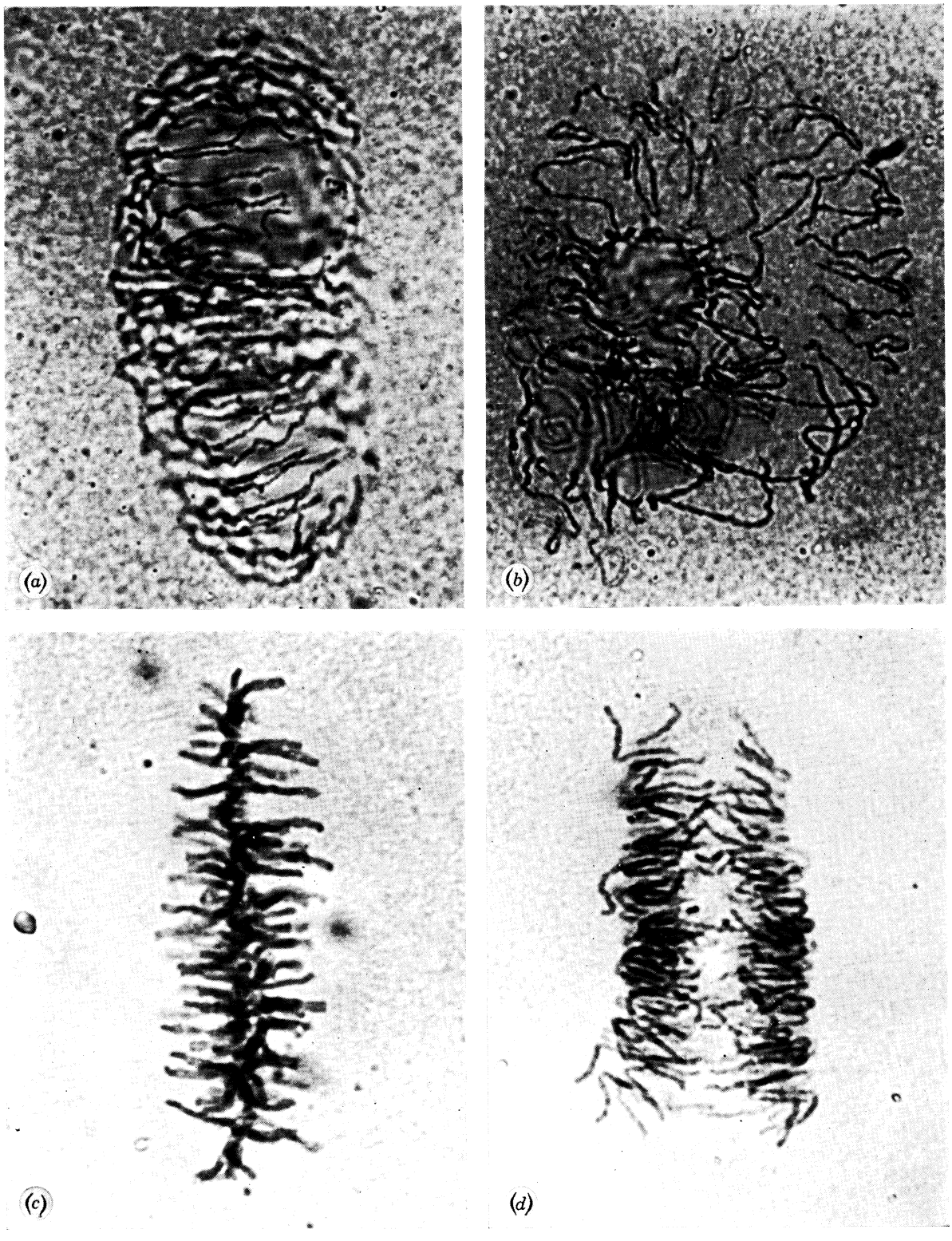

FIGURE 34. The endosperm in Chinese Spring grown at 20 °C showing: (*a*, *b*) two views of nuclei at prophase prior to the formation of a cellular endosperm (note the characteristic organization of the chromosomes and the prominent nucleoli (× 1375)); (*c*) a nucleus at metaphase (× 1705); (*d*) a nucleus at anaphase (× 1705).

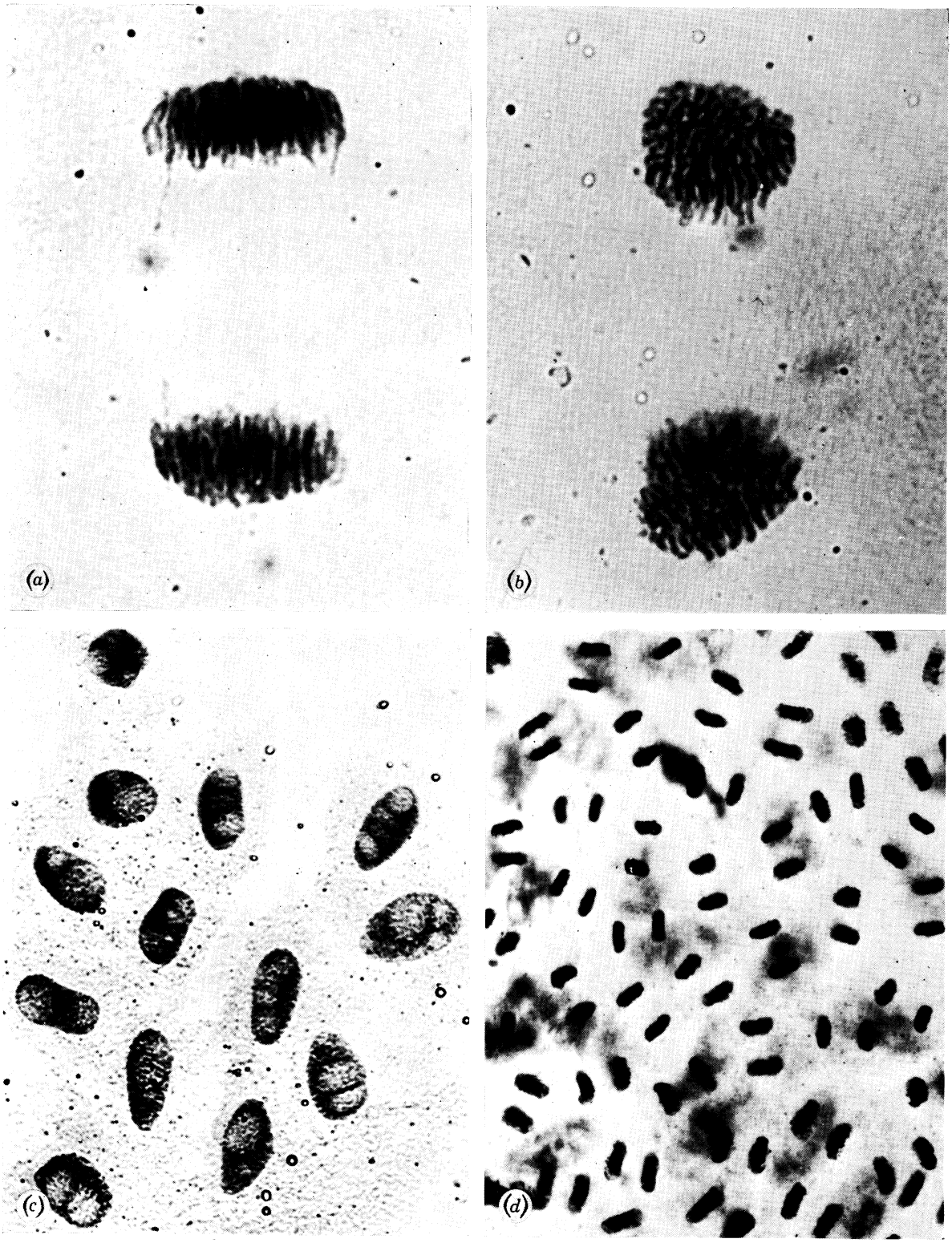

FIGURE 35. The endosperm in Chinese Spring grown at 20 °C showing: (*a*, *b*) nuclei at telophase; (*c*) interphase nuclei with several nucleoli (× 330); (*d*) synchronous mitosis in a patch of cells in an endosperm consisting of several thousand cells (× 305).

all at G_1 with 3*C* DNA contents, then nuclei at *S*-phase with values between 3*C* and 6*C*, next more nuclei at G_2 all with the 6*C* DNA amount and finally more cells at prophase of mitosis all with 6*C* amounts.

(*c*) *Early embryogeny*

According to Percival (1921) the ovum in wheat is divided into two cells by a transverse wall, and the large basal suspensor cell apparently undergoes little or no further development. Subsequently, the upper cell, from which the embryo develops, is divided by a wall parallel to the first, and then by a wall at right angles through both the cells produced, giving a five-celled embryo.

We saw several young embryos whose development conformed to the pattern described above (figures 39*a*, *b*, *d*), however, we also saw many others whose development differed from the pattern described by Percival (see figures 39*e* to *j*). For instance, although the first division in the ovum was usually transverse, two embryos were seen in which the first division was longitudinally oblique (figure 39*e*). Another embryo was seen to consist of a linear row of four cells, but only one example of this type was noted. A third embryo type had a longitudinal division in the upper cell (figure 39*f*). In the fourth and commonest type of variant development, after the second division, the central cell divided twice to give a quartet of cells before the first division occurred in the upper cell (figure 39*h*). Some embryos were seen (figures 39*i*, *j*) which showed that variant types continued to develop beyond the earliest stages just described. We cannot be certain whether all the various types of embryo develop into mature seed, but since variants constituted at least 50 % of all the embryos seen, and seed is set in up to 90 % of pollinated florets, there is probably more than one viable embryogeny in Chinese Spring.

(*d*) *The timing of early endosperm and embryo development*

(i) *Endosperm*

Early endosperm development was synchronous until about the tenth division cycle which occurred approximately 72 h after pollination in plants grown at 20 °C. Until this time the endosperm consisted of free nuclei in a common cytoplasm, but thereafter it became a cellular tissue. Until the tenth division cycle, the mean nuclear cycle time in the endosperm was calculated from counts of the number of endosperm nuclei observed in division at known intervals after fertilization. For instance, two endosperm nuclei were seen in division 11 h after pollination, that is, 5 h after division in the primary endosperm nucleus. The duration of the second division cycle was, therefore, about 5 h. (N.B. The first endosperm division cycle was taken as the time for the arrival of the sperm nucleus at the polar nuclei until division of the primary endosperm nucleus.) After the tenth division cycle, the mean endosperm cell cycle time was estimated from counts of the numbers of endosperm nuclei in ovules fixed at known intervals after pollination. Such calculations showed that the rate of division was much faster during early development than at later stages. Sixteen endosperm nuclei at mitosis were observed in an ovule fixed 24 h after pollination, that is, about 23.5 h after the arrival of the sperm nucleus in the embryo sac. The mean nuclear cycle time for the first five division cycles at 20 °C was, therefore, about 4.7 h. For the sixth to the tenth inclusive division cycles it was about 9.6 h (tables 3 and 4). After the tenth division cycle, when the endosperm consisted of about 1024 nuclei the cell cycle time suddenly became much longer, having a duration of about 16 h (table 4). This change was probably caused by the transition of the endosperm from a non-cellular to a cellular tissue, an event which occurred at the same time. By the end of the fifth

day after pollination the endosperm contained up to about 5000 nuclei on average. Development remained quite synchronous in groups of adjacent endosperm cells after it had become asynchronous in the endosperm as a whole.

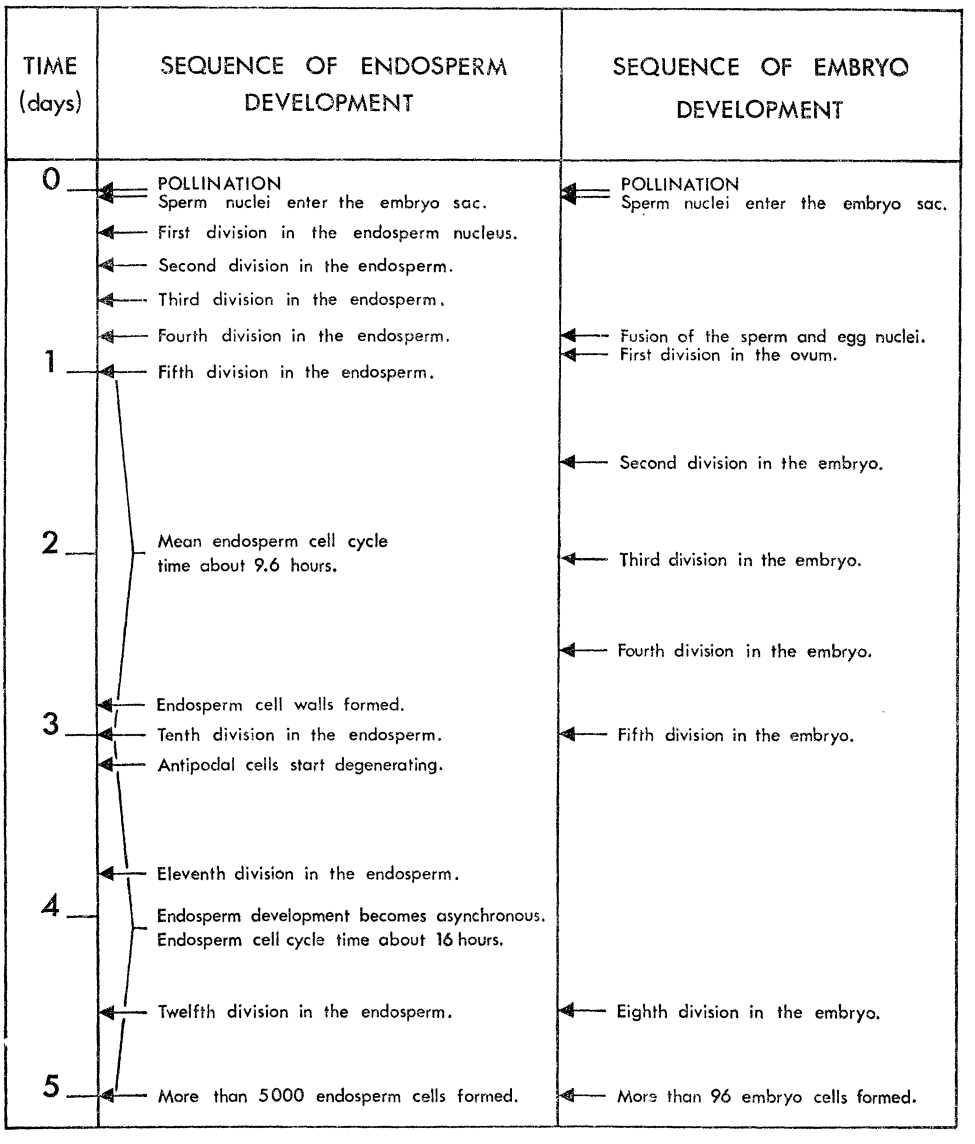

FIGURE 36. The time and sequence of early development in the embryo and endosperm of Chinese Spring wheat grown at 20 °C.

(ii) *Embryo*

The first division in the zygote occurred about 22 h after pollination in plants grown at 20 °C. The second embryo division, usually in the upper cell, occurred about 17 h after the first. The third embryo division which produced a 5-celled embryo, occurred about 55 h after pollination. A 9-celled embryo was produced about 65 h after pollination and 17- or 18-celled embryos were formed about 80 h after pollination. Ninety-six hours after pollination the sixth cell cycle in the embryo was often complete. Embryos fixed 120 h after pollination contained from about 96 to 190 cells and some nuclei had completed more than eight division cycles. The time and sequence of development in the embryo and endosperm is summarized in figure 36.

(*e*) *The relative growth of the embryo and the endosperm*

Although the sperm nucleus going to the egg reached its destination before the other sperm nucleus reached the polar nuclei, the rates of fertilization and of subsequent development were much faster in the endosperm than in the embryo. Thus at 20 °C, division occurred about 6 h after pollination in the primary endosperm nucleus but about 22 h after pollination in the zygote. At least four nuclear division cycles were completed in the endosperm before the first division in the zygote occurred, so that by 24 h after pollination, the ratio of endosperm nuclei to embryo cells was about 5:1. The number of endosperm cells remained much higher than

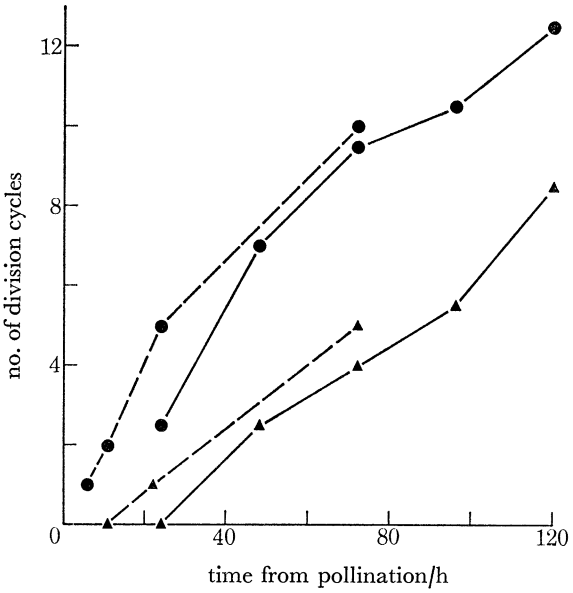

FIGURE 37. The rate of growth of the endosperm (●) and the embryo (▲) of Chinese Spring grown at 20 °C in a controlled environment cabinet (– – – –) and at 20 ± 2 °C in a glasshouse (————).

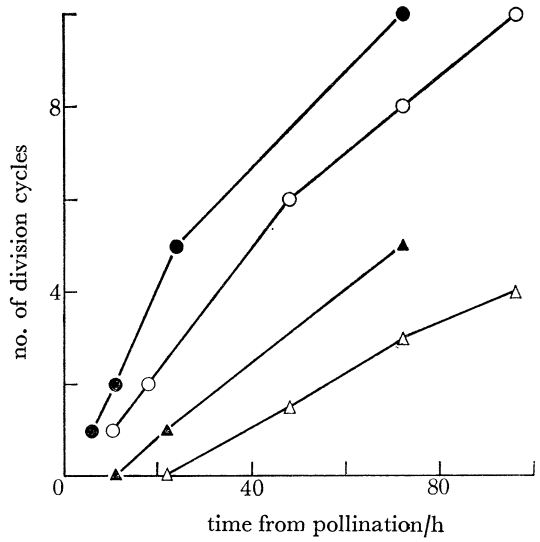

FIGURE 38. The relative growth rates of the endosperm and the embryo of Chinese Spring wheat grown at 15 and 20 °C. ●, endosperm at 20 °C; ○, endosperm at 15 °C; ▲, embryo at 20 °C; △, embryo at 15 °C.

the number of embryo cells throughout the first 5 days of seed development (figure 36) and the mean ratio of endosperm to embryo cells increased steadily (table 4). For instance, at 72 h after pollination the endosperm contained 600 to 1000 cells while the embryo contained only about 25 to 28 giving a ratio of endosperm to embryo nuclei of up to about 36:1. By the fifth day after pollination the mean ratio of endosperm cells to embryo cells was about 60:1 and the endosperm and embryo contained up to about 11000 and 190 cells respectively. In other words,

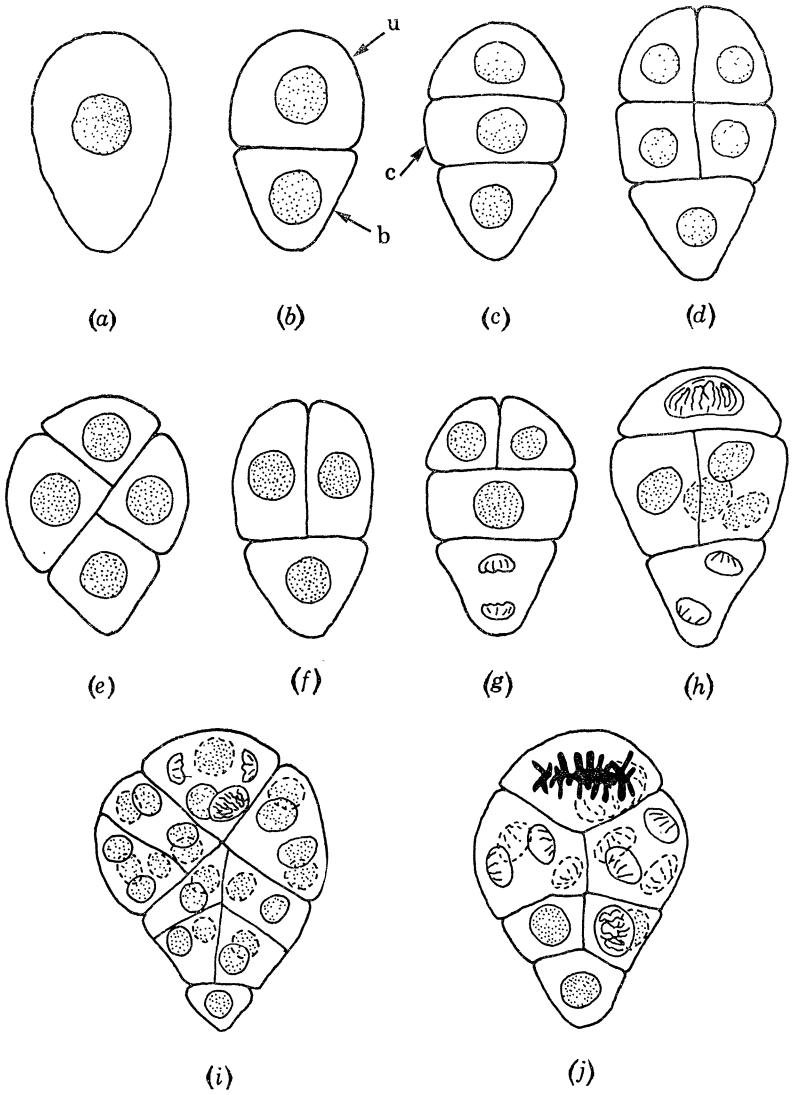

FIGURE 39. Normal and variant embryogeny in Chinese Spring wheat grown at 20 °C. (*a–d*) The sequence of early embryo development in wheat according to Percival (1921): u, upper cell; b, basal cell; c, central cell. (*e–j*) Diagrammatic illustration, of several embryos whose development differed from that described by Percival (1921). A full description of these is given in §6*c*.

by the end of the fifth day after pollination the endosperm had completed about 12.5 ± 0.5 division cycles, while the embryo had undergone only about 8.5 ± 0.5 division cycles (figure 37). Essentially similar relationships between the numbers of embryo and endosperm nuclei during the first 5 days of seed development were obtained from plants grown at 20 ± 1 °C in a controlled environment cabinet and from plants grown at 20 ± 2 °C in a glasshouse (figure 37, tables 4 to 6).

The sequence of nuclear cycle times in the endosperm differed considerably from that seen in the embryo. In the endosperm the nuclear cycle time from the first until the fifth division remained fairly constant at about 4.5 h, but subsequently it became increasingly long, until about the twelfth division cycle it was about 18 h. In the embryo, however, the early cell cycles from the first division until the fifth division had a mean duration of about 12.5 h in plants grown at 20 °C in a growth cabinet (table 6). The data for plants grown in the glasshouse (table 4) show that successive cell cycles in the embryo may be decreasing from about 19 h (the second embryo cell cycle) to less than 10 h (by the eighth embryo cell cycle).

TABLE 4. THE NUMBER OF DIVISION CYCLES AND THE MEAN DIVISION CYCLE TIME IN THE ENDOSPERM AND THE EMBRYO OF CHINESE SPRING GROWN AT 20 ± 2 °C IN A GLASSHOUSE.

The ratio of the number of endosperm cells to the number of embryo cells is also given at 1–5 days after anthesis.

	endosperm		embryo		
time after anthesis (h)	no. of division cycles	mean division cycle time (h)	no. of division cycles	mean division cycle time (h)	mean ratio of embryo endosperm cell numbers
24	2.5 ± 0.5	9.6	—	19.2	5:1
48	7.0 ± 1.0	5.3	2.5 ± 0.5		25:1
72	9.5 ± 0.5	9.6	4.0	16.0	36:1
96	10.5 ± 0.5	16.0	5.5 ± 0.5	16.0	44:1
120	12.5 ± 0.5		8.5 ± 0.5	8.0	60:1

(*f*) *Changes in nuclear and cell size in the developing embryo*

A comparison of embryos with from 5 to 25 cells, showed that cell and nuclear volume decreased as the number of embryo cells increased. A 5-celled embryo was 139 μm long and 89 μm wide, while a 25-celled embryo was 141 μm long and 99 μm wide. Thus, the total size of the embryo increased very little while the number of embryo cells increased fivefold. Consequently, the mean cell volume in the 25-celled embryo was about 20 to 25 % of the mean cell volume in the 5-celled embryo. Similarly, in the 5-celled embryo, the mean volume of two prophase nuclei was about 23×10^3 μm³, while in a 10-celled embryo the mean volume of two prophase nuclei was 7.1×10^3 μm³, and in the 25-celled embryo the mean volume of three prophase nuclei was 3.8×10^3 μm³. Thus, the mean volume of prophase nuclei was only about one-sixth as much in the 25-celled embryo as in the 5-celled embryo.

The cell cycle time apparently decreased from about 19.0 h to less than 10.0 h as the number of embryo cells increased from 1 to about 190 during early embryo development. It would be interesting if the developmental behaviour of the young embryo were the reverse of that already noted in the developing archesporium where the cell cycle time increased with successive divisions as cell volume increased, since then in both instances cell cycle time would be positively correlated with cell size.

(*g*) *The effect of temperature on fertilization time and early seed development*

Meiosis in Chinese Spring wheat has a Q_{10} of 2.3 (see §3*a*) over the temperature range 15 to 25 °C. It would be interesting to know whether temperature has a similar relationship to pollination time and the rates of endosperm and embryo development as it does to meiotic time. The above experiments were repeated at 15 °C and the development timed until the tenth division cycle in the endosperm tissue was completed. The results (table 5, figure 38) show that

at 15 °C the sequence of development was similar to that observed at 20 °C. The rate of development, however, was much slower at 15 °C than at 20 °C. Thus, the pollen tube grew down the style and discharged the male nuclei into the embryo sac within about 70 min at 15 °C compared with 41 min at 20 °C. Similarly, the first division in the endosperm nucleus occurred about 10.5 h after pollination at 15 °C compared with 6 h after pollination at 20 °C (and about 5 h after pollination at 23 °C). In plants grown at 15 °C the tenth division in the endosperm occurred at about 96 h after pollination while in plants grown at 20 °C the tenth division in the endosperm occurred at about 72 h after pollination. In Chinese Spring wheat meiosis lasted 24 h at 20 °C and 42 h at 15 °C (Bennett *et al.* 1972), that is, 1.75 times longer at

TABLE 5. THE EFFECT OF TEMPERATURE ON THE RATE OF EARLY ENDOSPERM DEVELOPMENT IN CHINESE SPRING GROWN AT 15 AND 20 °C

	20 °C		15 °C		
stage of development	time after pollination (h)	mean division cycle time (h)	time after pollination (h)	mean division cycle time (h)	expected time at 15 °C (h)
arrival of ♂ nucleus at polar nucleus	0.7	5.3	1.2	9.3	1.2
					9.3
1st division of endosperm nucleus	6.0	4.5	10.5	7.5	7.8
2nd division in endosperm	11.0		18.0		
5th division in endosperm	24.0		—	7.5	7.8
6th division in endosperm	—	9.6	48.0		
8th division in endosperm	—		72.0	12.0	16.8
10th division in endosperm	72.0		96.0		

TABLE 6. THE NUMBER OF DIVISION CYCLES AND THE MEAN DIVISION CYCLE TIME IN THE EMBRYO OF CHINESE SPRING GROWN AT 15 AND 20 °C IN A GROWTH CABINET

	20 °C		15 °C	
time after pollination (h)	no. of division cycles	mean division cycle time (h)	no. of division cycles	mean division cycle time (h)
11	< 1.0	—	< 1.0	
22	1.0	22.0	< 1.0	32.0
48	—	12.5	1.5 ± 0.5	24.0
72	5.0	—	3.0	24.0
96	—	—	4.0	

15 °C than 20 °C. To test whether the effect of temperature on pollination and early seed development is similar to its effect on meiosis, the observed times for pollination and endosperm development at 20 °C were multiplied by 1.75 to give 'expected times'. These expected times were then compared with the observed times obtained at 15 °C (table 5). Up until about the fifth endosperm division cycle there is very good agreement between the 'expected' and the obtained results. For instance, the expected fertilization time at 15° C is 72 min and the observed time was 70 min. Similarly, the expected mean endosperm cell cycle time for the first four division cycles is 7.8 h while the observed mean was 7.5 h. After the fifth endosperm division cycle the observed endosperm cell cycle times were shorter than the expected times (table 5).

(*h*) *Discussion*

The timing of pollination and subsequent embryo development deduced from our results differs greatly from that given by Percival (1921). For instance, Percival stated that the pollen tube did not appear until about 1.5 to 2 h after pollination, whereas in the present work both male gametes had entered the embryo sac by 41 min after pollination in Chinese Spring at 20 °C. Similarly, Percival stated that fusion of the sperm nucleus with the egg occurred at between 30 and 40 h after pollination, whereas in our material it occurred not more than about 20 to 22 h after pollination. Lastly, Percival noted that the embryo was 10 to 15 celled, 8 to 10 days after pollination, while in our material it had reached this stage not more than 3 days after pollination. The differences between our results and those reviewed by Percival (1921) could be due to intervarietal variation or to different temperatures for the two experiments. Percival, unfortunately, did not state the temperature at which he made his observations.

Our results show considerable agreement with those obtained in more recent studies. D'Souza (1970), working on the wheat variety Koga II grown at 20 ± 2 °C with a 16 h day, noted that pollen started to germinate about 15 min after pollination. Furthermore, pollen viability fell to 0 % by 45 min after dehiscence in air with 40 % relative humidity. The time for the start of growth of the pollen tube given by Percival must, therefore, be in some doubt, since growth begins much sooner in Koga II (D'Souza 1970), Norin 26 (Hoshikawa 1960) and Chinese Spring wheat, in rye and Triticale (D'Souza 1970), in barley (Pope 1944) and in wheat/rye crosses (Zeven & Heermert 1970). It is even doubtful that low temperature could be responsible for such slow development as Percival reported since in Norin 26 wheat the pollen tube penetrated the embryo sac 2 h after pollination at 10 °C and in barley penetration only took 2.3 h at 5 °C (Hoshikawa 1960).

The present result indicates that the effect of temperature on the time for penetration of the pollen tube into the embryo sac was similar to its effect on meiotic duration. This is also supported by data for penetration time in Norin 26 wheat (Hoshikawa 1960). In this variety penetration occurred at 120, 30 and 15 min at temperatures of 10, 20 and 30 °C respectively. Penetration time had a Q_{10} of about 2.8 in Norin 26 over the range 10–30 °C, compared with a Q_{10} of about 2.3 for meiotic time and penetration time in Chinese Spring over the temperature range 15 to 25 °C. In barley, a similar Q_{10} about 2.0 for penetration time, was found for the temperature range 10 to 30 °C (Pope 1937).

Our observation that the division in the primary endosperm nucleus occurred at about 6 h after pollination agrees with Hoshikawa's work (1959) on Norin 50 and 67 wheat grown at 20 °C with constant light and 85 % relative humidity. Similar results were recorded for barley grown at about 27 °C where a primary endosperm nucleus was seen at prophase 6 h after pollination (Pope 1944), and for *Elymus virginicus* grown in the field where the primary endosperm nucleus divided about 6 h after pollination (Beaudry 1951).

It is generally agreed that in wheat (Percival 1921), in barley (Pope 1944) and other grasses (Beaudry 1951), division of the primary endosperm nucleus occurs earlier than division in the zygote.

7. General discussion

The present work is a comprehensive and integrated study in a higher plant of the dynamic development of reproductive tissues. The period studied lasted 3 weeks and involved up to 20 inclusive nuclear division cycles. The importance of the work is twofold. *First*, it allows comparisons to be made between the behaviour of reproductive cells in those animals which have been intensively studied and in a higher plant species. *Second*, the availability of a detailed description of what is 'normal' for reproductive development in Chinese Spring opens the way for comparative studies with the wide range of mutant or chromosomally different genotypes of Chinese Spring and other wheat forms which are available, and which vary considerably in their behaviour during reproductive development (Sears 1954; Kempanna 1963; Riley, Chapman & Belfield 1966). It seems reasonable to hope that studies of premeiotic development will lead to increased understanding of the causal sequence of nuclear and cellular characters which directly or indirectly control chromosome pairing (Bayliss & Riley 1972*a*; Dover & Riley 1972). Similarly, studies of both pollen and embryo sac development may lead to the development of techniques for producing haploid plants (Bennett & Hughes 1972; Oram 1971) in wheat.

The development studied in the present work covers a wide range of nuclear conditions and types of cellular organisation. These are briefly considered below with respect to: (*a*) rate of cell or nuclear development; (*b*) nuclear and cell volume; (*c*) nuclear ploidy level; (*d*) male and female reproductive development.

(*a*) *The rate of cell or nuclear development*

The rate of cell or nuclear development at 20 °C was very variable. Nuclear cycle times ranged from about 60 h in the microspore to only about 4.5 h in the endosperm. Cell cycle times in diploid cells ranged from about 55 h in some male archesporial cells to about 9 h in some embryo cells. In haploid nuclei the cycle times range from about 60 h in the microspore to about 12 h for some nuclei in the embryo sac. It was previously noted (Bennett & Smith 1972) that male premeiotic, meiotic and postmeiotic development comprised cell cycles with extremely long durations compared with the cell cycle time in somatic root-tip meristem cells which lasts about 12.5 h at 20 °C. Possible explanations for this slow development have been discussed previously (Bennett & Smith 1972).

(*b*) *Nuclear and cell volume*

Chromosome and nuclear volume vary considerably between normal diploid somatic cells within the same organism, and such variation often reflects real differences in RNA and protein content (Bennett 1970). The range of nuclear volumes noted in the present study is much larger than the range of nuclear sizes previously detected in root-tip and shoot-apex meristem cells of several higher plant species. Thus, the volume of nuclei containing the 4*C* nuclear DNA amount ranged from about 23×10^3 μm^3 in some embryo cells to less than 1×10^3 μm^3 in some somatic cells in the tapetum and nucellus. Even greater extremes of size are found if nuclei at different ploidy levels are compared. For instance, the volume of a haploid sperm nucleus was about 240 μm^3 while the volume of some antipodal cell nuclei reached about 160×10^3 μm^3. Furthermore, the mean density of DNA is very variable between nuclei ranging from 0.15 pg/μm^3 in the sperm nucleus, to 0.0025 pg/μm^3 in an unfertilized egg.

The wheat nucleus exists in several widely different conditions. Comparison of the complex and different types of nuclear and chromosomal structure in, for instance, the metabolically inactive and dense haploid sperm nucleus, the normal somatic diploid nucleus, the triploid endosperm nucleus, the meiotic nucleus, and the highly polyploid antipodal cell nucleus reveals a remarkable diversity of nuclear and chromosomal architecture. This diversity emphasizes how little is understood of how 'function modifies form' with respect to the internal organization of the chromosome itself, or of the chromosomes within the nucleus. In both male and female cell lines the transition from sporophyte to gametophyte, and later the reverse transition, was marked by sudden changes in nuclear organization. In the gametophytes too, both the rate at which nuclear characters changed, and the range of very different nuclear types seen among a few nuclei, illustrates the impressive plasticity of higher plant nuclei.

It was noted in the present work that cell cycle time in male archesporial cells increased with successive cell cycles as meiosis was approached, and that this phenomenon was accompanied by a gradual increase in nuclear and cell volume. Similarly, in the young embryo, the cell cycle time apparently decreased during successive cell cycles while nuclear and cell size decreased. Van't Hof & Sparrow (1963) demonstrated a positive relationship between nuclear volume and cell cycle time in comparisons of unrelated diploid species. This, together with the present intraspecific instance of a similar correlation between nuclear volume and cell cycle time re-emphasizes the important role of nucleotypic characters (Bennett 1971) in relation to the rate of cell development.

(*c*) *Nuclear ploidy level*

Nuclear cycle times have been estimated for haploid, diploid and triploid nuclei in the present work, and nuclear cycles observed in antipodal nuclei with between 1*C* and 200 *C* DNA amounts. There has been a considerable discussion about the effects of increased nuclear DNA content on cell cycle time in polyploids (Palitti, Rocchi, Mercanti & Olivieri 1972). Examples are cited in which the cell cycle time in polyploids is longer than (Evans, Rees, Snell & Sun 1970), the same as (Yang & Dodson 1970) and shorter than (Gupta 1969) that in related diploid species. Comparison of the duration of meiosis in all types of polyploid species with its duration in related diploid species has consistently shown that the duration of meiosis decreased with increasing ploidy level (Bennett & Smith 1972; Finch & Bennett 1972; Bennett 1973). It is interesting to note, therefore, that in the present work the fastest cell cycle at 20 °C occurred in nuclei with the highest ploidy level, that is in endosperm nuclei. Furthermore, the minimum cell cycle time for haploid (embryo sac), diploid (embryo) and triploid (endosperm) nuclei were about 12.0, 9.0 and 4.5 h respectively. These results show that in somatic cells, as previously found in meiotic cells, the minimum cell cycle time decreased with increasing ploidy level. Thus, an increase in nuclear DNA content which results from an increase in ploidy level does not necessarily increase the duration of the cell cycle. This conclusion is supported by the behaviour of antipodal cell nuclei (figure 37) which showed no proportional increase in nuclear cycle time over the first seven cycles of endo-reduplication despite the vast increase in nuclear DNA content resulting from their high level of polyploidy.

(*d*) *Male and female reproductive development*

Since the duration of male and female meiosis in Chinese Spring wheat are very similar, it has been concluded that the rates of meiosis in p.m.cs and e.m.cs are both subject to similar nucleotypic control (Bennett *et al.* 1973). Not only do male and female meiosis both have similar durations, but, they occur almost synchronously within individual florets. It was noticeable, however, in the present work that the nuclear cycle times for haploid embryo sac nuclei were on average much shorter than for haploid nuclei in the microspore. It is clear, therefore, that the prolonged nuclear cycle times in the microspore are not caused by the haploid condition of the nuclei involved. It is suggested that the long microspore cell cycle times are an adaptive feature ensuring that the microspores mature concurrent with the onset of stigmatic receptiveness and embryo sac maturity ready for fertilization. Fertilization involving male and female gametes produced within a single floret is common in wheat and is obviously advantageous to this inbreeding species.

References

Avivi, L., Feldman, M. & Bushuk, W. 1970 The mechanism of somatic association in common wheat, *Triticum aestivum* L. III. Differential affinity for nucleotides. *Genetics* **66**, 449–461.

Banerjee, U. C. 1967 Ultrastructure of the tapetal membranes in grasses. *Grana palynol.* **7**, 365–377.

Bayliss, M. W. 1972 An analysis of meiosis in *Triticum aestivum*. Ph.D. thesis. University of Cambridge.

Bayliss, M. W. & Riley, R. 1972*a* Evidence of pre-meiotic control of chromosome pairing in *Triticum aestivum*. *Genet. Res. Camb.* **20**, 201–212.

Bayliss, M. W. & Riley, R. 1972*b* An analysis of temperature dependant asynapsis in *Triticum aestivum*. *Genet. Res. Camb.* **20**, 193–200.

Beaudry, J. R. 1951 Seed development following the mating *Elymus virginicus* L. × *Agropyron repens* (L) Beauv. *Genetics* **36**, 109–133.

Bennett, M. D. 1970 Natural variation in nuclear characters of meristems in *Vicia faba*. *Chromosoma* **29**, 317–335.

Bennett, M. D. 1971 The duration of meiosis. *Proc. R. Soc. Lond.* B **178**, 277–299.

Bennett, M. D. 1973 The duration of meiosis. In *British Society for developmental biology Symposium*, The cell cycle in development and differentiation (eds. M. Balls & F. S. Billet). Cambridge University Press.

Bennett, M. D., Chapman, V. C. & Riley, R. 1971 The duration of meiosis in pollen mother cells of wheat, rye and *Triticale*. *Proc. R. Soc. Lond.* B **178**, 259–275.

Bennett, M. D., Finch, R. A., Smith, J. B. & Rao, M. K. 1973 The time and duration of female meiosis in wheat, rye and barley. *Proc. R. Soc. Lond.* B **183**, 301–319.

Bennett, M. D. & Hughes, W. G. 1972 Additional mitosis in wheat pollen induced by Ethrel. *Nature, Lond.* **240**, 566–568.

Bennett, M. D. & Smith, J. B. 1972 The effect of polyploidy on meiotic duration and pollen development in cereal anthers. *Proc. R. Soc. Lond.* B **181**, 81–107.

Bennett, M. D., Smith, J. B. & Kemble, R. 1972 The effect of temperature on meiosis and pollen development in wheat and rye. *Can. J. Genet. Cytol.* **14**, 615–624.

Bird, A. P. & Birnstiel, M. L. 1971 A timing study of DNA amplification in *Xenopus laevis* oocytes. *Chromosoma* **35**, 300–309.

Bonnet, O. T. 1966 Inflorescences of maize wheat, rye, barley and oats. Their initiation and development. *Bull. Ill. agric. Exp. Stn* no. 721.

Callan, H. G. 1972 Replication of DNA in the chromosomes of eukaryotes. *Proc. R. Soc. Lond.* B **181**, 19–41.

Coggins, L. N. & Gall, J. G. 1972 The timing of meiosis and DNA synthesis during early oogenesis in the toad *Xenopus laevis*. *J. Cell Biol.* **52**, 569–576.

Conger, A. D. & Fairchild, M. 1953 A quick freeze method for making smear slides permanent. *Stain Technol.* **28**, 281–283.

Crone, M., Levy, E. & Peters, H. 1965 The duration of premeiotic DNA synthesis in mouse oocytes. *Expl Cell Res.* **39**, 668–688.

De Vries, A. P. 1971 Flowering biology of wheat particularly in view of seed production – a review. *Euphytica* **20**, 152–170.

Dover, G. A. & Riley, R. 1973 The effect of spindle inhibitors applied before meiosis on meiotic chromosome pairing. *J. Cell. Sci.* **12**, 143–161.

D'Souza, L. 1970 Untersuchungen über die Eignung des Weizens als Pollenspender bei der Fremdbefruchtung, verglichen mit Roggen, Triticale und Secalotricum. *Z. PflZücht.* **63**, 246–269.

Evans, G. M., Rees, H., Snell, C. L. & Sun, S. 1970 The relation between nuclear DNA amount and the duration of the mitotic cell cycle. In *Chromosomes today*, **3**, 24–31.

Feldman, M., Mello-Sampayo, T. & Sears, E. R. 1966 Somatic association in *Triticum aestivum*. *Proc. natn Acad. Sci. U.S.A.* **56**, 1192–1199.

Finch, R. A. & Bennett, M. D. 1972 The duration of meiosis in diploid and autotetraploid barley. *Can. J. Genet. Cytol.* **14**, 507–515.

Ghosal, S. K. & Mukherjee, B. B. 1971 The chronology of DNA synthesis, meiosis and spermiogenesis in the male mouse and golden hamster. *Can. J. Genet. Cytol.* **13**, 672–682.

Gillies, C. B. 1972 Reconstruction of the *Neurospora crassa* pachytene karyotype from serial sections of synaptonemal complexes. *Chromosoma* **36**, 119–130.

Gupta, S. B. 1969 Duration of mitotic cycle and regulation of DNA replication in *Nicotiana plumbaginifolia* and a hybrid derivate of *N. tabacum* showing chromosome instability. *Can. J. Genet. Cytol.* **11**, 133–142.

Henderson, S. A. 1969 Chiasma localisation and incomplete pairing. In *Chromosomes today* **2**, 56–60 (eds C. D. Darlington & K. R. Lewis). Edinburgh: Oliver and Boyd.

Heslop-Harrison, J. 1969 An acetolysis-resistant membrane investing tapetum and sporogenous tissue in the anthers of certain Compositae. *Can. J. Bot.* **47**, 541–542.

Hoshikawa, K. 1959 Cytological studies of double fertilization in wheat (*Triticum aestivum* L.). *Proc. Crop Sci. Soc. Japan* **28**, 143–146.

Hoshikawa, K. 1960 Studies on the pollen germination and pollen tube growth in relation to fertilization in wheat. *Proc. Crop Sci. Soc. Japan* **29**, 333–336.

John, B. & Lewis, K. R. 1965 In *The meiotic system*. Protoplasmatologia, VI. New York: Springer Verlag.

Kasha, K. J. & Burnham, C. R. 1963 The location of interchange break-points in barley. II. Chromosome pairing and the intercross method. *Can. J. Genet. Cytol.* **7**, 620–632.

Kempanna, C. 1963 Investigation into the genetic regulation of chromosome behaviour in *Triticum aestivum* L. Thesis, University of Cambridge.

Kofman-Alfaro, S. & Chandley, A. C. 1970 Meiosis in the male mouse. An autoradiographic investigation. *Chromosoma* **31**, 404–420.

Law, C. N. 1968 Genetic analysis using inter-varietal chromosome substitutions. *Proc. 3rd int. Wheat Genet. Symp. Canberra*, pp. 331–342. Canberra: Australian Academy of Science.

Maheshwari, P. 1950 *An introduction to the embryology of angiosperms*. New York: McGraw-Hill.

McLeish, J. & Sunderland, N. 1961 Measurements of deoxyribonucleic acid (DNA) in higher plants by Feulgen photometry and chemical methods. *Expl Cell Res.* **24**, 527–540.

Monesi, V. 1962 Autoradiographic study of DNA synthesis and the cell cycle in spermatogonia and spermatocytes of mouse testis using tritiated thymidine. *J. Cell Biol.* **14**, 1–18.

Morrison, J. W. 1955 Fertilization and post fertilization development in wheat. *Can. J. Bot.* **33**, 168–176.

Oram, R. N. 1972 Apomixis in wheat. *Australian wheat newsletter.*

Palitti, F., Rocchi, A., Mercanti, A. & Olivieri, G. 1972 Chromosome studies on polyploid cell strains of Chinese Hamster. IV. Duration of the mitotic cell cycle. *Caryologia* **25**, 365–371.

Percival, J. 1921 In *The wheat plant*. London: Duckworth and Co.

Pope, M. N. 1944 Some notes on technique in barley breeding. *J. Hered.* **35**, 99–111.

Ramanna, M. S. & Mutsaerts, M. C. A. 1971 Unusual behaviour of growing pollen tubes in the styles and ovules of *Spinacia oleracea* L. *Euphytica* **20**, 145–151.

Riley, R. 1960 The diploidisation of polyploid wheat. *Heredity* **15**, 407–429.

Riley, R., Chapman, V. & Belfield, A. M. 1966 Induced mutation affecting the control of meiotic chromosome pairing in *Triticum aestivum*. *Nature, Lond.* **211**, 368–369.

Riley, R., Chapman, V. & Johnson, R. 1968 The incorporation of alien disease resistance in wheat by genetic interference with the regulation of meiotic chromosome synapsis. *Genet. Res.* **12**, 199–219.

Sears, E. R. 1954 The aneuploids of common wheat. *Bull. Mo. agric. Exp. Stn* no. 572.

Van't Hof, J. & Sparrow, A. H. 1963 A relationship between DNA content, nuclear volume, and minimum mitotic cycle time. *Proc. natn. Acad. Sci. U.S.A.* **49**, 897–902.

Wettstein, R. & Sotelo, J. R. 1967 Electron microscope serial reconstruction of the spermatocyte. I. Nucleus at pachytene. *J. Microsc.* **6**, 557–576.

Wimber, D. E. & Prensky, W. 1963 Autoradiography with meiotic chromosomes of the male newt *Triturus viridescens* using ^{3}H thymidine. *Genetics* **48**, 1731–1738.

Wollam, D. A. M., Ford, E. H. R. & Millen, J. W. 1966 The attachment of pachytene chromosomes to the nuclear membrane in mammalian spermatocytes. *Expl Cell Res.* **42**, 657–661.

Yang, D. P. & Dodson, E. O. 1970 The amounts of nuclear DNA and the duration of DNA synthesis period (*S*) in related diploid and autotetraploid species of oats. *Chromosoma* **31**, 309–320.

Zeven, A. C. & Heermert, C. van. 1970 Germination of pollen of *S. segetale* on *T. aestivum* stigmas and growth of pollen tubes. *Euphytica* **19**, 175–179.

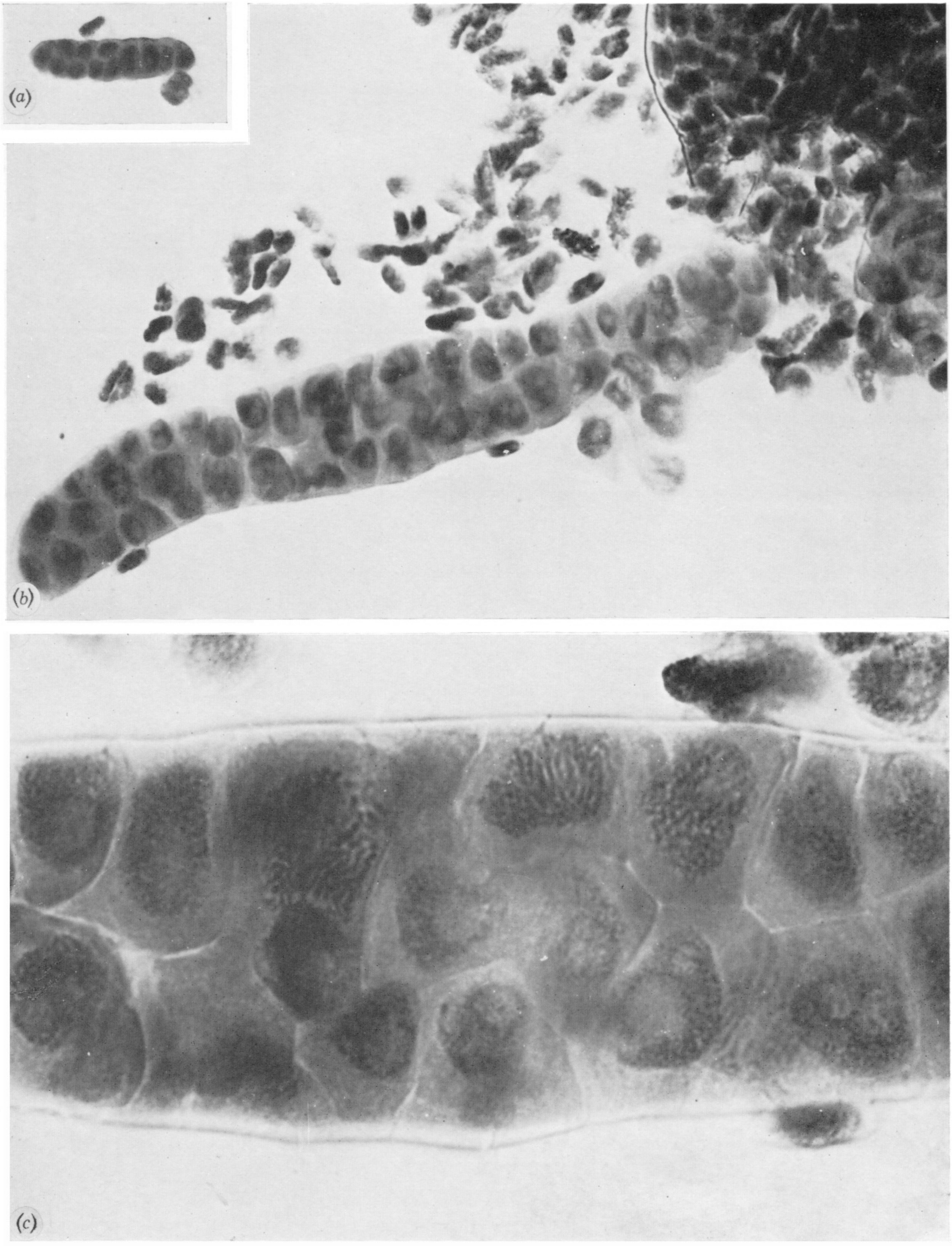

FIGURE 7. Complete archesporial columns extruded from loculi of anthers containing (*a*) 12 archesporial cells and (*b*) about 70 cells. (Magn. × 375.) In (*c*), which is a detailed view of part of the column in (*b*), premeiotic archesporial cells including several at prophase are seen. (Magn. × 1230.)

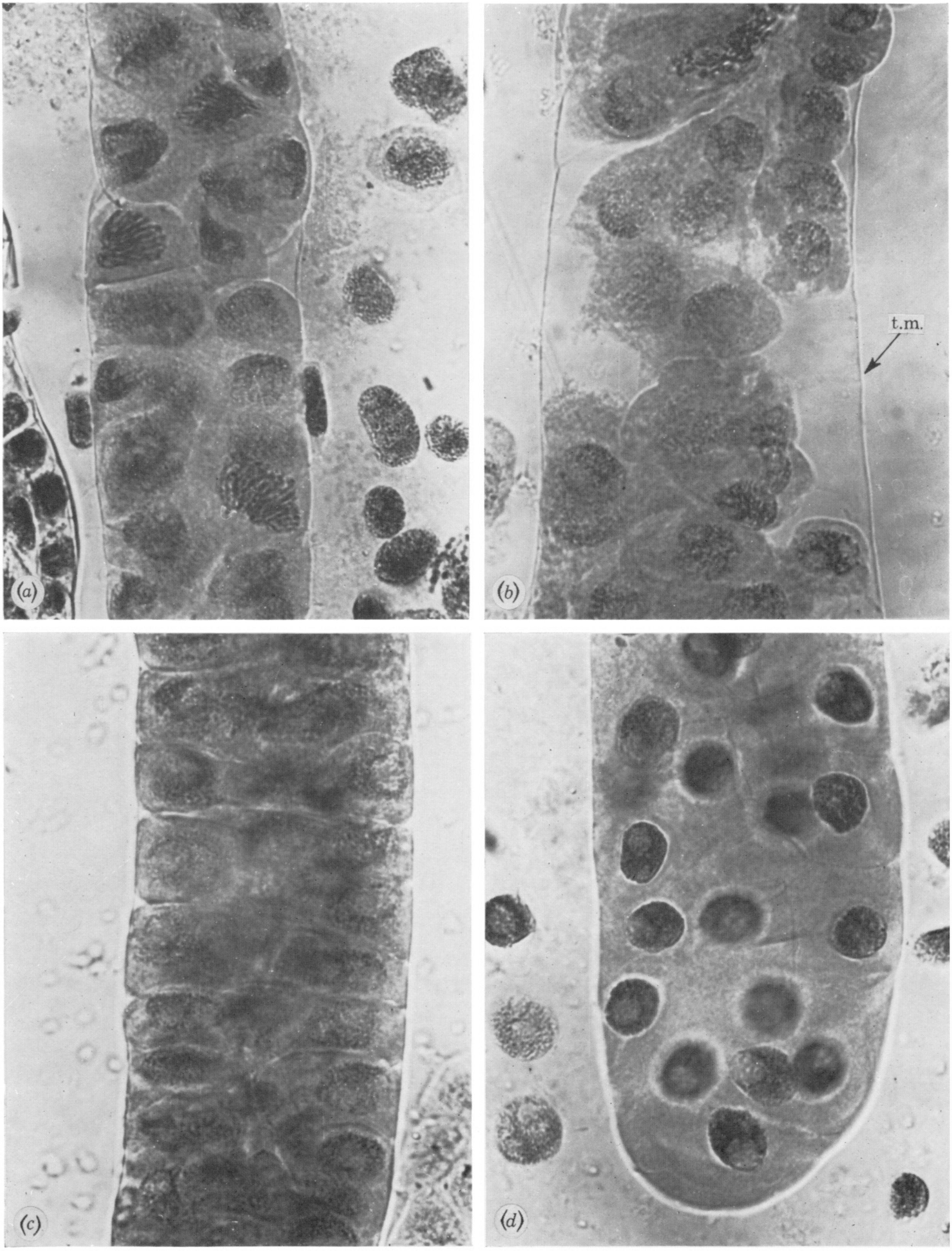

FIGURE 8. Detailed views of parts of extruded columns of archesporial cells containing aceto-carmine stained nuclei at premeiotic mitosis (*a*, *b*), stage 1 of premeiotic interphase (*c*) and stage 2 or premeiotic interphase (*d*). In (*b*), which shows the effect of gentle heating, the tapetal membrane (t.m.) is clearly visible. (Magn. × 815.)

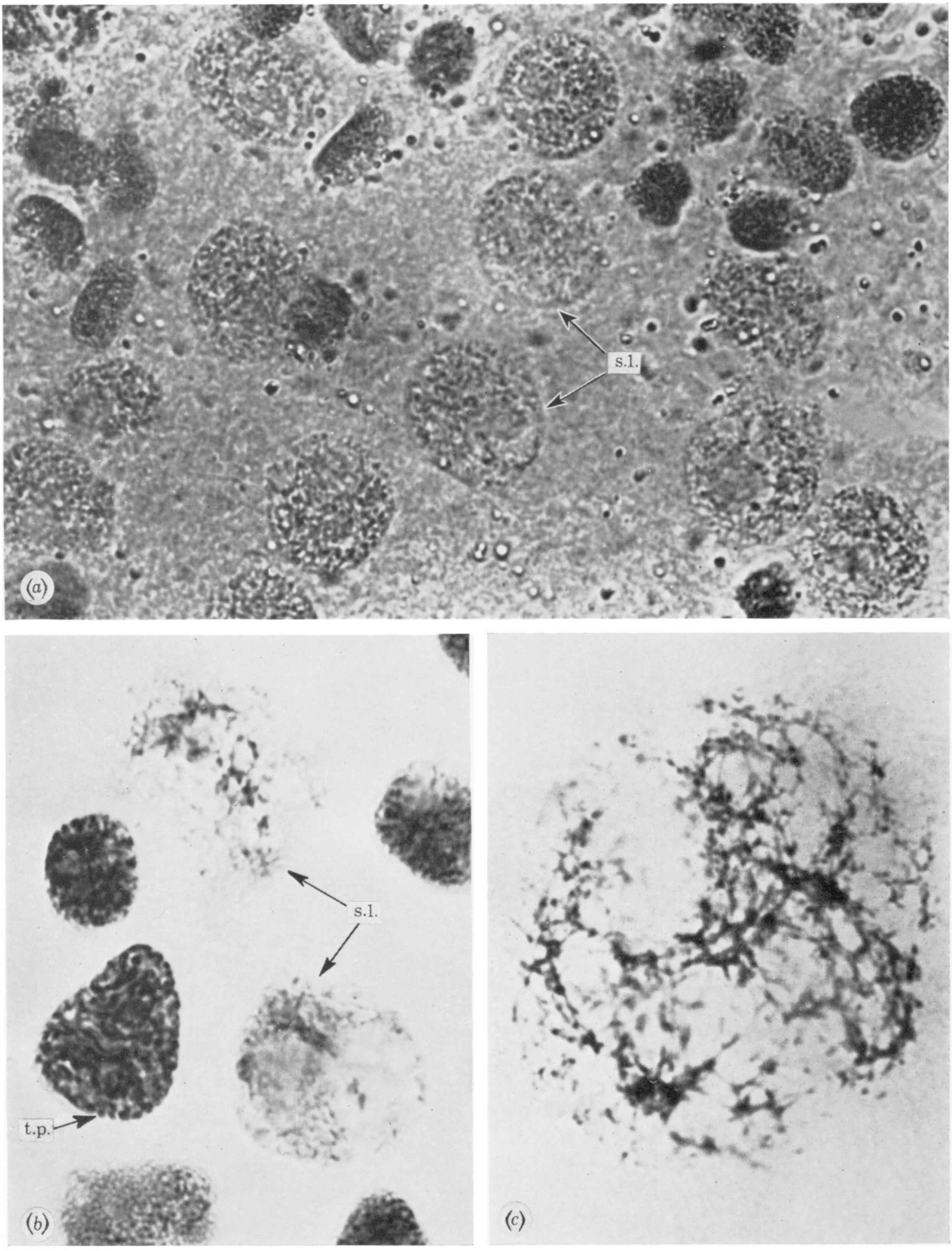

FIGURE 9. Nuclei at stage 1 (s.1) of premeiotic interphase stained using (*a*) aceto-carmine (× 1055), (*b*) the normal Feulgen method (× 825) and (*c*) the modified Feulgen method (× 3190). A tapetal nucleus at prophase (t.p.) is also included for comparison in (*b*).

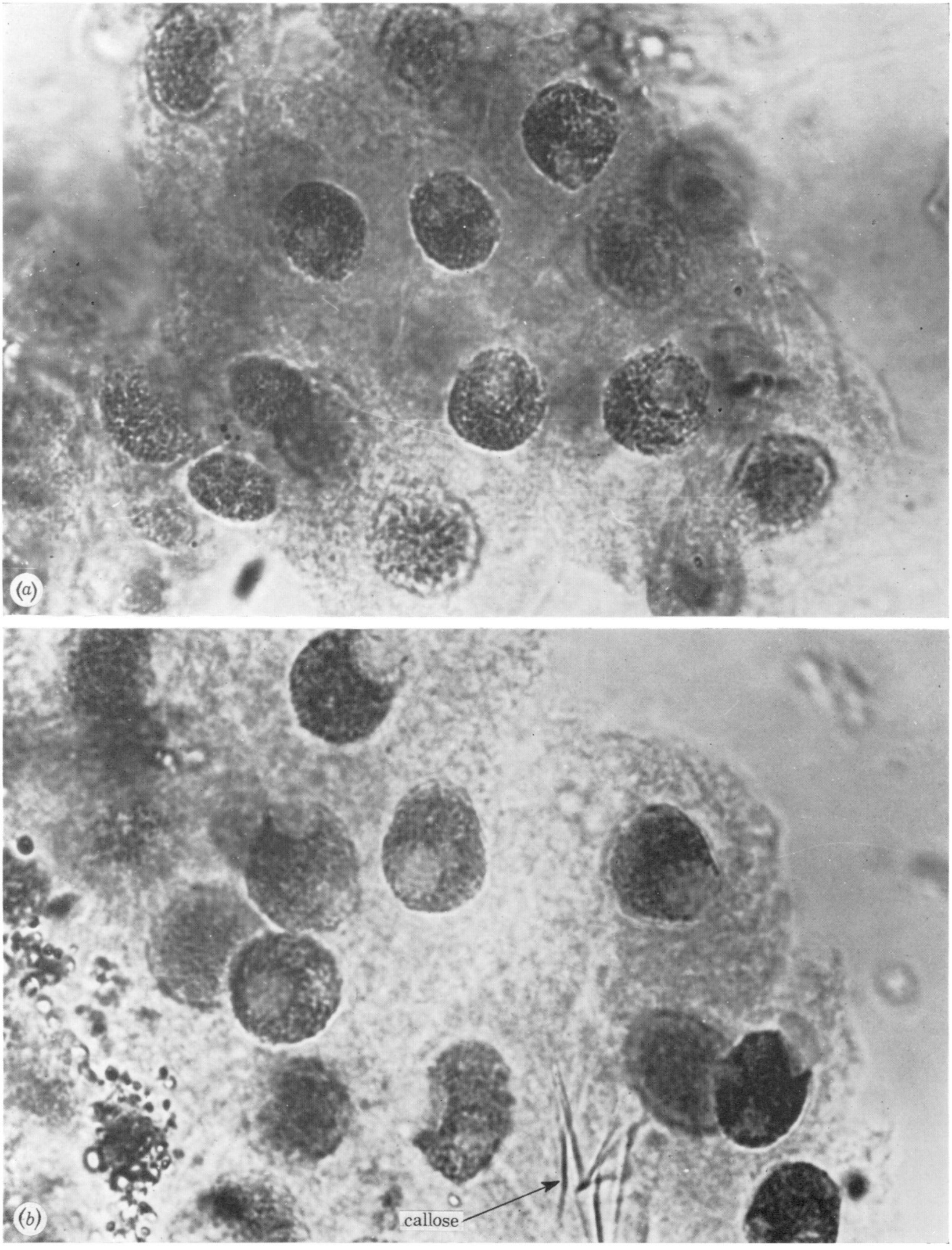

FIGURE 10. Nuclei at stage 2 (*a*) and early stage 3 (*b*) of premeiotic interphase seen in aceto-carmine stained anther squashes. (Magn. × 1145.) Note the migration of the nucleolus to the nuclear periphery and the presence of callose in (*b*).

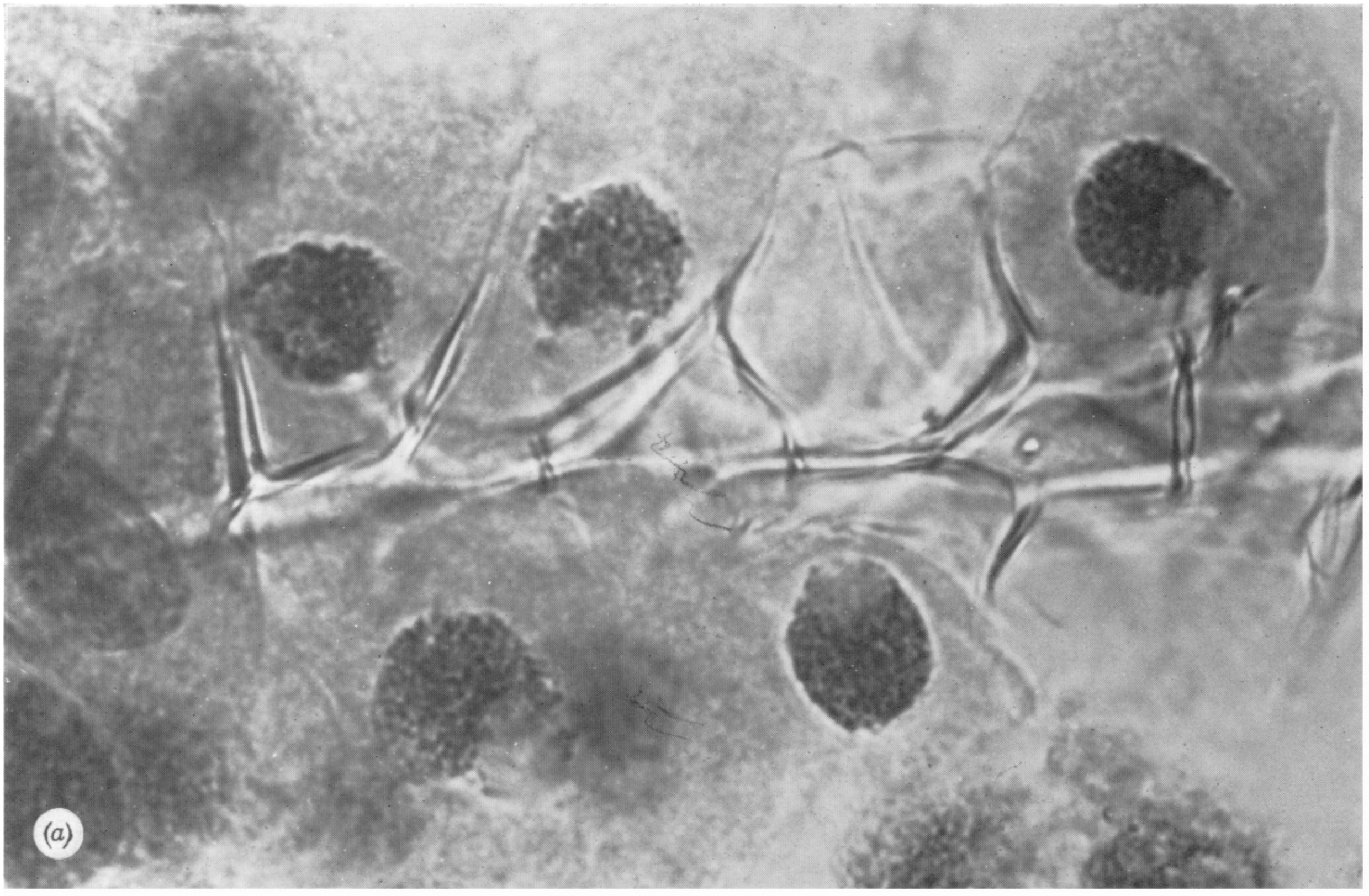

FIGURE 11. (*a*) Nuclei at midstage 3 of premeiotic interphase seen in part of an extruded column of archesporial cells stained in aceto-carmine. Note the central spine of callose within the column and the characteristic position of the nucleolus (× 1145). (*b*) Very early leptotene nuclei in part of an extruded column of archesporial cells from an anther stained in aceto-carmine (× 1145). (*c*) Surface view of the tapetal membrane showing pores of up to 2 μm in diameter in a Feulgen stained anther containing p.m.cs at leptotene (× 2200).

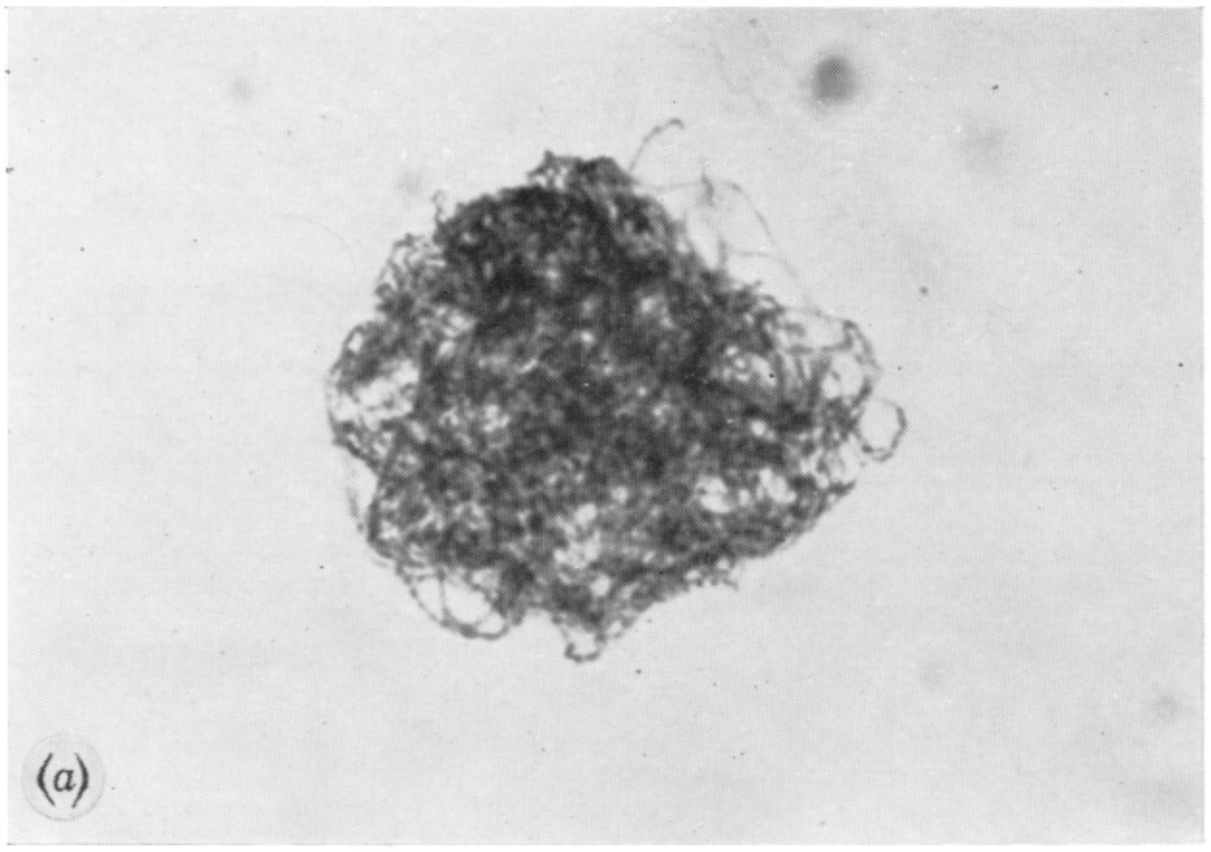

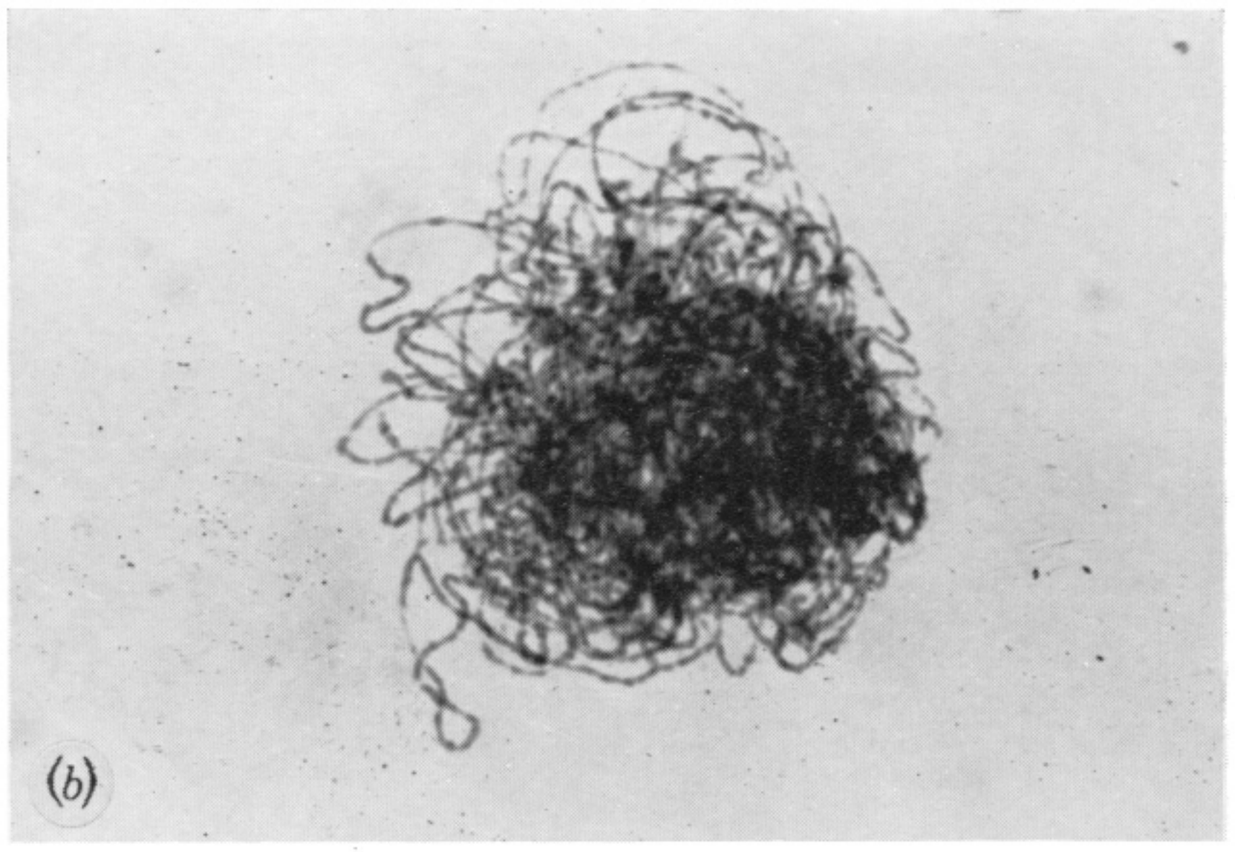

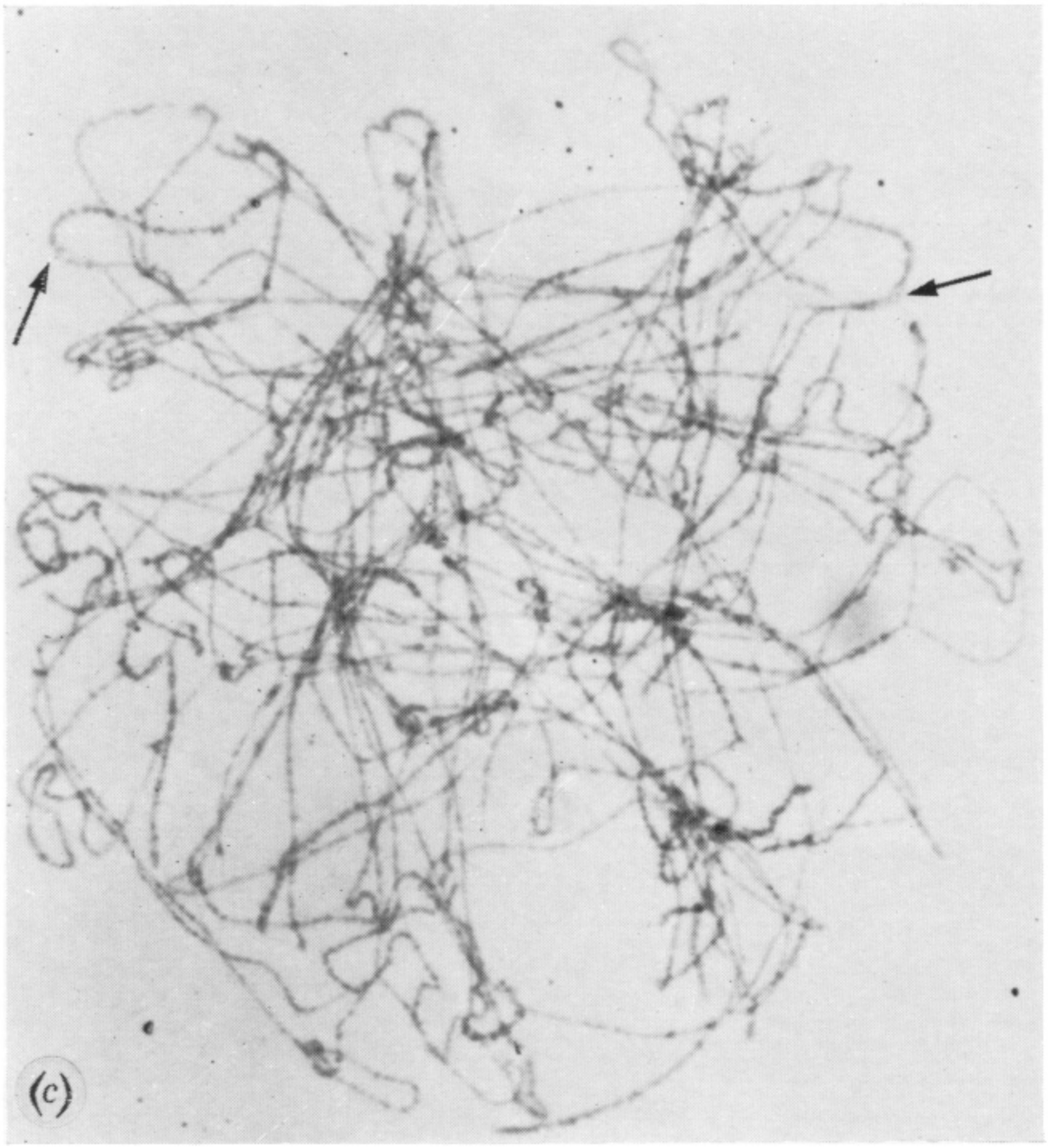

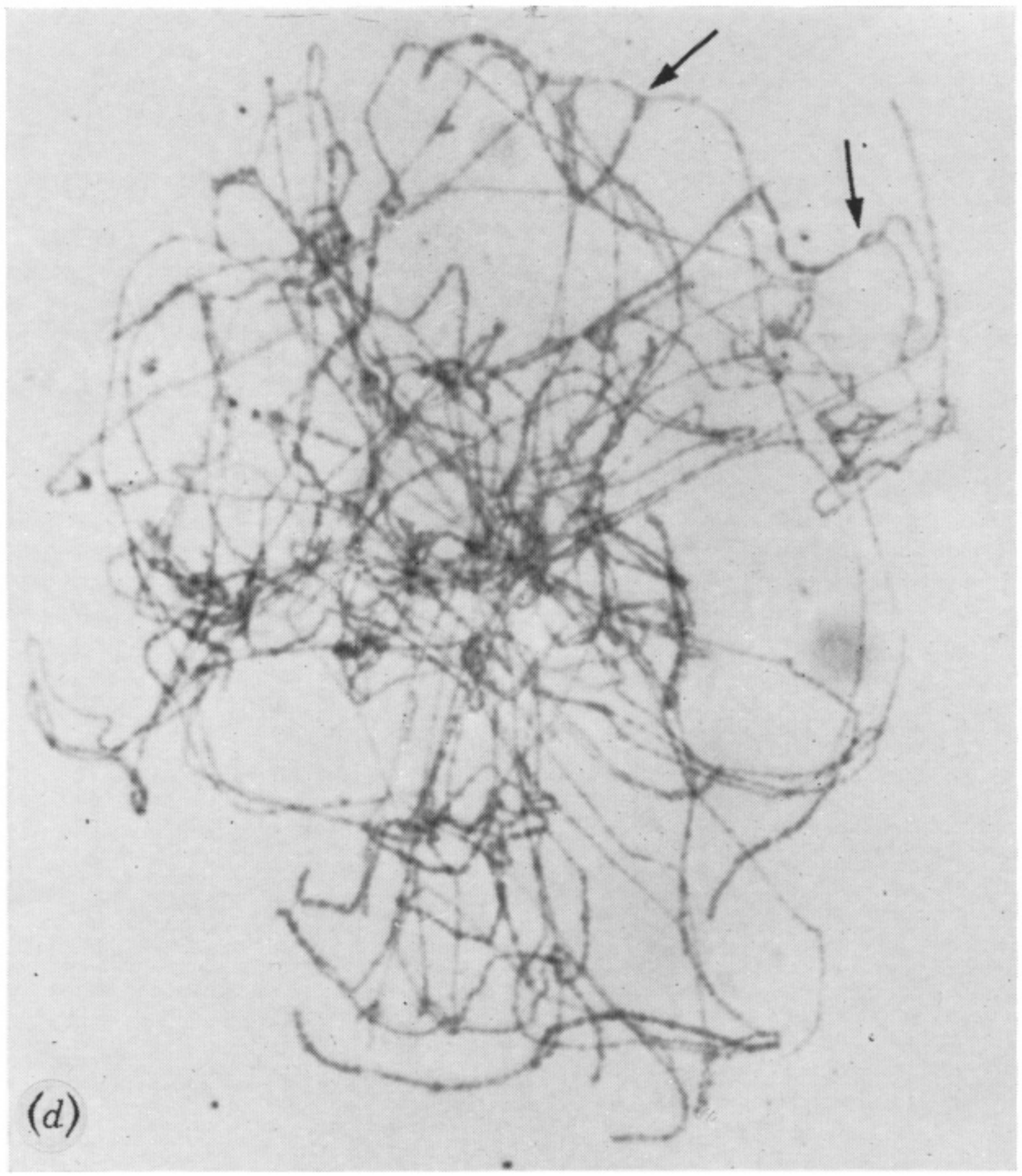

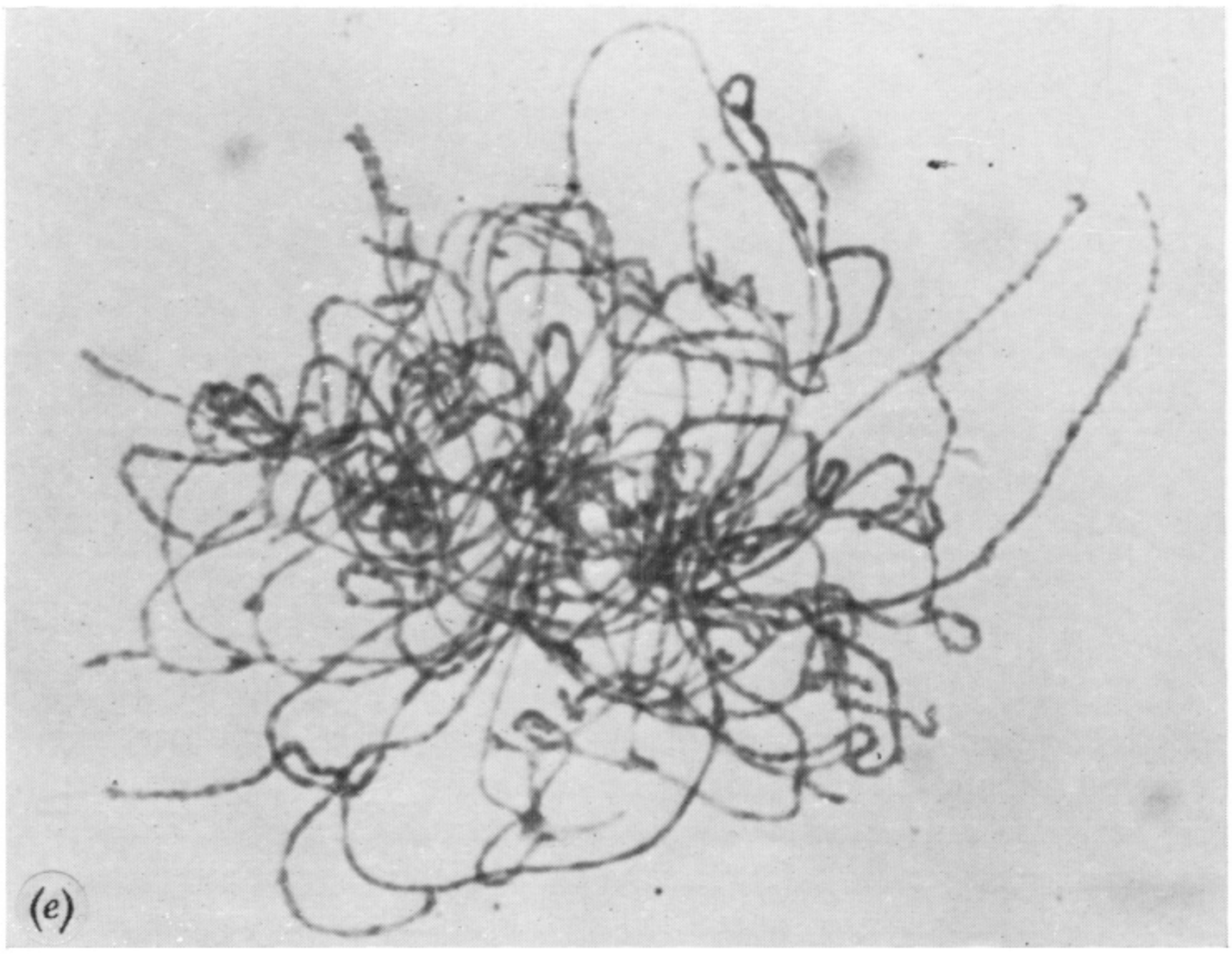

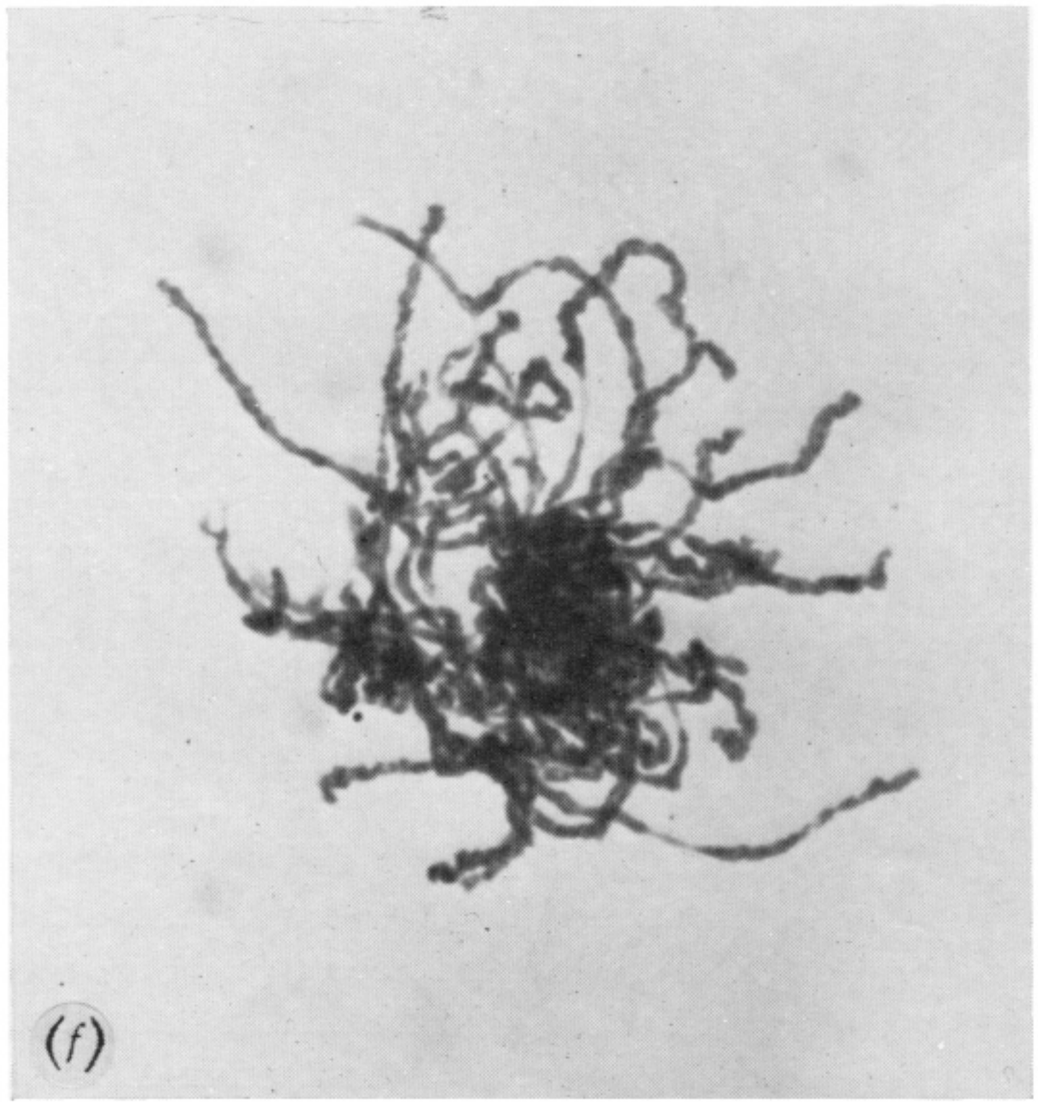

FIGURE 15. Nuclei of pollen mother cells at: (*a*) early leptotene, (*b*) late leptotene, (*c*) early zygotene, (*d*) late zygotene, (*e*) early pachytene; and (*f*) late pachytene. (Magn. × 2000.) (N.B. Some junctions between regions of paired and unpaired chromosomes are indicated by arrows in (*c*) and (*d*).)

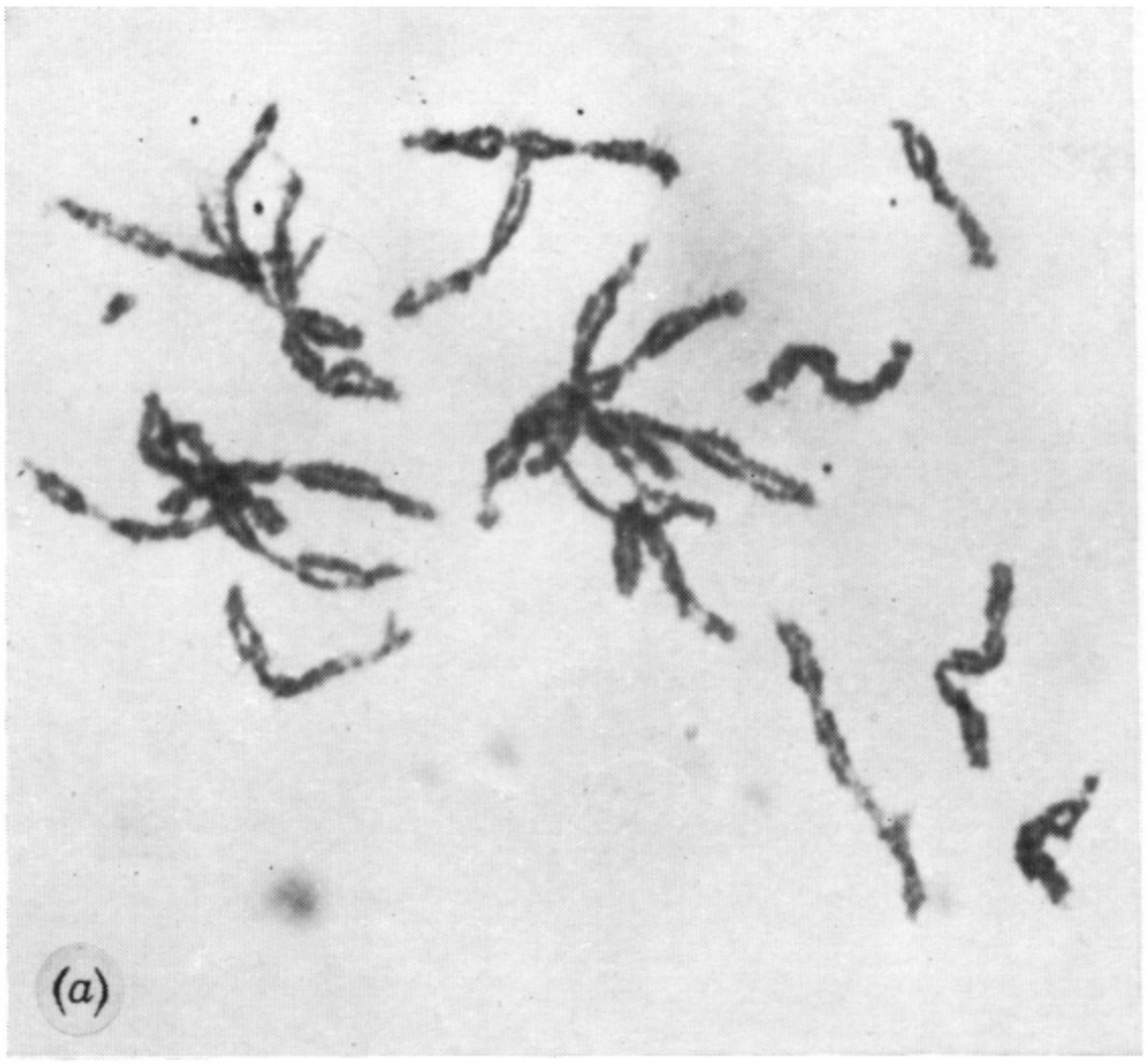

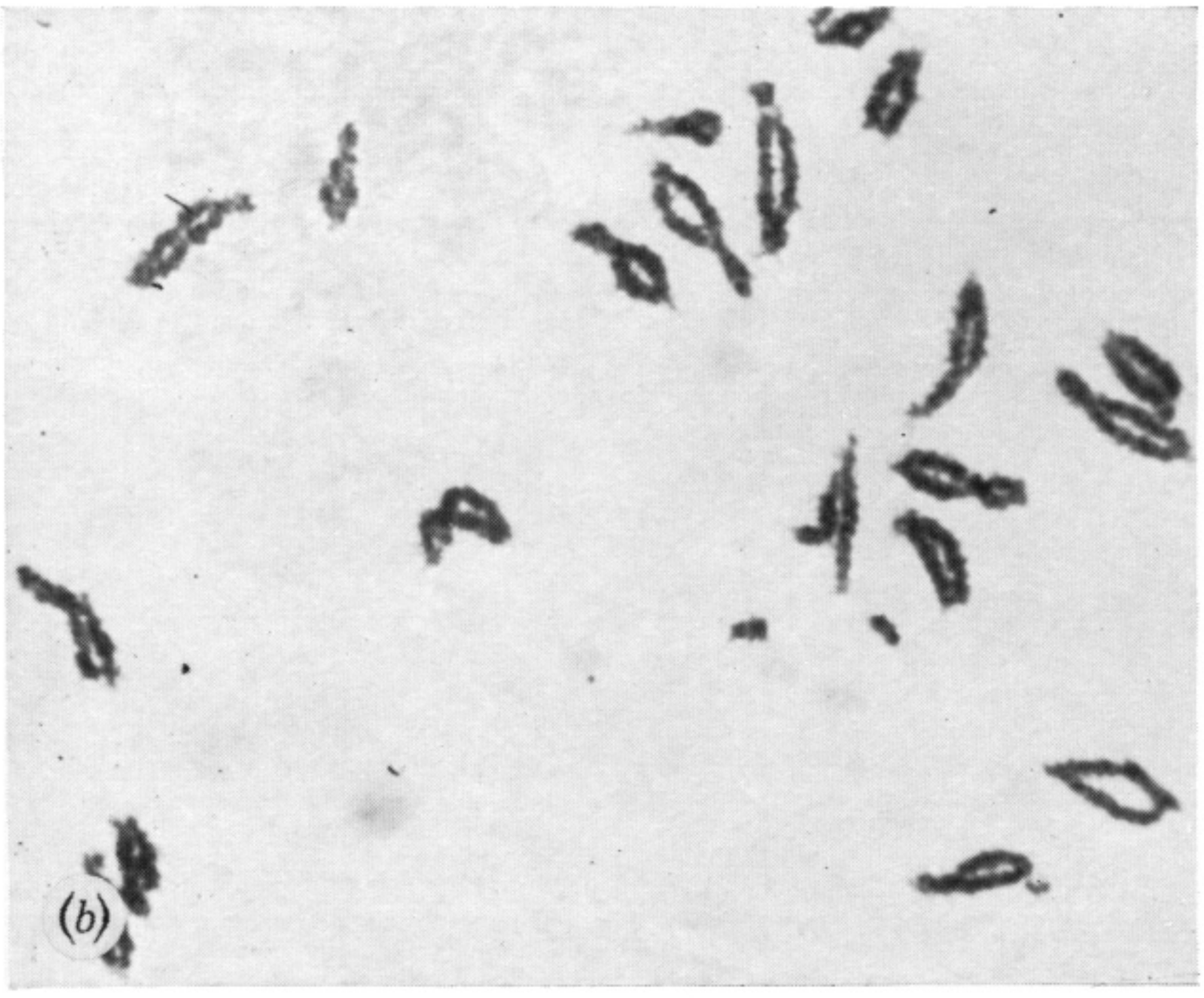

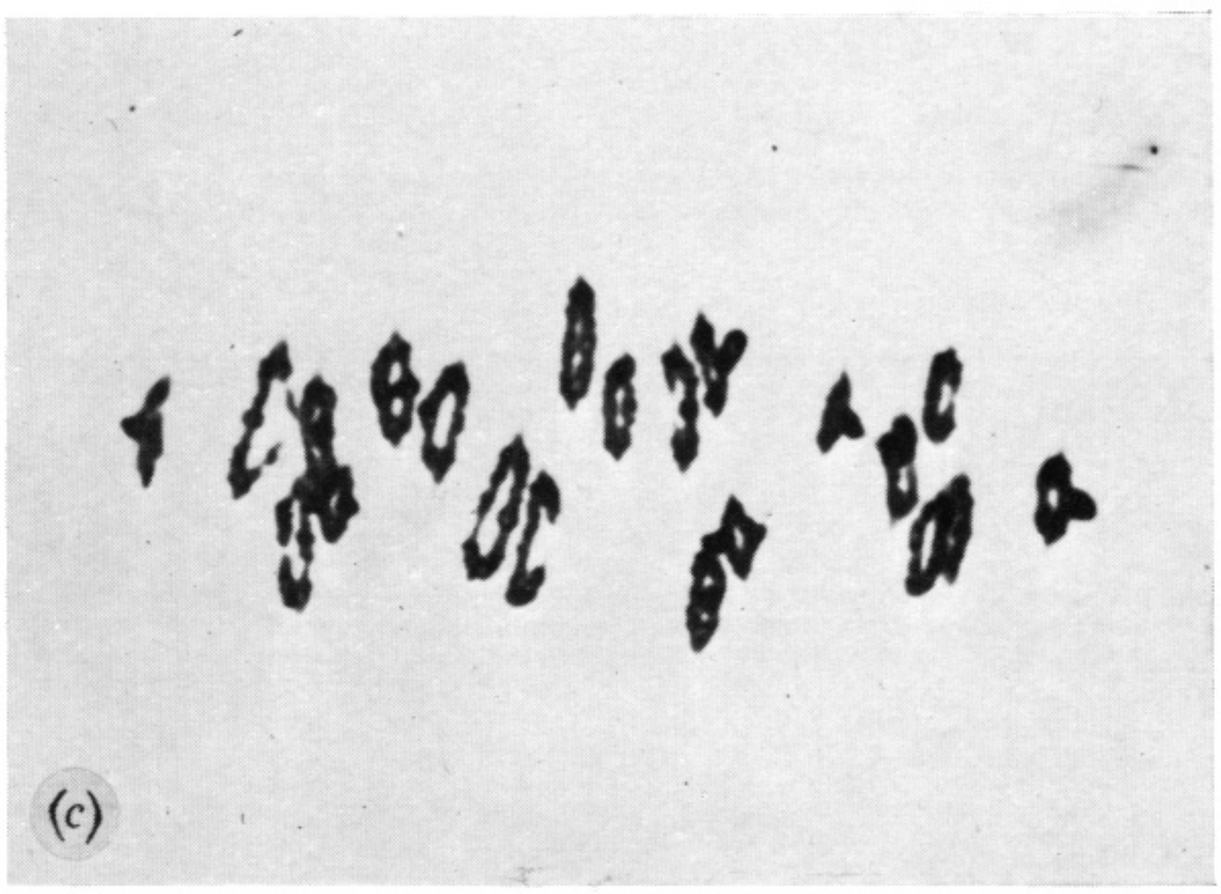

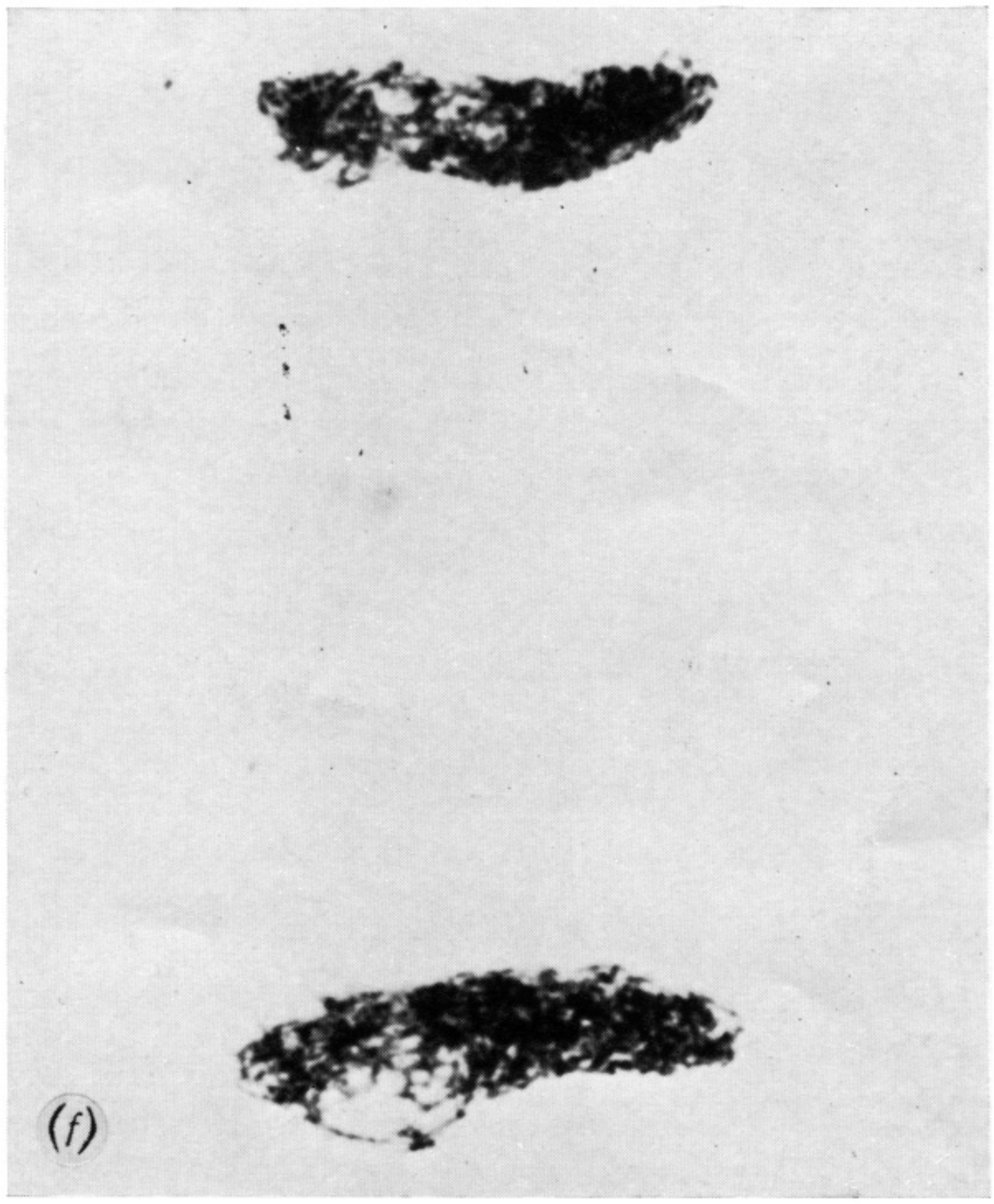

FIGURE 16. Nuclei of pollen mother cells at: (*a*) diplotene, (*b*) diakinesis, (*c*) first metaphase, (*d*) first anaphase (early), (*e*) first anaphase (late), (*f*) first telophase. (Magn. × 2200.)

FIGURE 17. Nuclei of pollen mother cells at: (*a*) second prophase, (*b*) second metaphase, (*c*) second anaphase, (*d*) second telophase, (Magn. × 2200.) Nuclei of embryo sac mother cells at: (*e*) diakinesis, (*f*) second metaphase. (Magn. × 1210.)

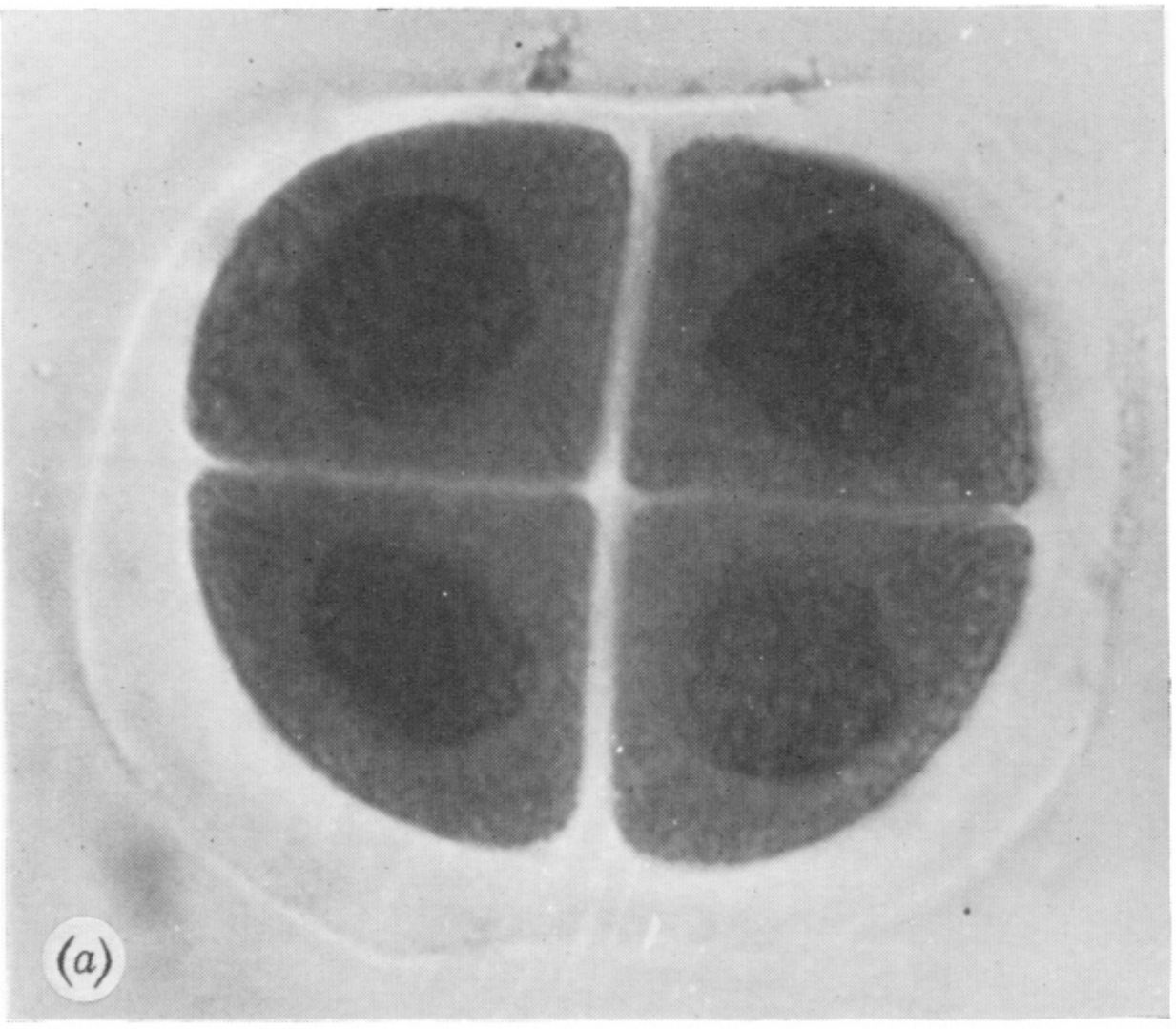

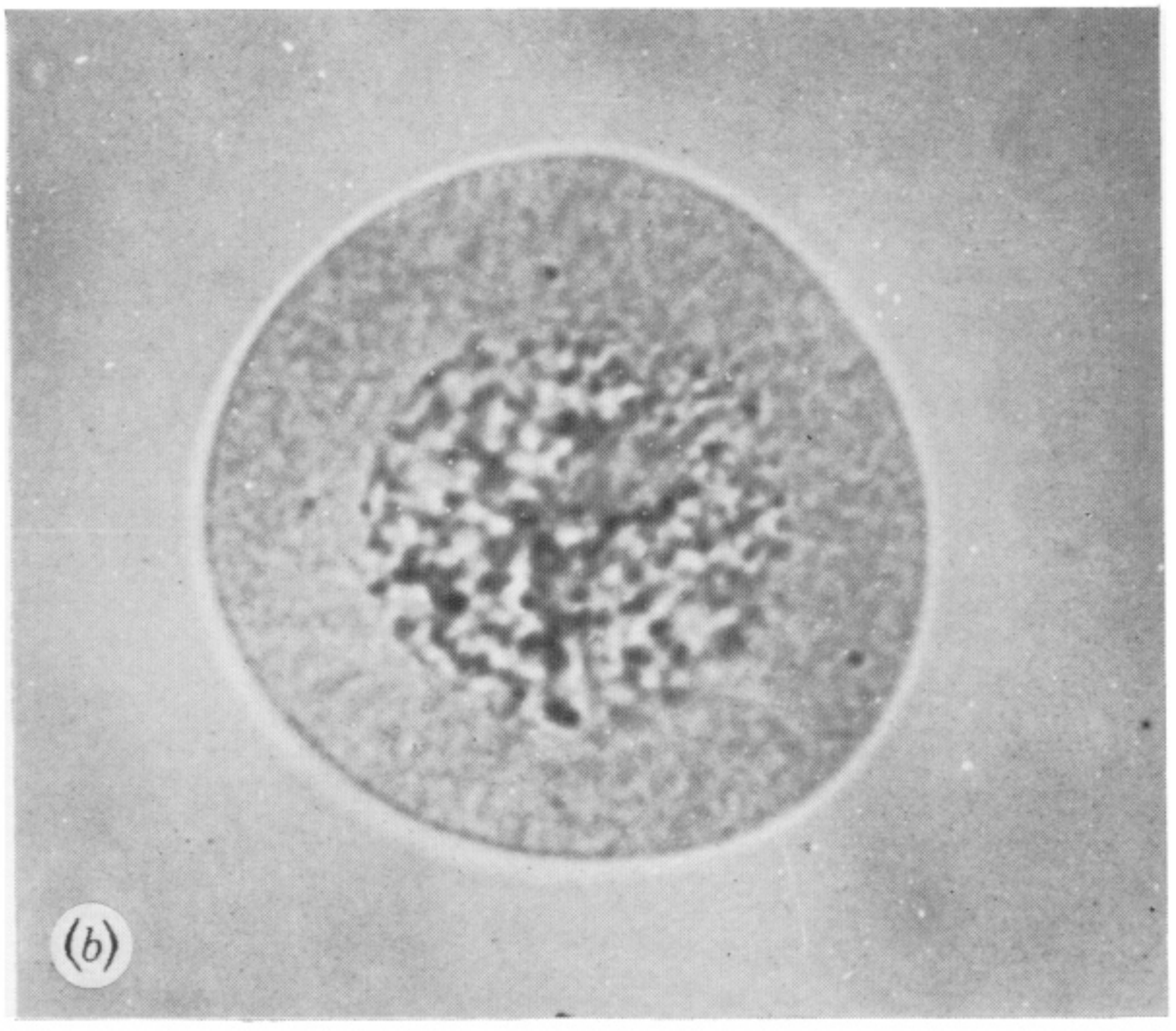

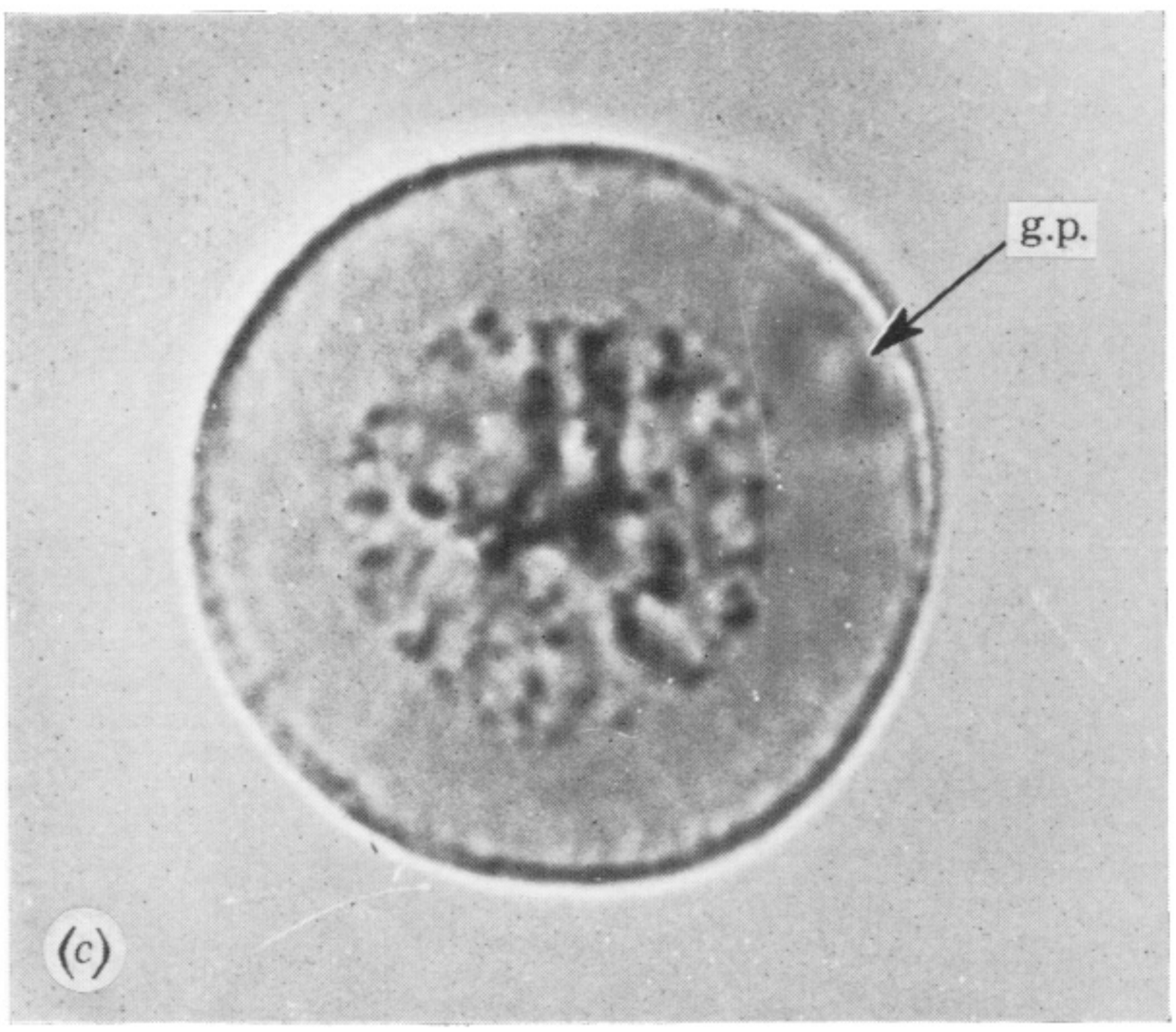

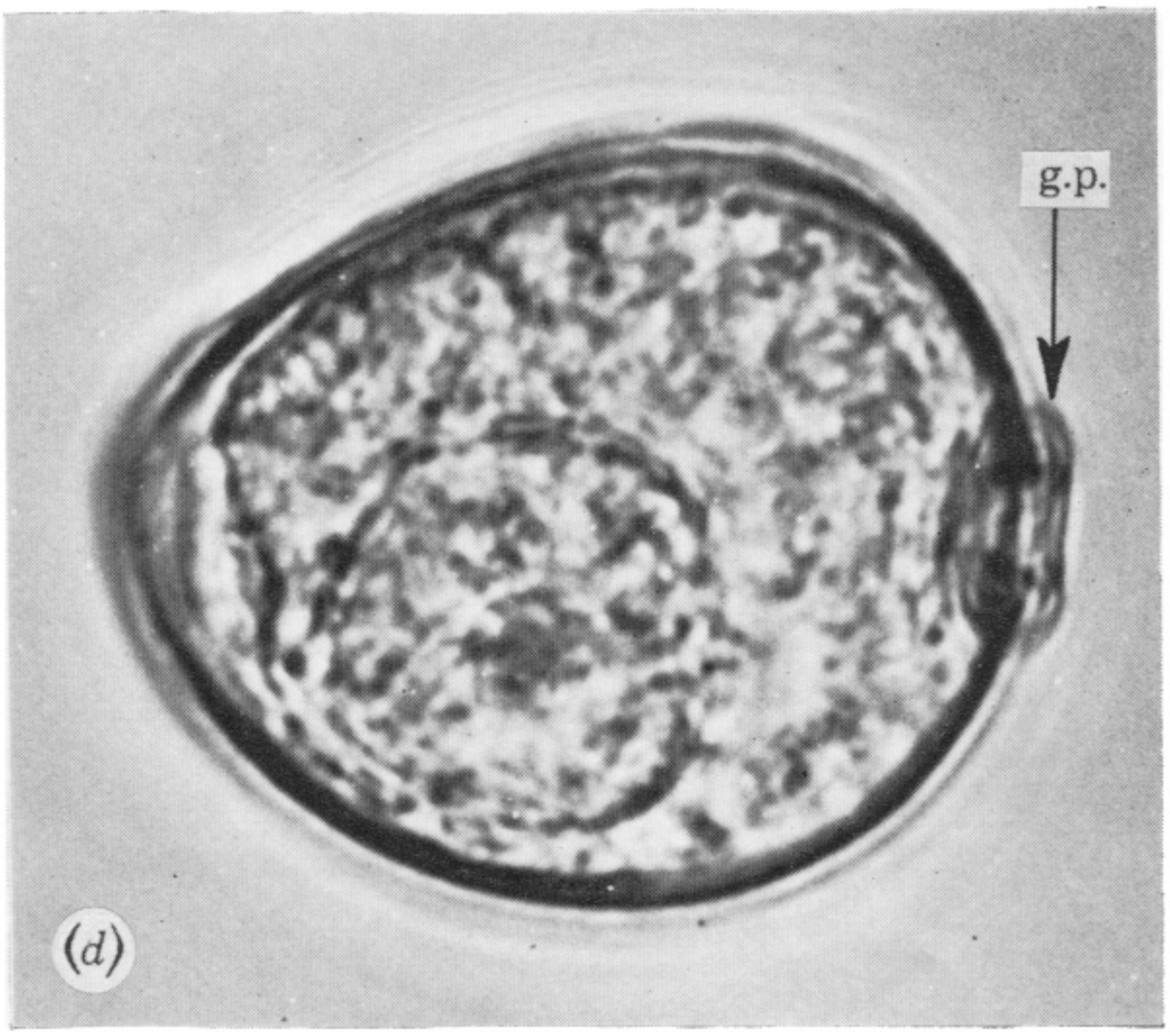

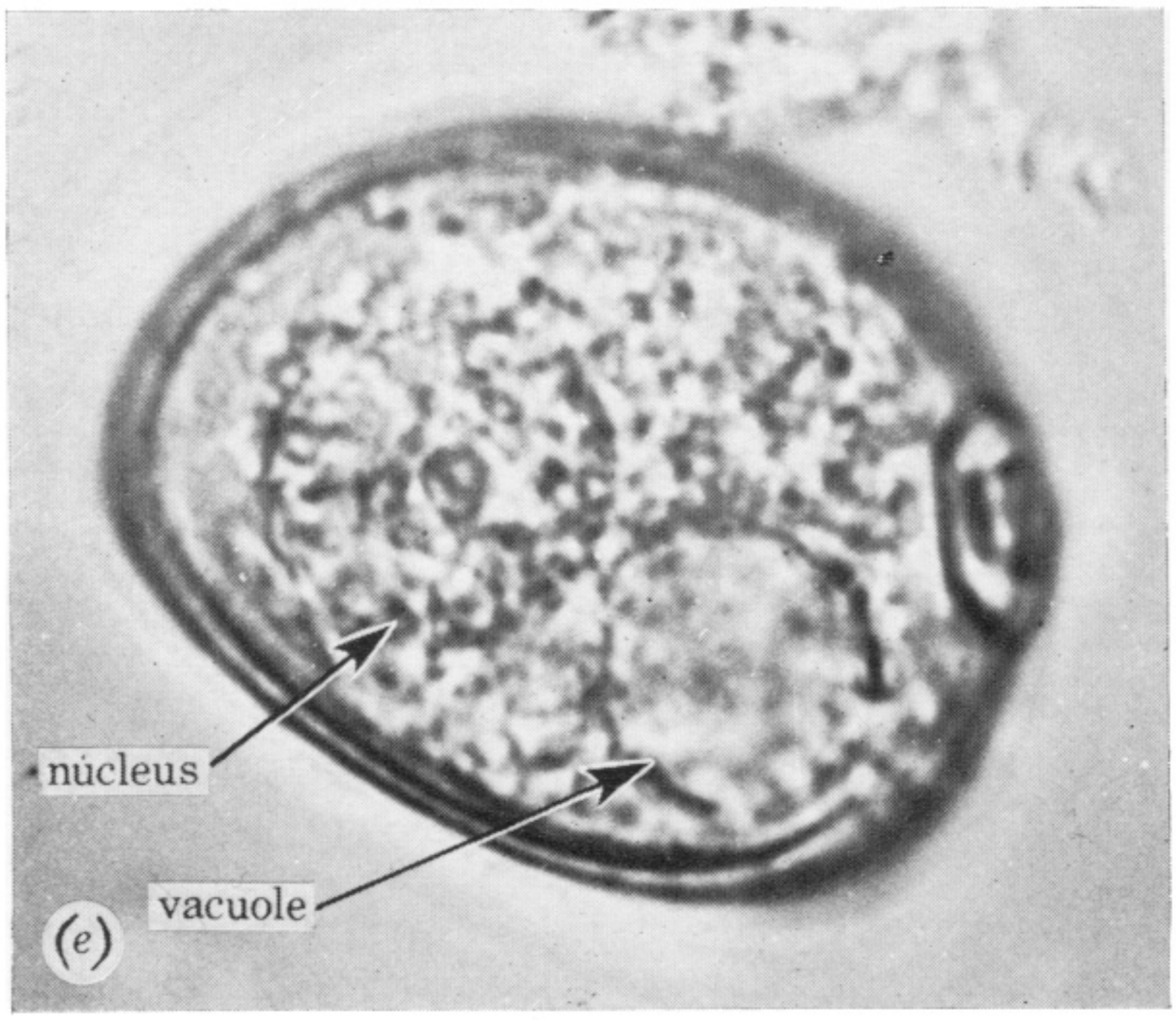

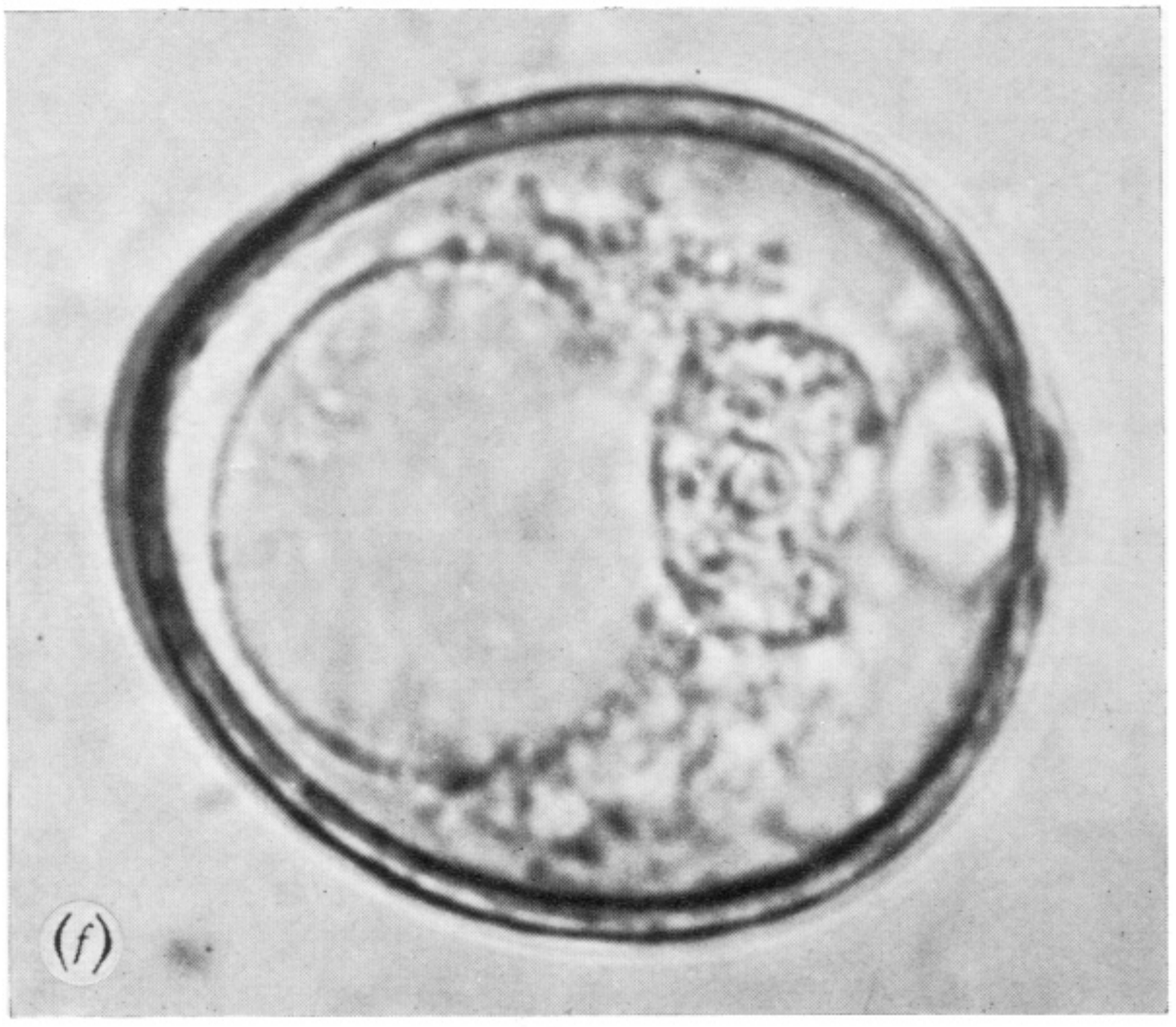

FIGURE 20. Pollen development in Chinese Spring wheat grown at 20 °C showing: (*a*) late tetrad stage (× 1375); (*b*) young pollen without a germ pore (× 1650); (*c*) young pollen with germ pore (g.p.) just visible; (*d*) young pollen with well formed germ pore but no single obvious vacuole; (*e*) young pollen soon after the appearance of a single obvious vacuole; (*f*) young pollen about 18 h after breakdown of the tetrad wall. (*c* to *f*, magn. × 2255.)

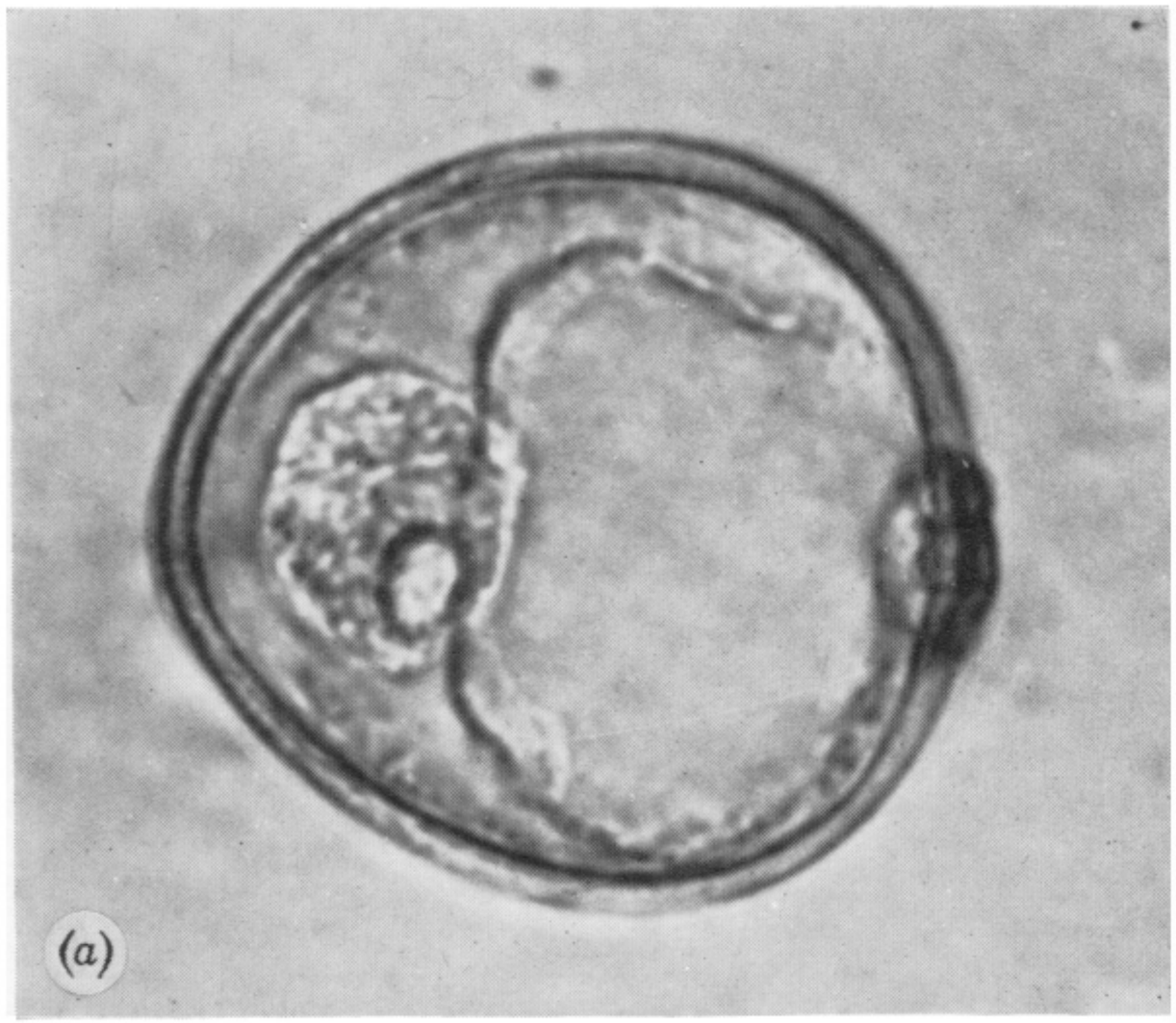

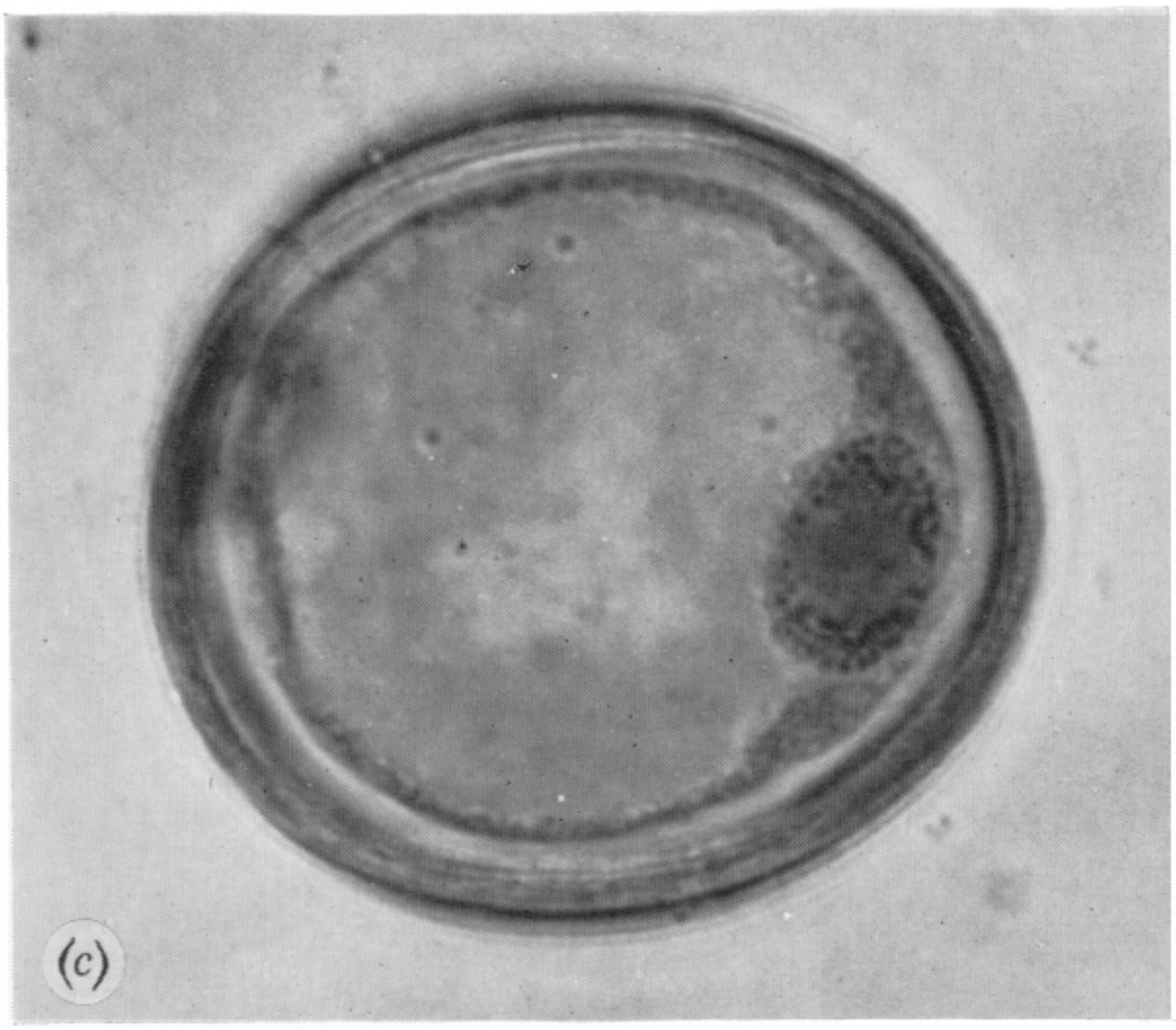

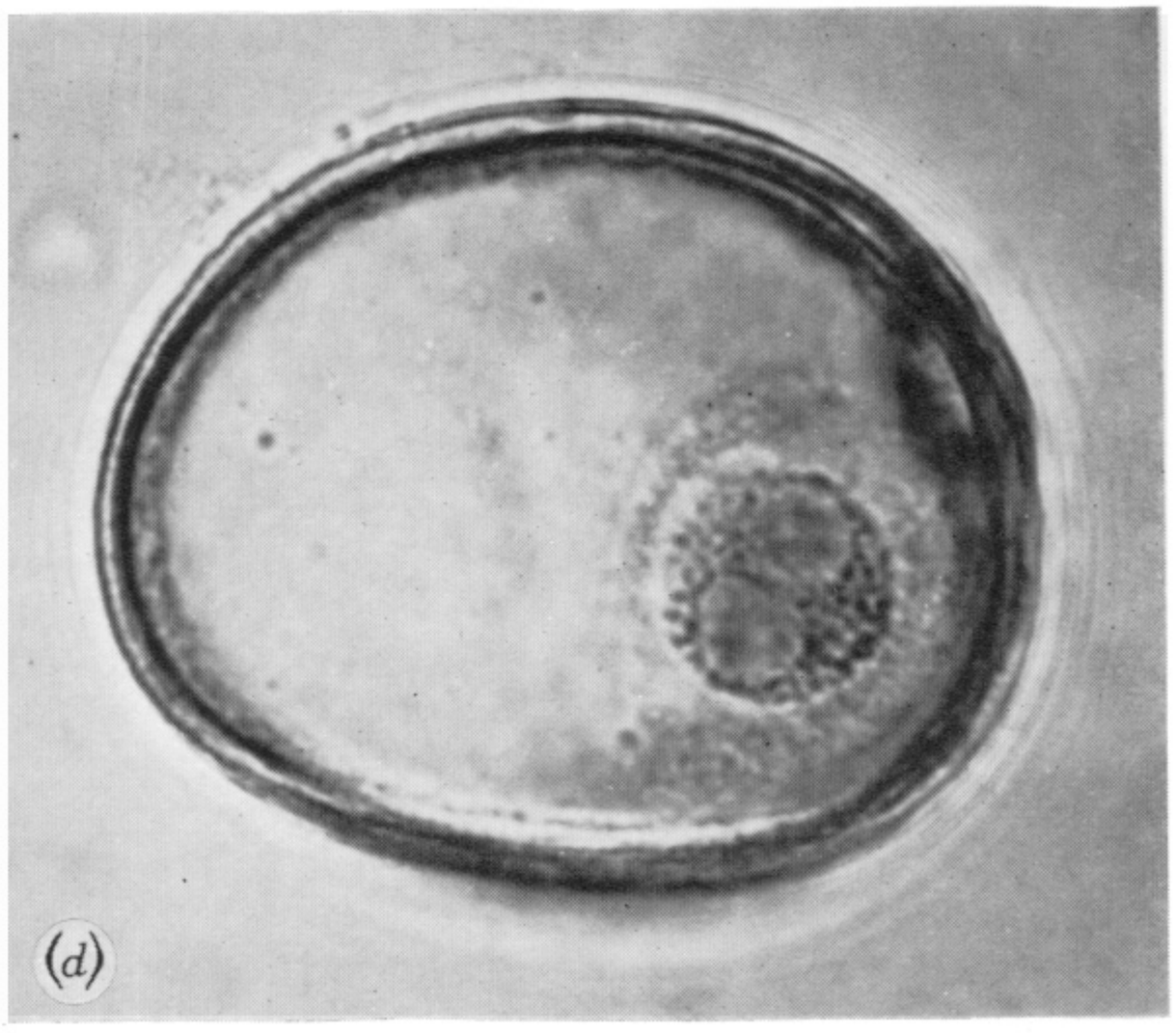

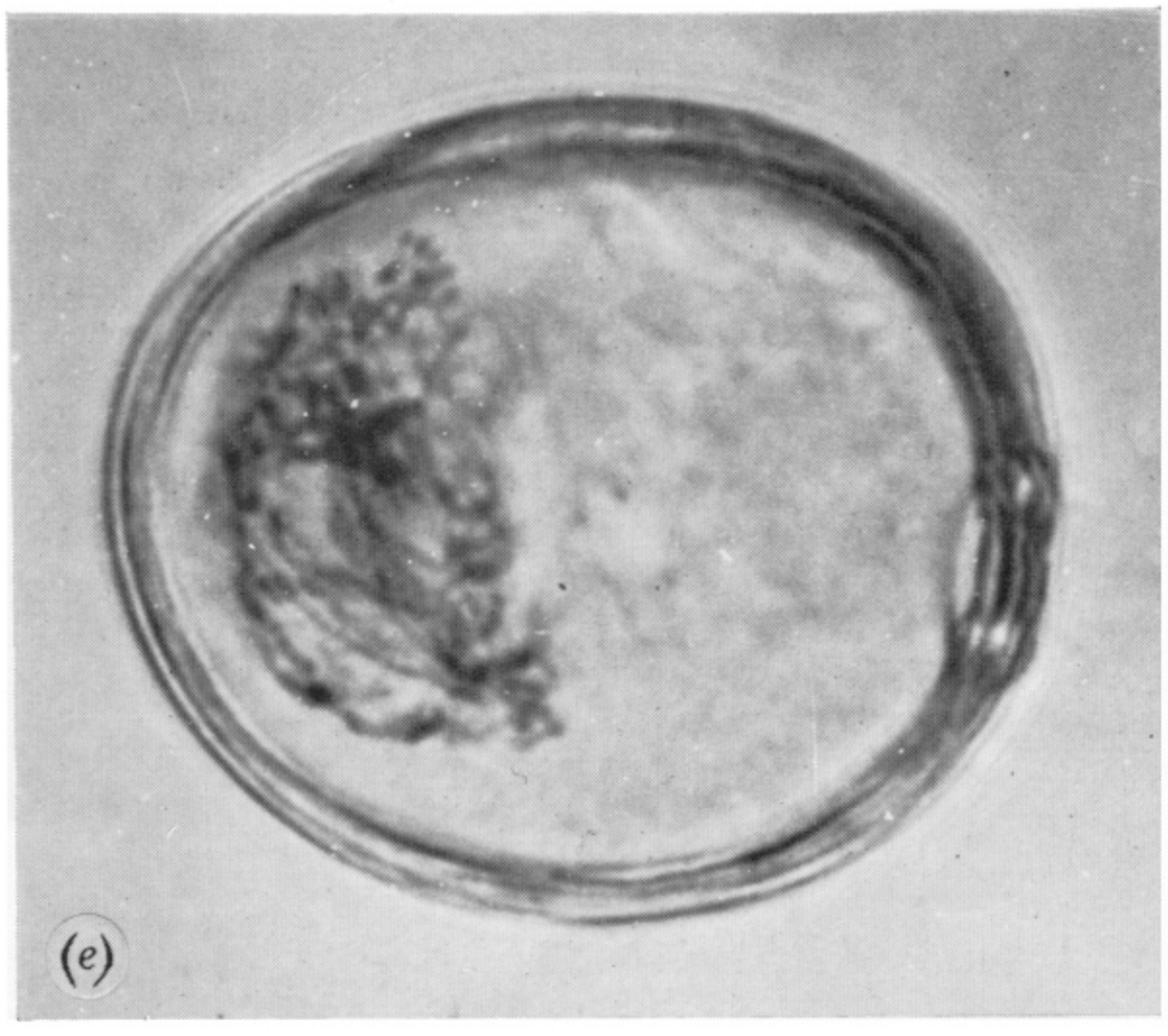

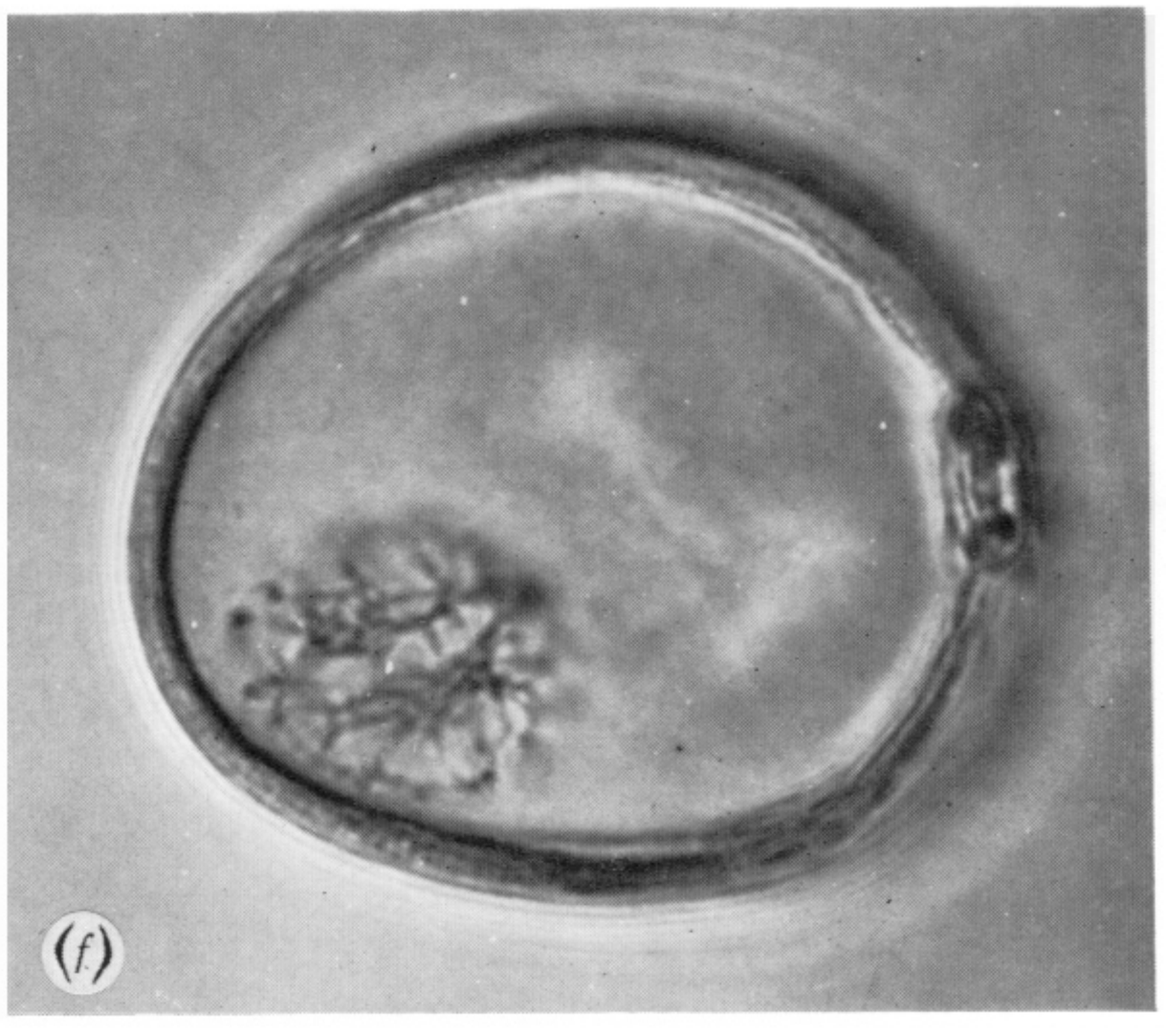

FIGURE 21. Pollen development in Chinese Spring wheat grown at 20 °C showing: (*a* to *c*) The increasing size of the microspore and the vacuole. Note the nucleus may be at either pole; either under the pore (*b*) and (*d*) or at the other end of the spore (*a*) and (*c*). (*c*, *d*) Nuclear contraction before first pollen grain mitosis probably concurrent with DNA synthesis phase. (*e*, *f*) Early and late stages of prophase of first pollen grain mitosis. (Magn. × 1430.)

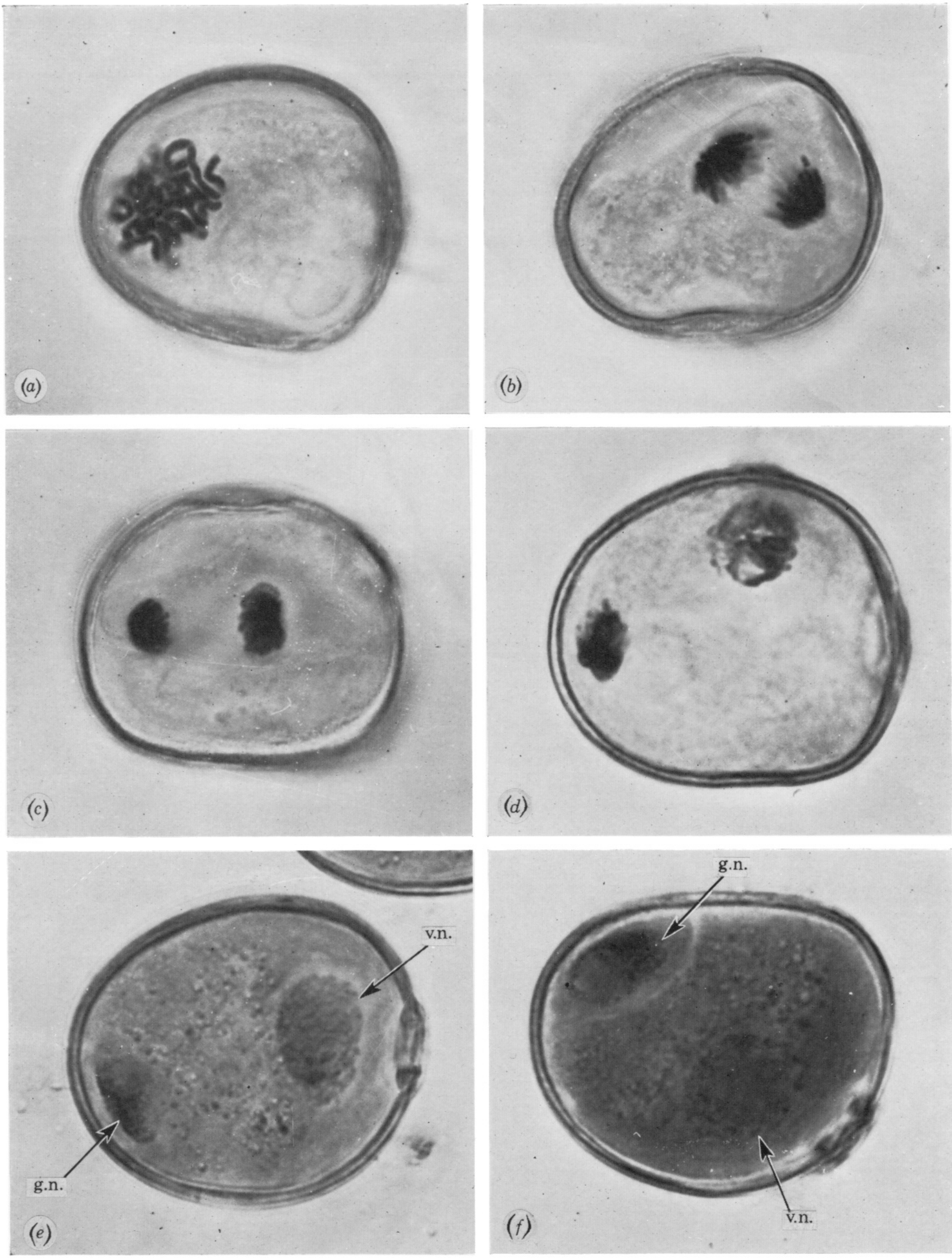

FIGURE 22. Pollen development in Chinese Spring wheat grown at 20 °C showing: (*a*) metaphase of p.g.m.1; (*b*) anaphase of p.g.m.1; (*c*) telophase of p.g.m.1; (*d*) migration of the nuclei to opposite poles of the microspore after p.g.m.1; (*e*) differentiation of the generative nucleus (g.n.) and vegetative nucleus (v.n.) (note the first appearance of starch granules); (*f*) pollen grain half way between p.g.m.1 and p.g.m.2 showing the organization of a separate cell around the generative nucleus, and numerous starch granules around the vegetative nucleus. (Magn. × 1430.)

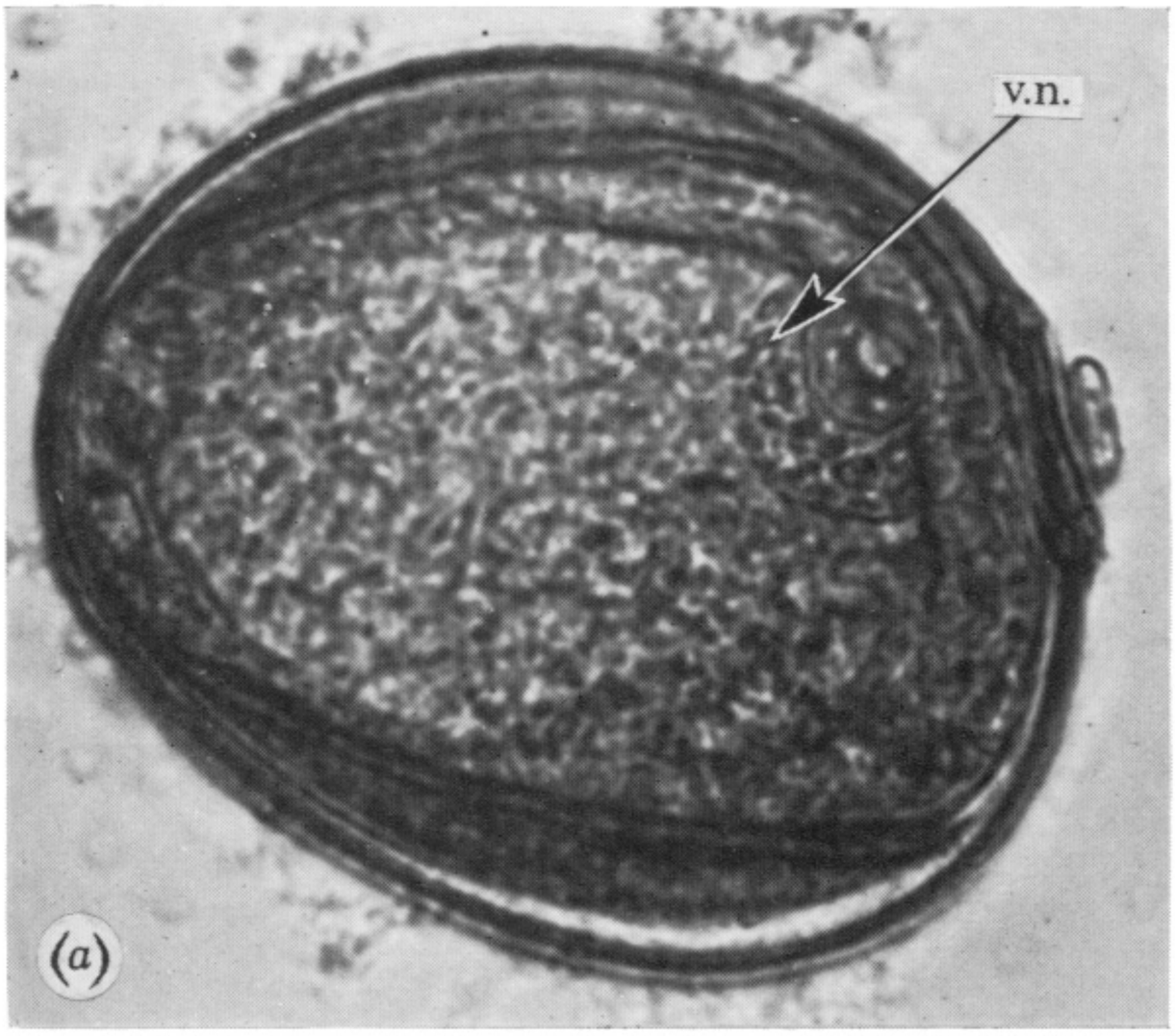

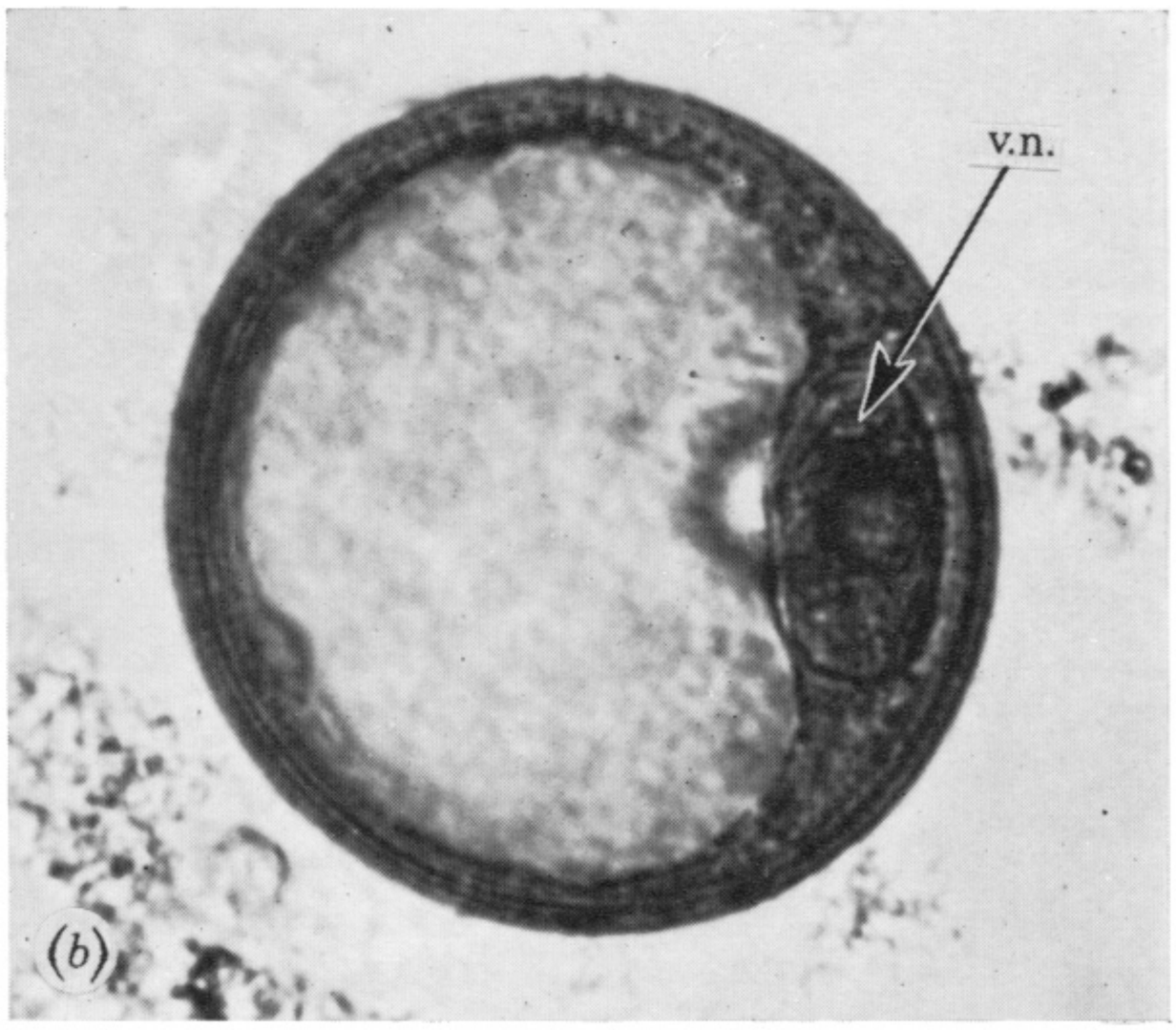

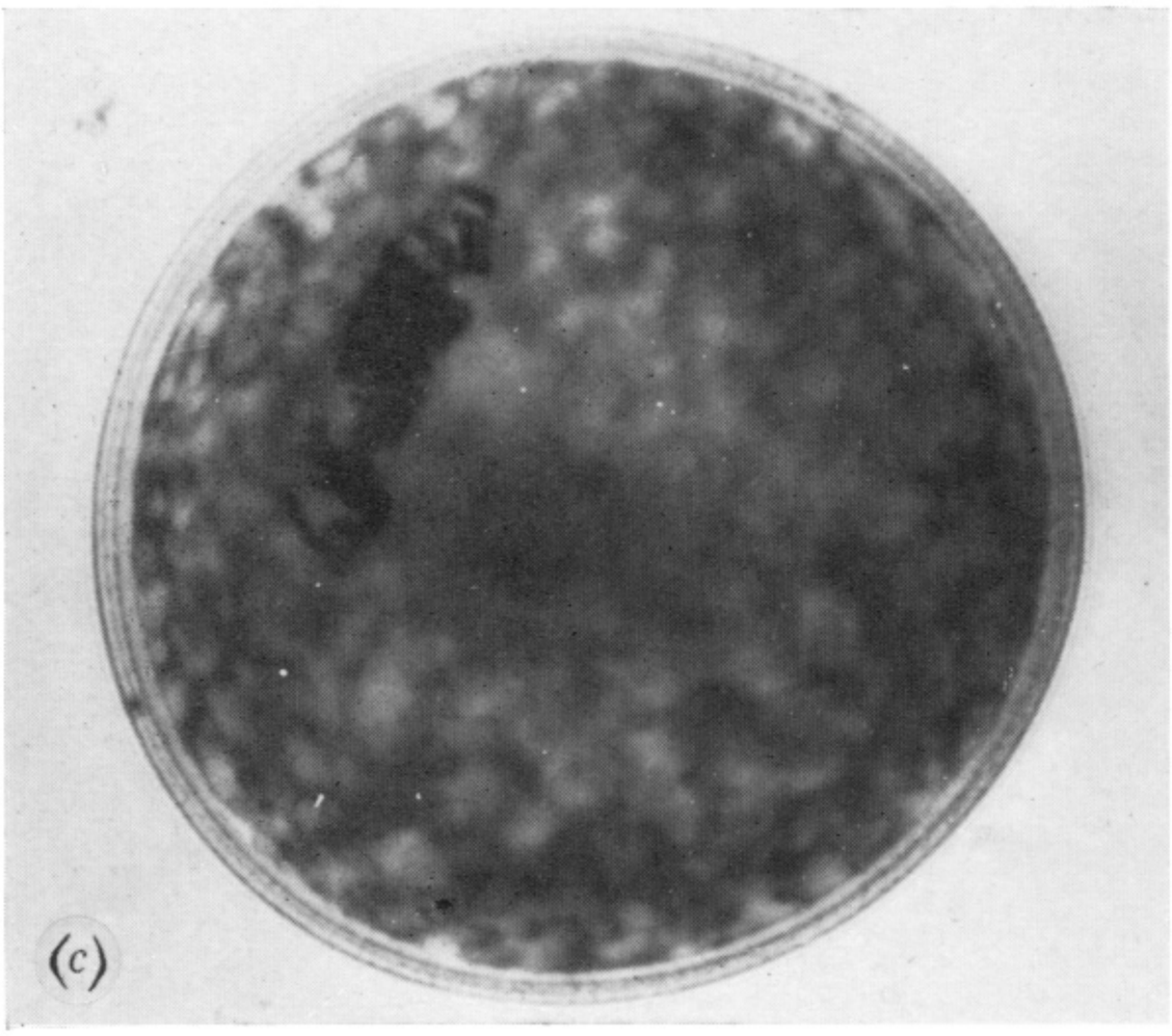

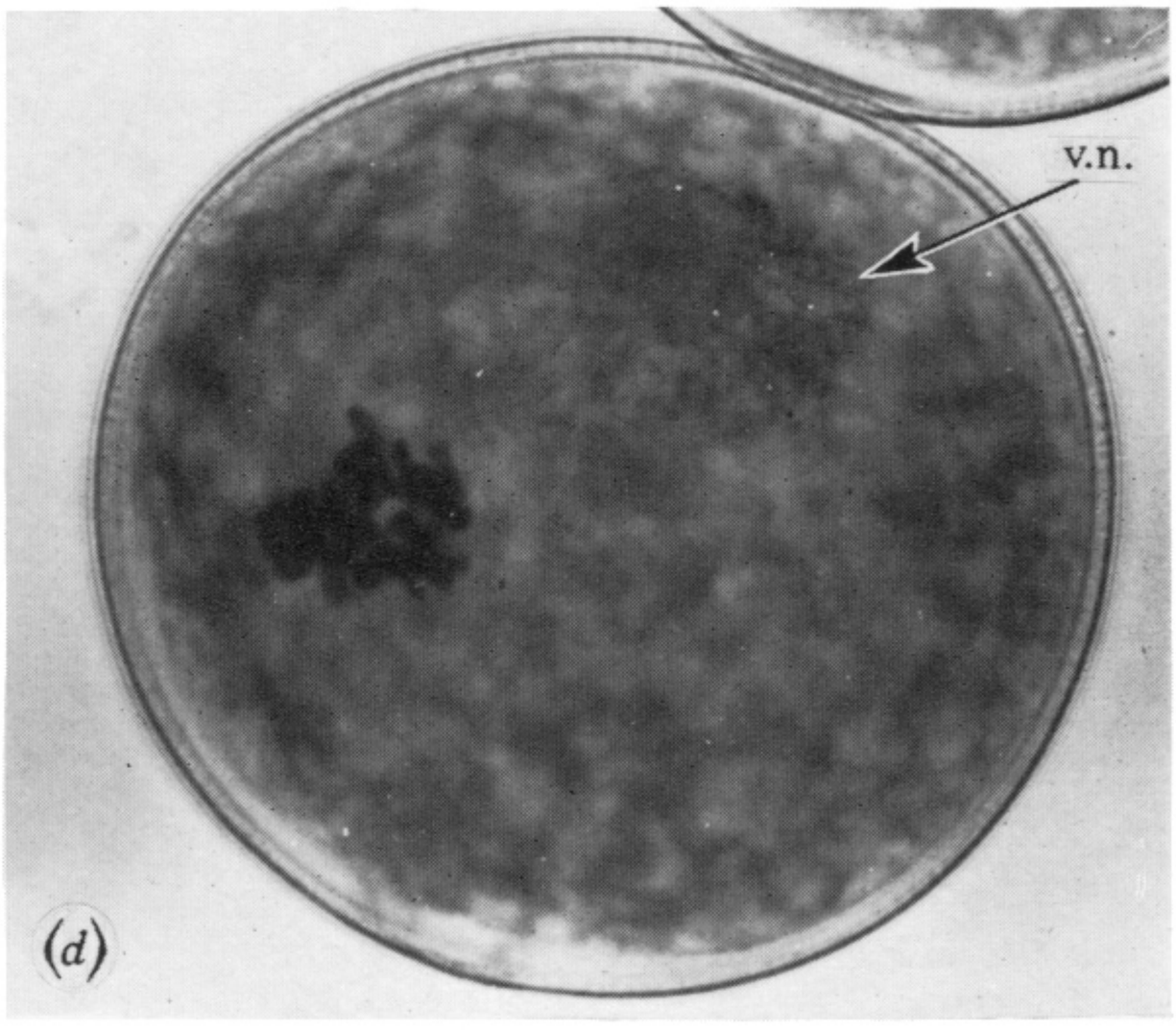

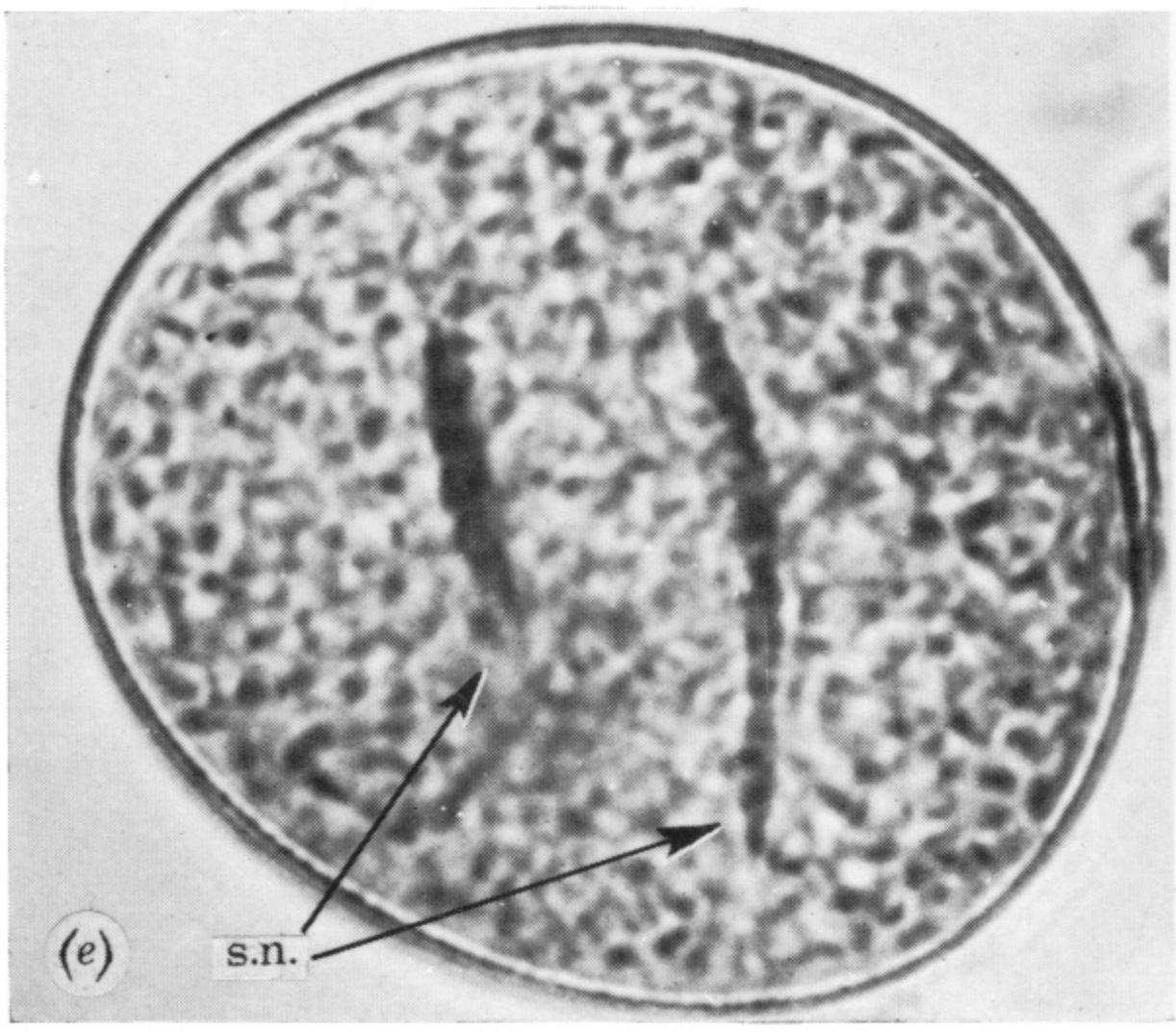

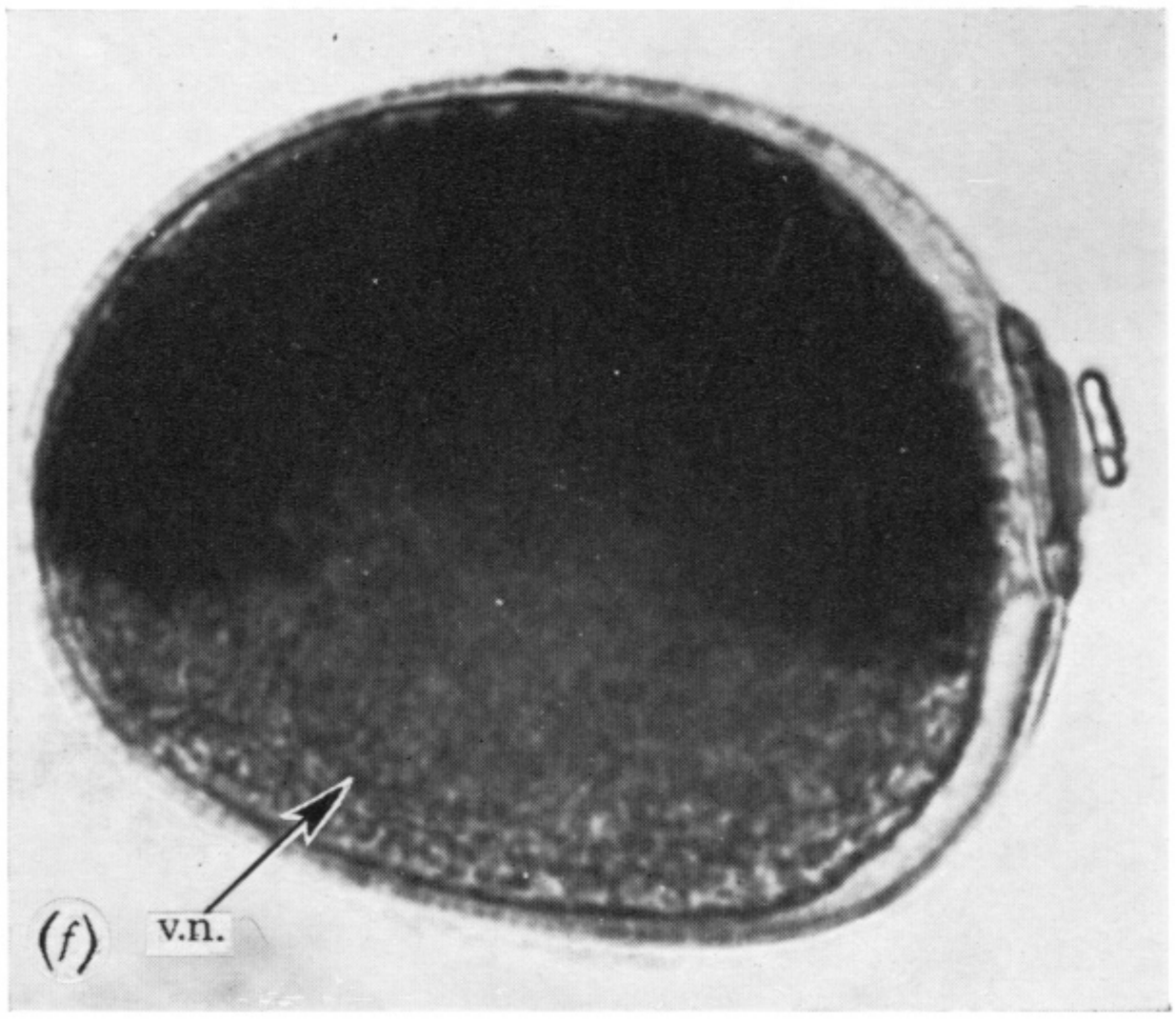

FIGURE 23. (*a*, *b*) Pollen grains later in the interval between p.g.m.1 and p.g.m.2 showing the size of the vacuole and the position and shape of the vegetative nucleus (v.n.); (*c*) late prophase of p.g.m.2; (*d*) metaphase of p.g.m.2; (*e*) almost mature pollen grain showing elongated sperm nuclei (s.n.); (*f*) Pollen at anther dehiscence stained in iodine solution showing the presence of starch granules on one side of the spore only away from the vegetative nucleus. (Magn. × 1320.)

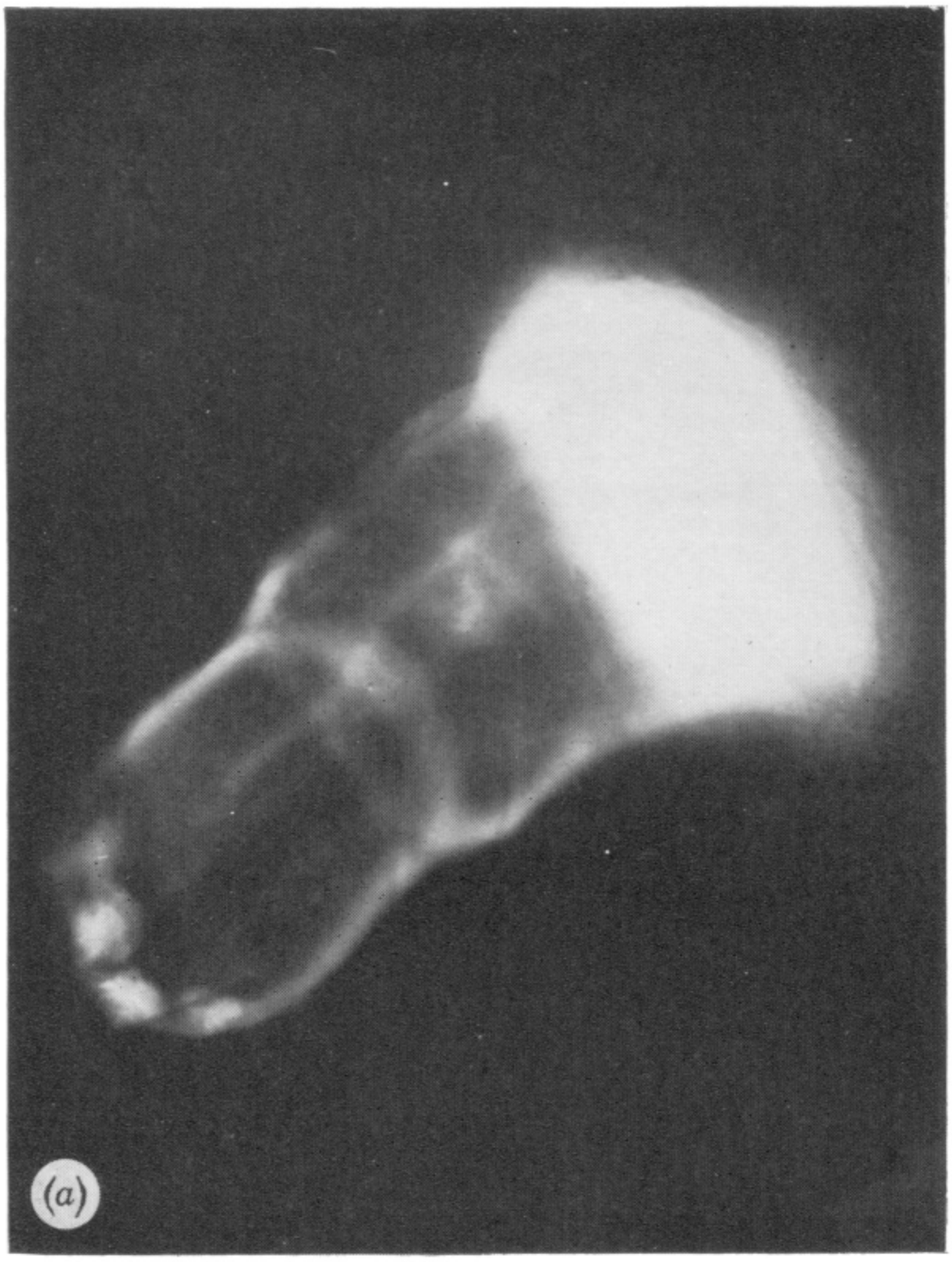

(a)

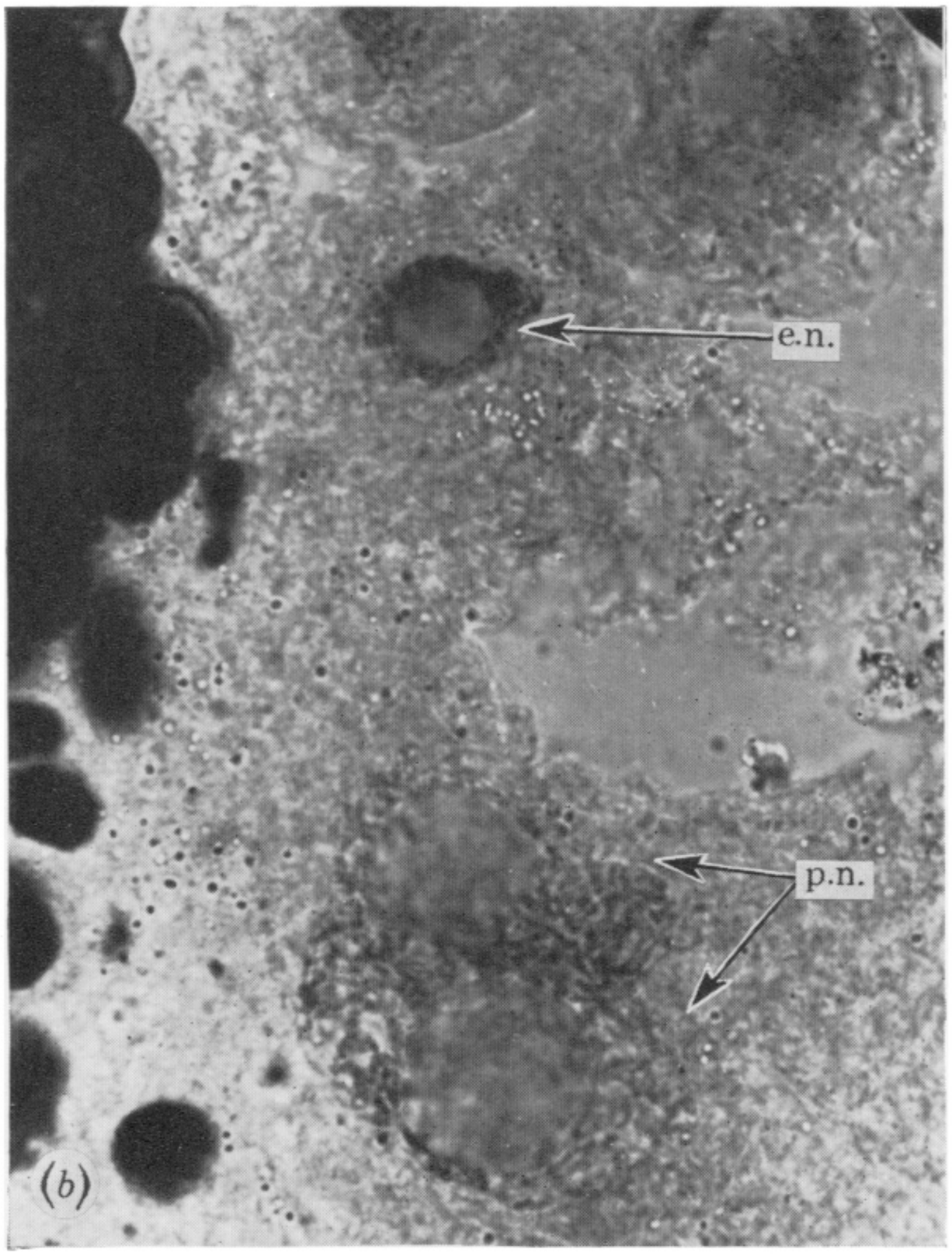

(b)

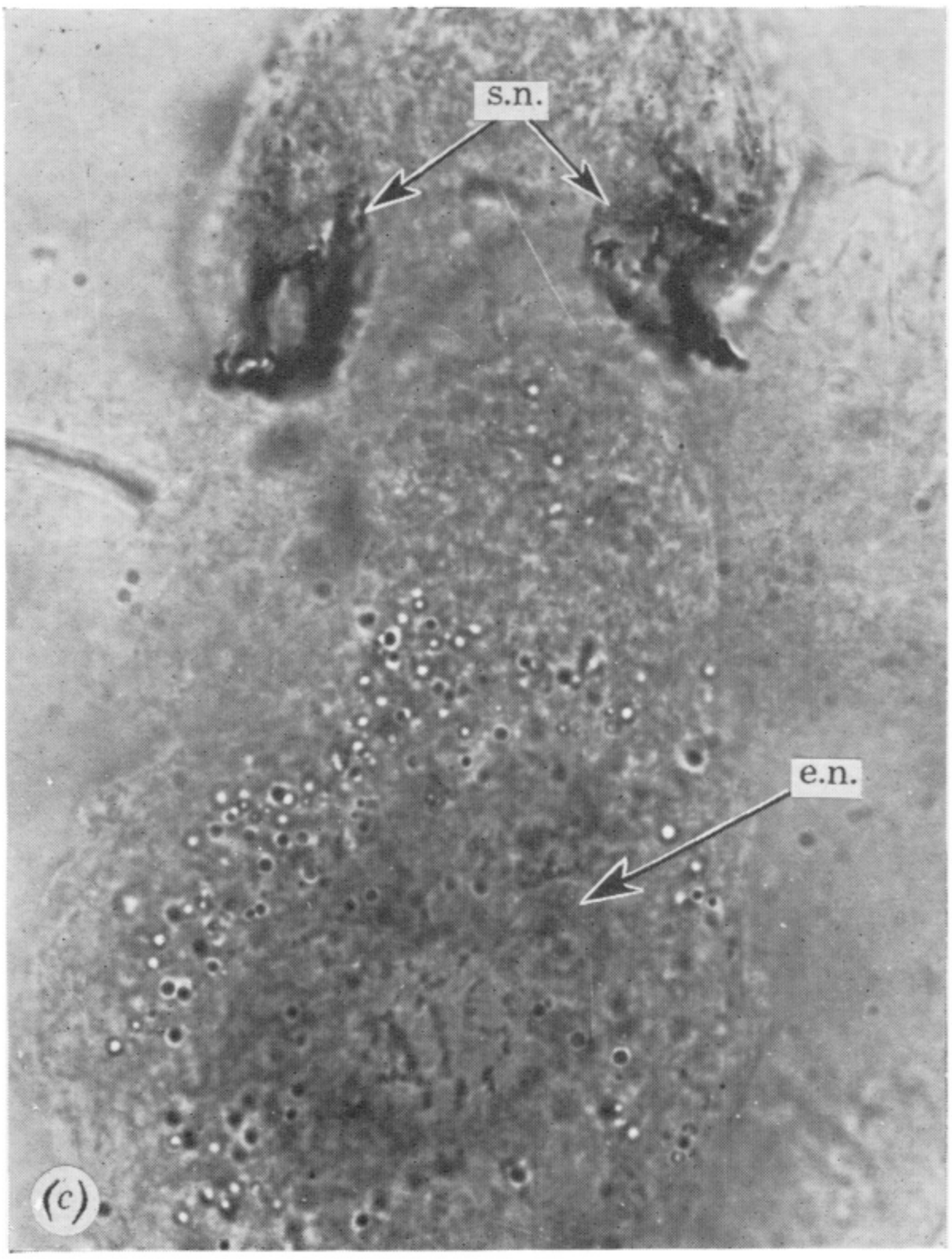

(c)

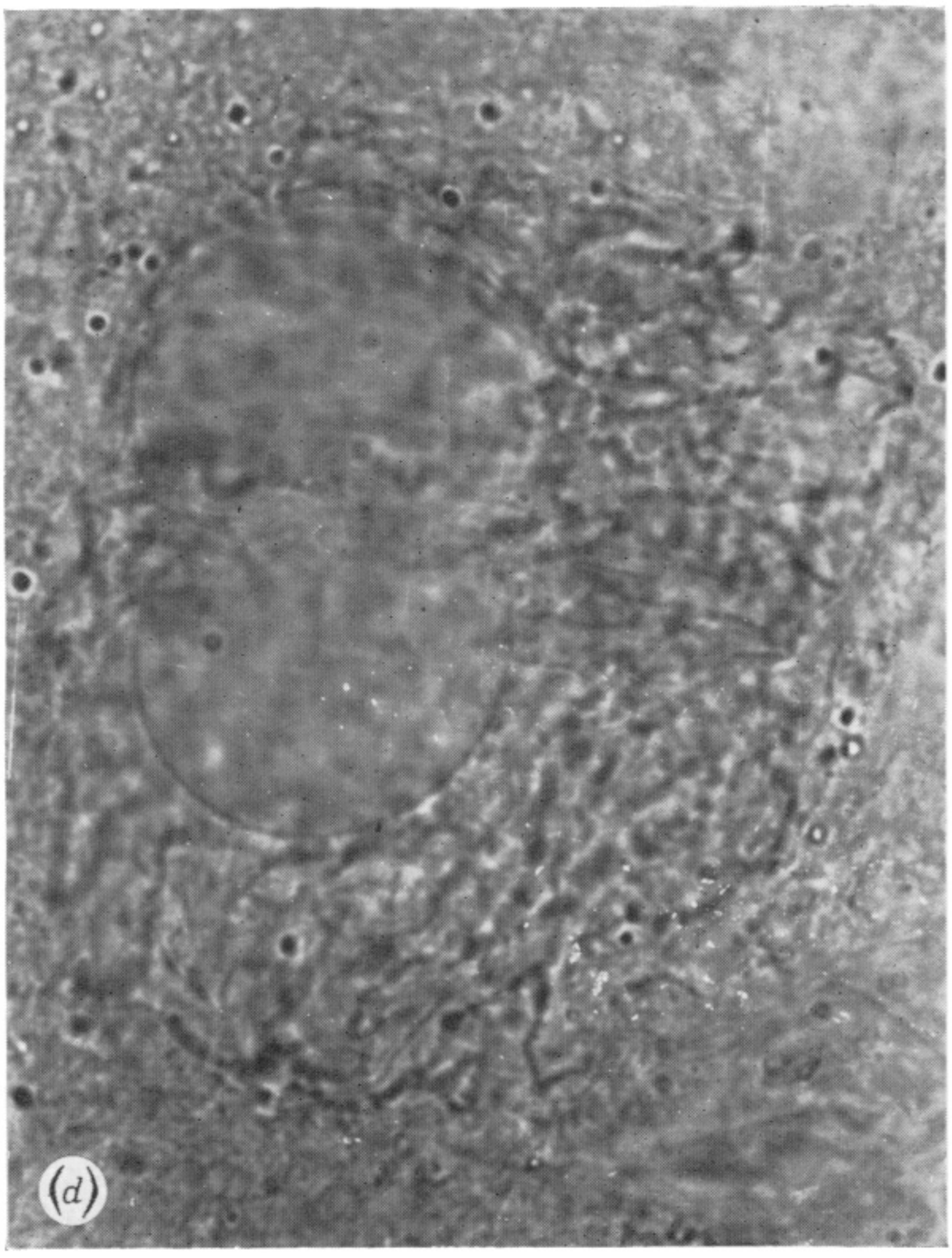

(d)

FIGURE 26. Embryo sac development in Chinese Spring wheat showing: (*a*) fluorescing callose around the female tetrad soon after the end of meiosis – the functional megaspore is at the bottom left-hand corner (× 1055); (*b*) part of an embryo sac about 4 days after meiosis showing the polar nuclei (p.n.), and the undifferentiated egg nucleus (e.n.) (× 1320); (*c*) part of an almost mature embryo sac prior to fertilisation showing the two degenerating synergid nuclei (s.n.) and the differentiated egg nucleus surrounded by refractile globules (bottom) (× 1045); (*d*) another part of the embryo sac in (*c*) showing the polar nuclei (× 1320).

FIGURE 27. Embryo sac development in Chinese Spring wheat at 20 °C showing: (*a*) prophase of mitosis in the functional megaspore (×1375); (*b*) metaphase of mitosis in the functional megaspore (×725); (*c*) a two-celled embryo sac at interphase (×880); (*d*) synchronous mitosis in the two-celled embryo sac (×1320); (*e*) a four-celled embryo sac at interphase (×965); (*f*) synchronous mitosis in the four-celled embryo sac (×945). (N.B. only the four pairs of dividing nuclei are included.)

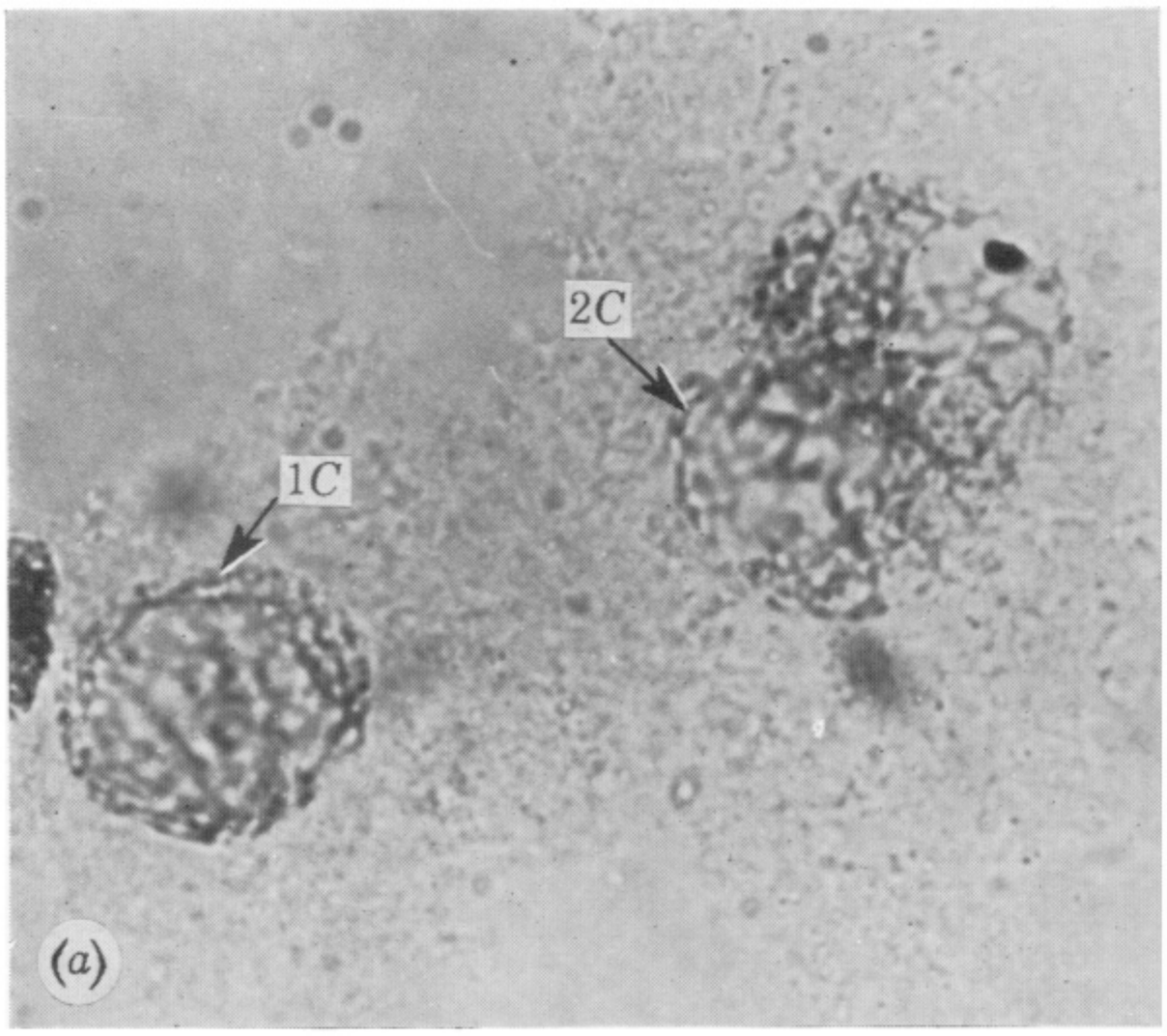

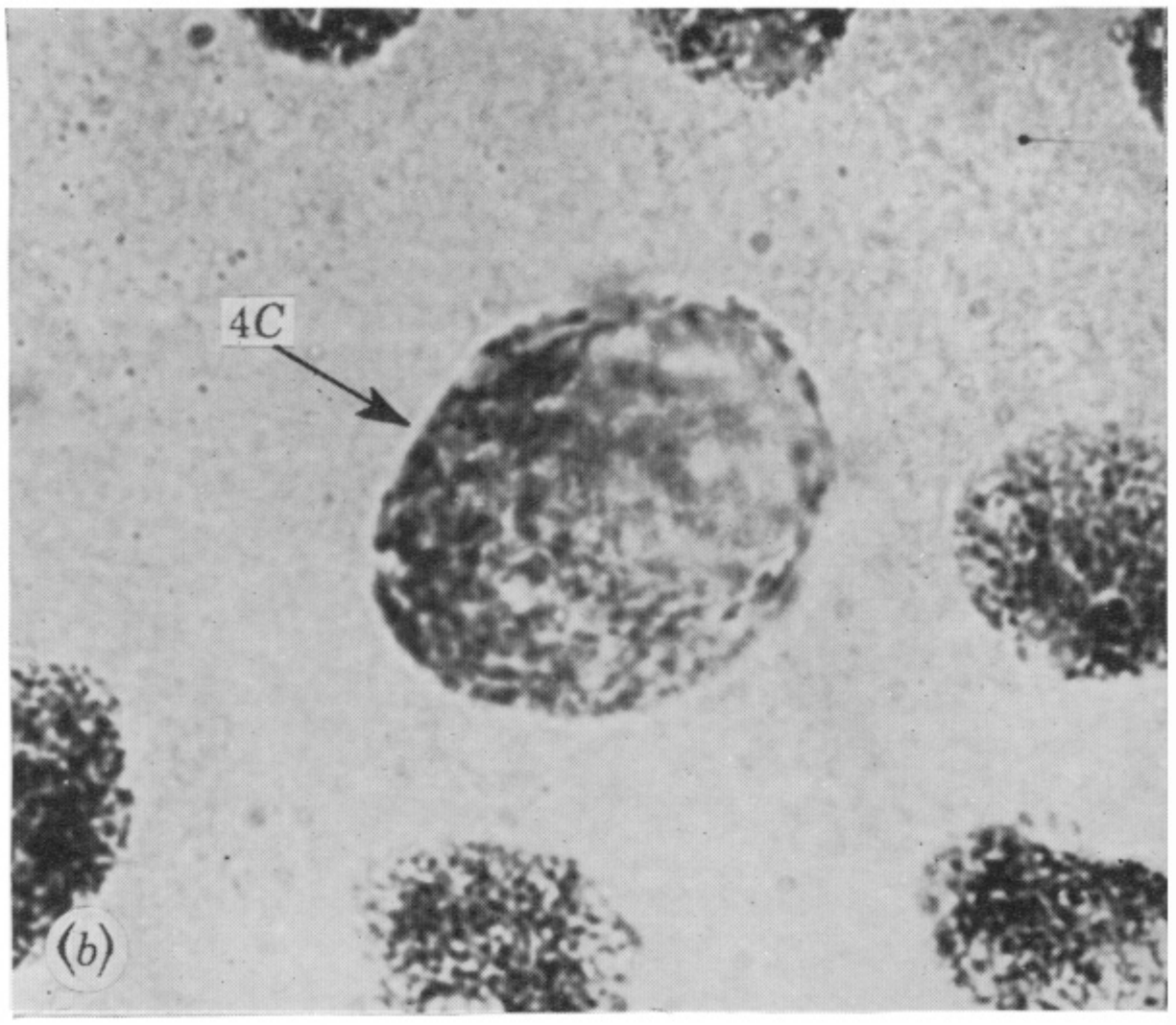

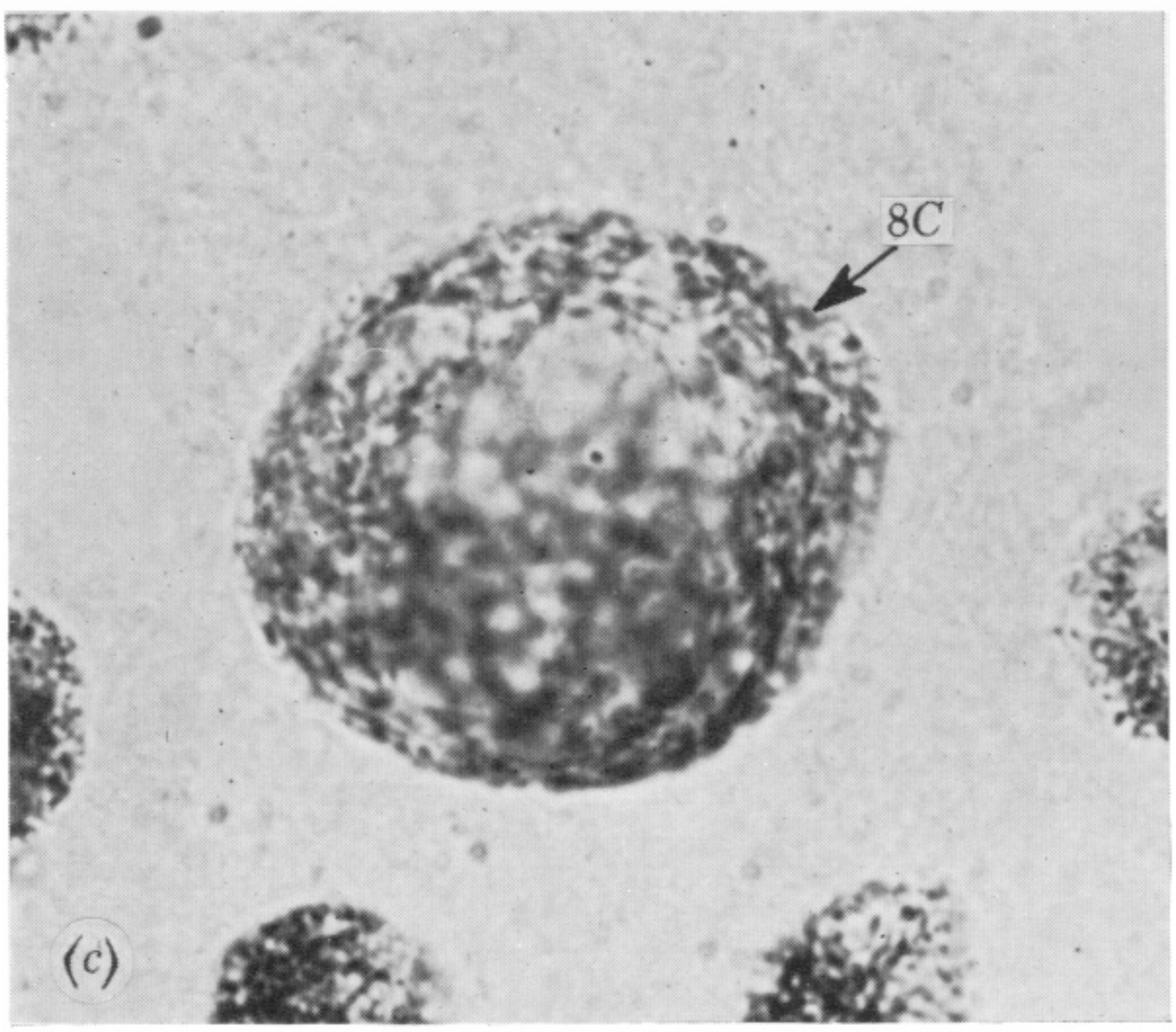

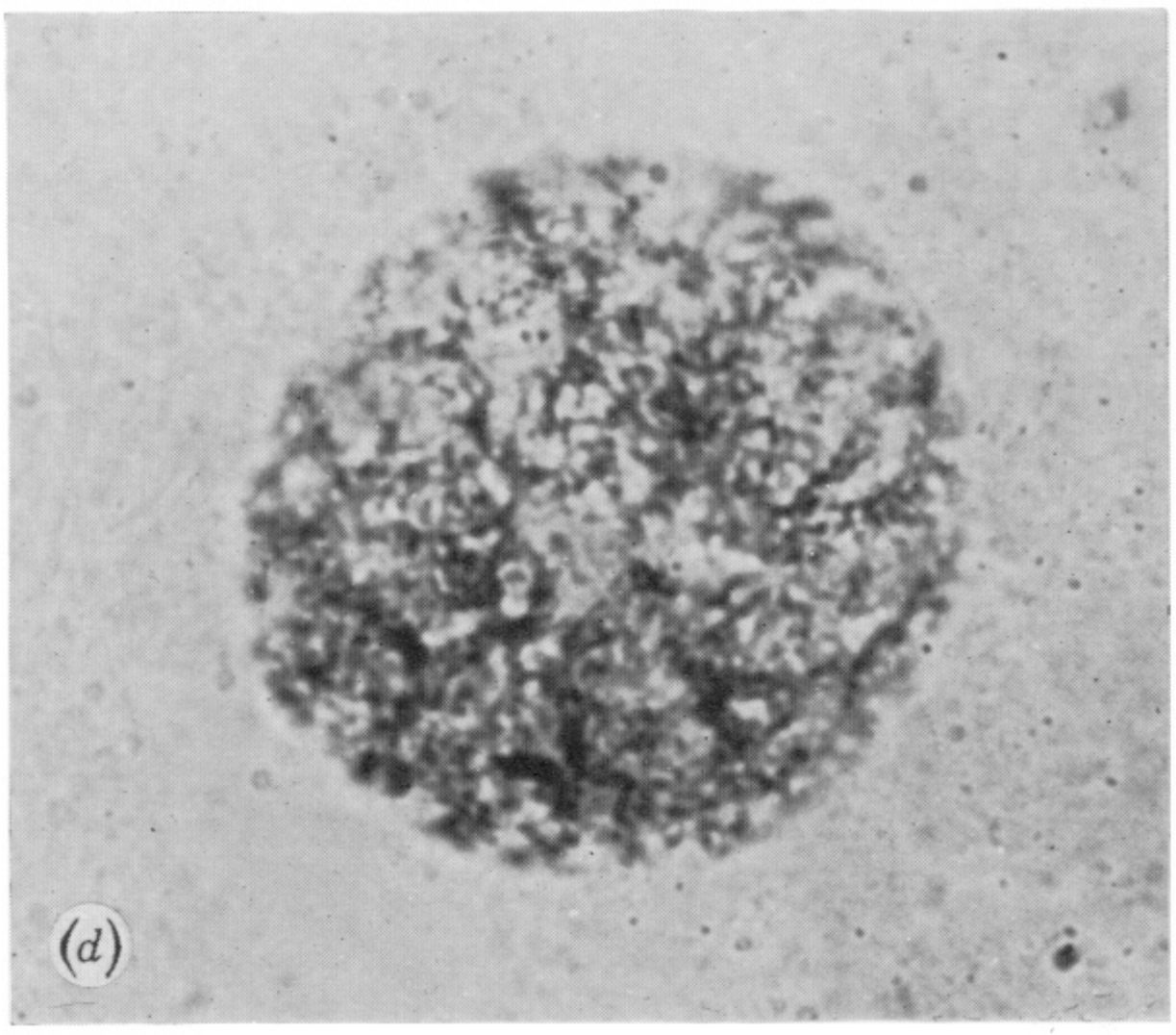

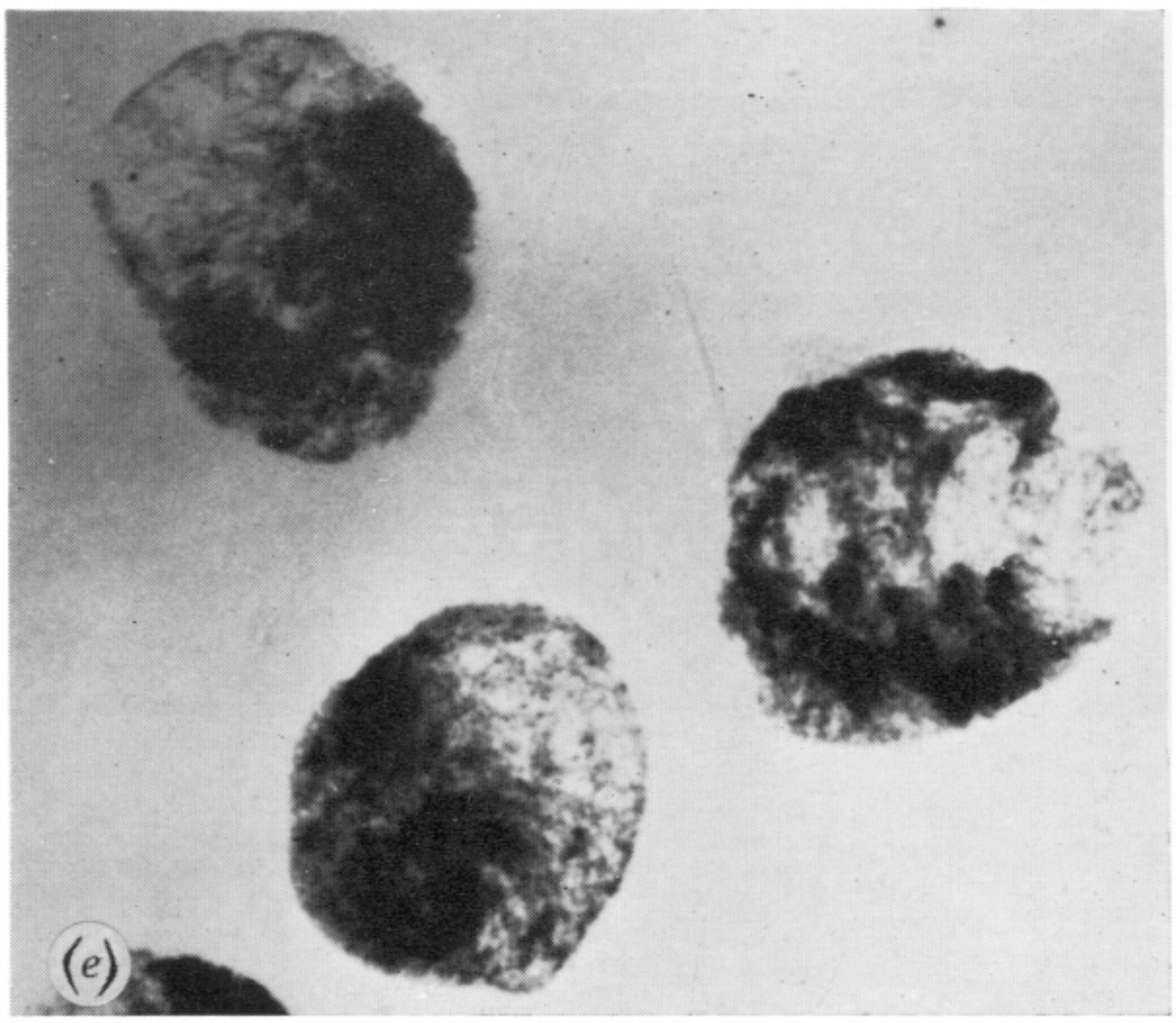

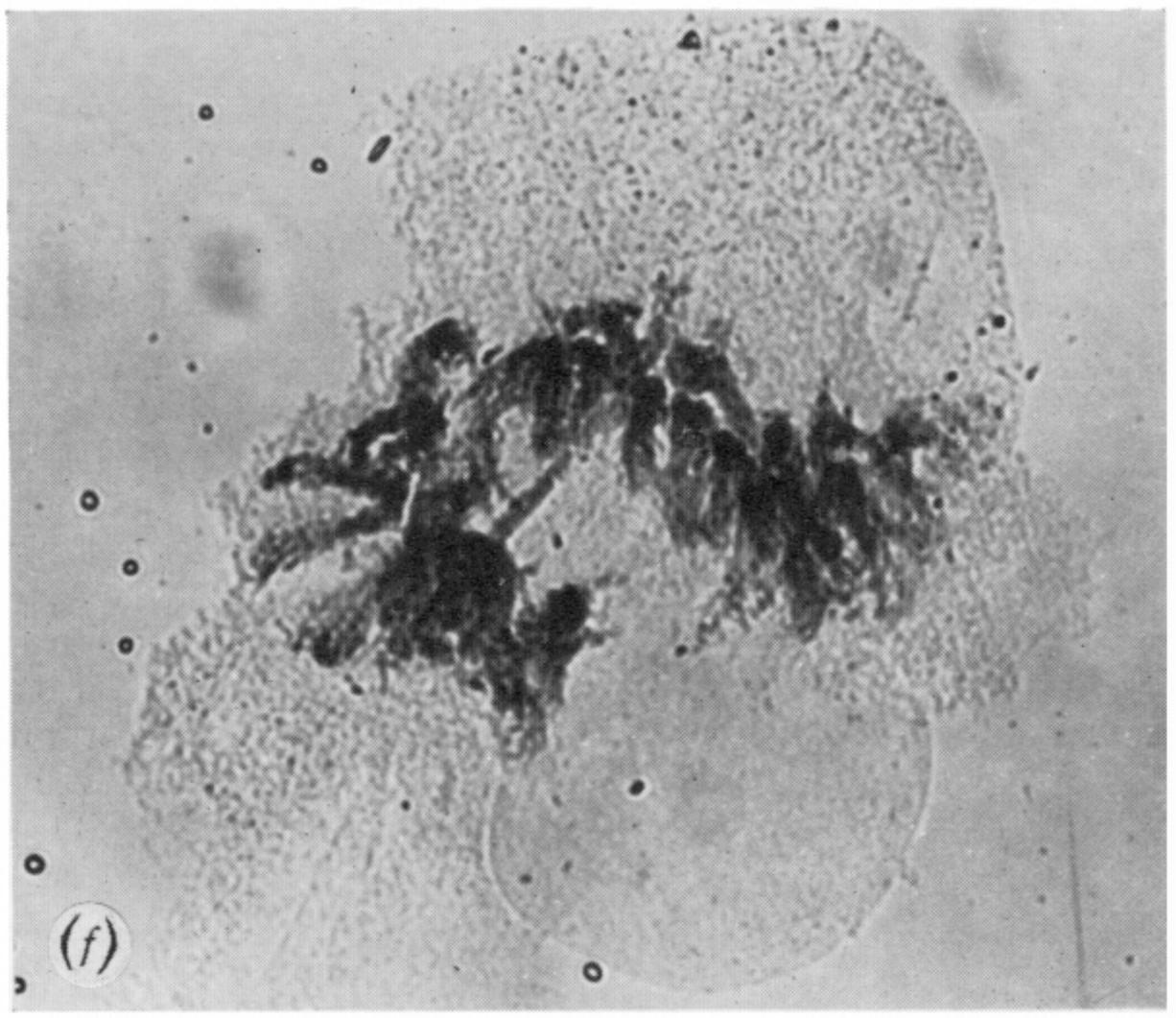

FIGURE 29. Antipodal nuclei in Chinese Spring wheat grown at 20 °C showing: (*a*) 1*C* and 2*C* nuclei; (*b*) a 4*C* nucleus; (*c*) an 8*C* nucleus; (*d*) a 16*C* nucleus; (*a–d* magn. × 1320); (*e*) 50–100*C* nuclei (× 285); (*f*) nucleus with more than 100*C* DNA content showing individual polyneme chromosomes and a very large nucleolus (× 275).

(a)

(b)

a single chromosome

(c)

endosperm nucleus

(d)

FIGURE 30. Antipodal nuclei in Chinese Spring wheat grown at 20 °C showing: (*a*) a single nucleus with about 100*C* DNA amount showing the arrangement of chromosomes with their centromeres all at one side of the nucleus (× 1045); (*b*) detail of polynemic chromosomes (× 2420); (*c*) a nucleus 3 days after pollination showing individual highly polynemic chromosomes (× 495); (*d*) degenerating antipodal nucleus with a triploid endosperm nucleus for comparison (× 750).

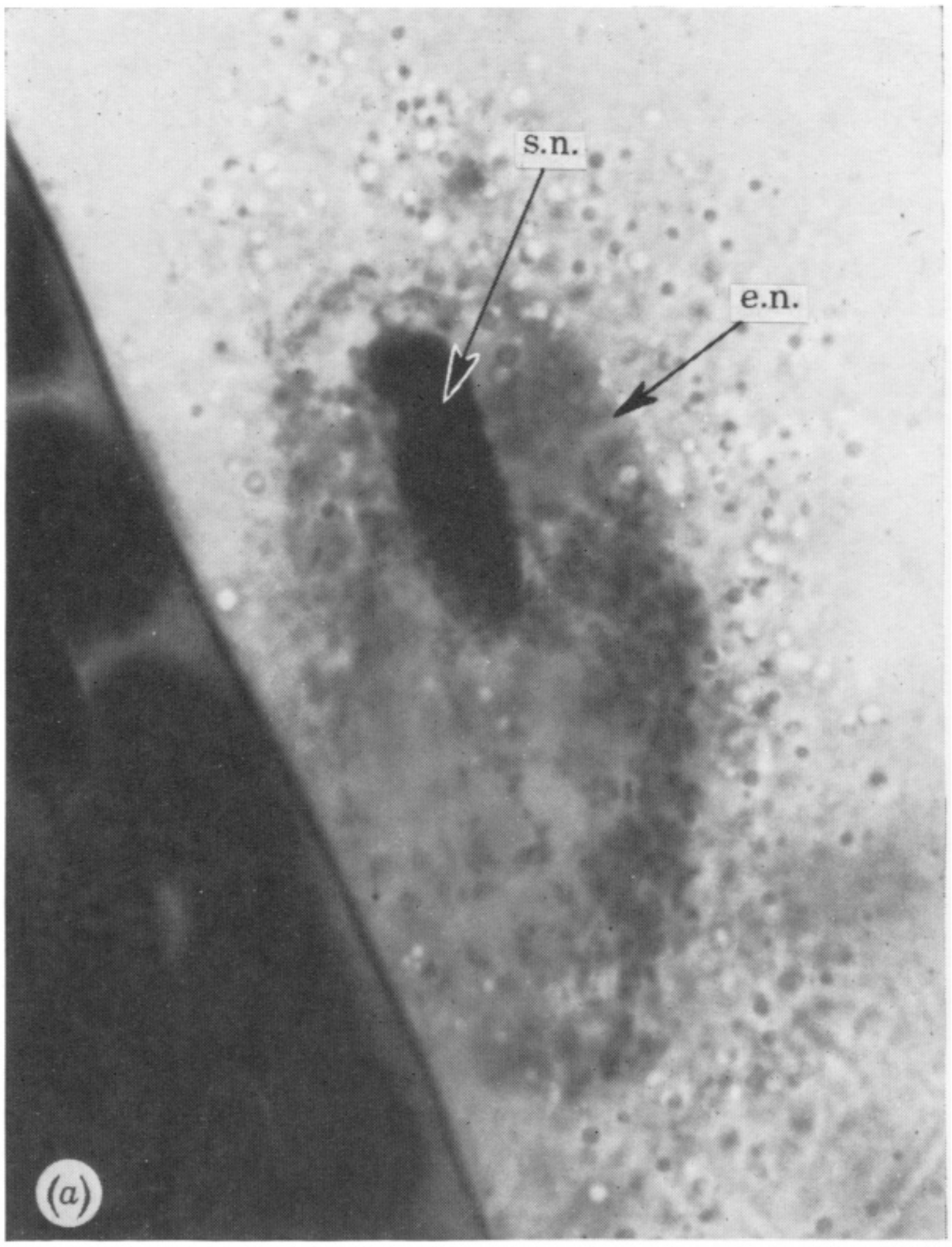

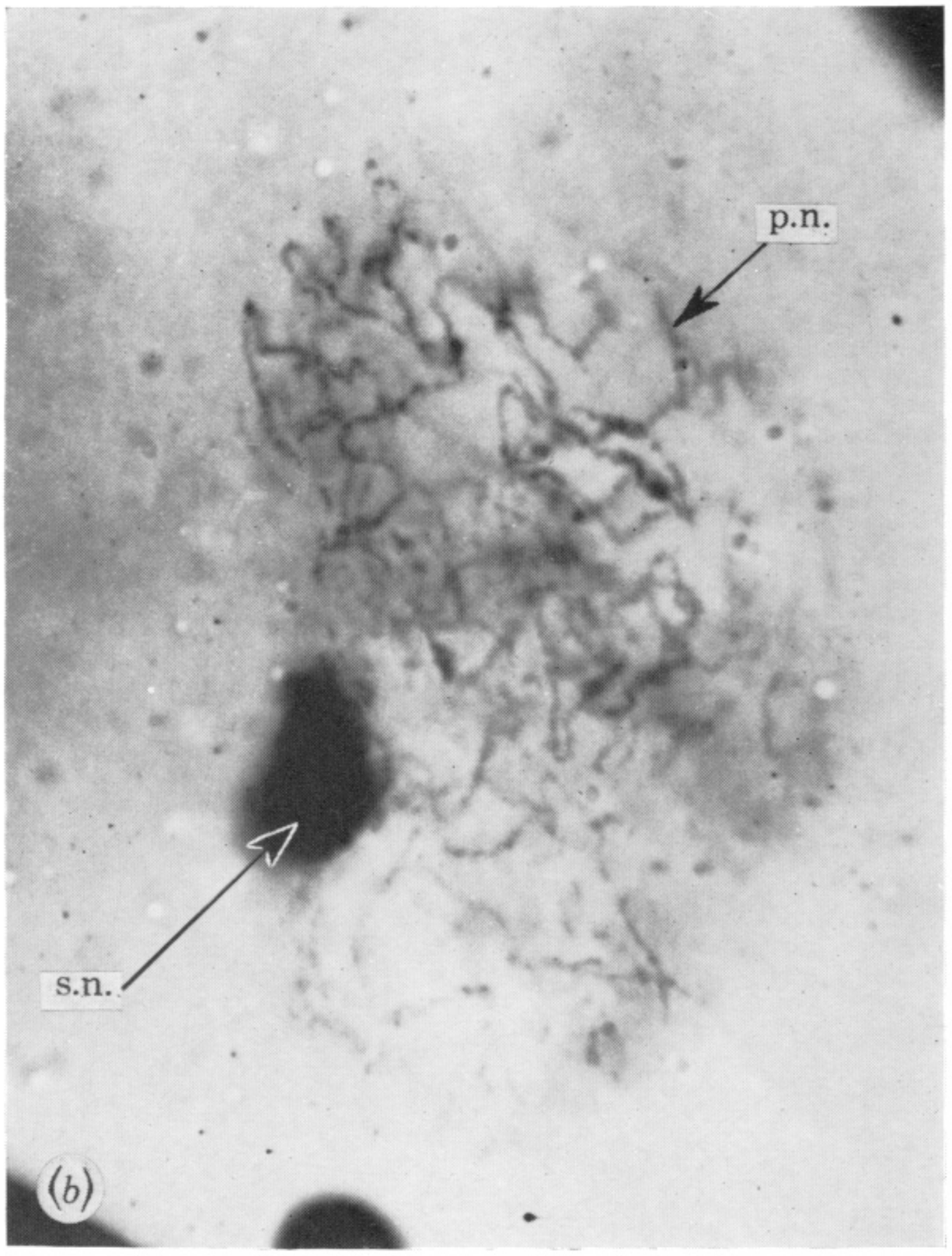

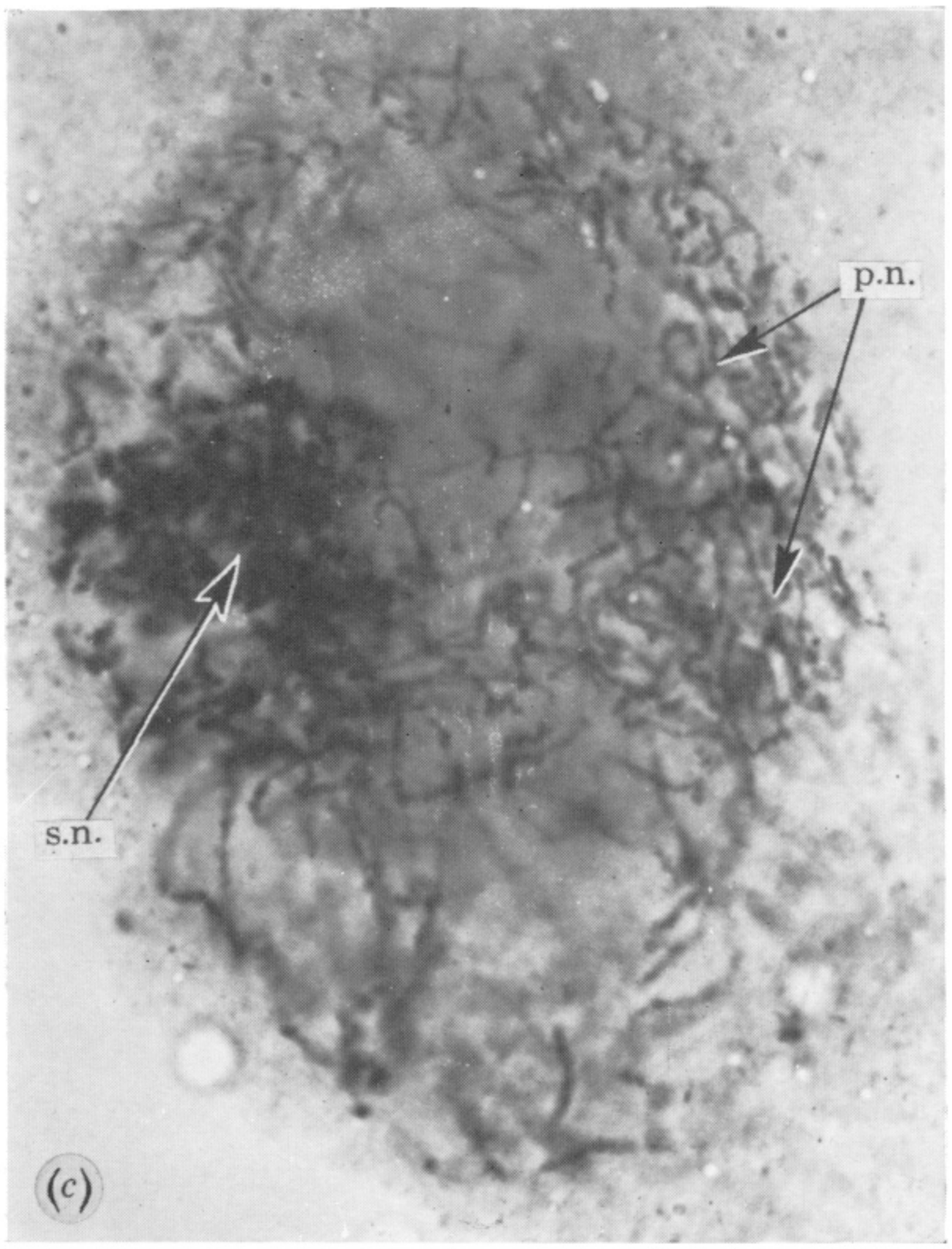

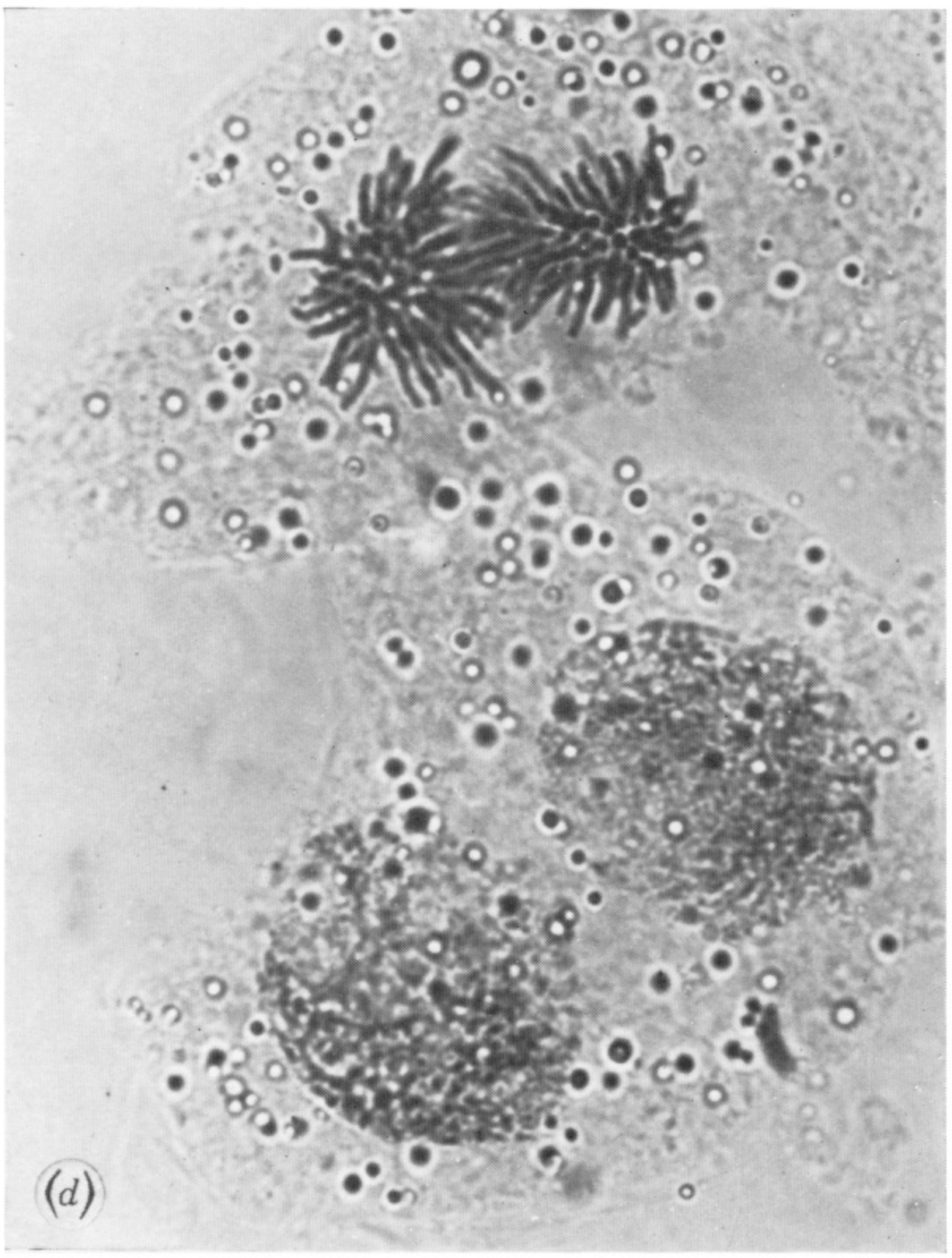

FIGURE 33. (*a*) An egg nucleus (e.n.) and a sperm nucleus (s.n.) about 3 h after pollination at 20 °C in Chinese Spring wheat (× 1320); (*b*) a polar nuclei (p.n.) and a sperm nucleus about 1 h after pollination at 20 °C in Chinese Spring wheat (× 1100); (*c*) a polar nuclei and a differentiating sperm nucleus about 3 h after pollination at 20 °C in Chinese Spring (× 1485); (*d*) typical young embryo cells from a five-celled embryo showing characteristic refractile globules in the cytoplasm (× 1210).

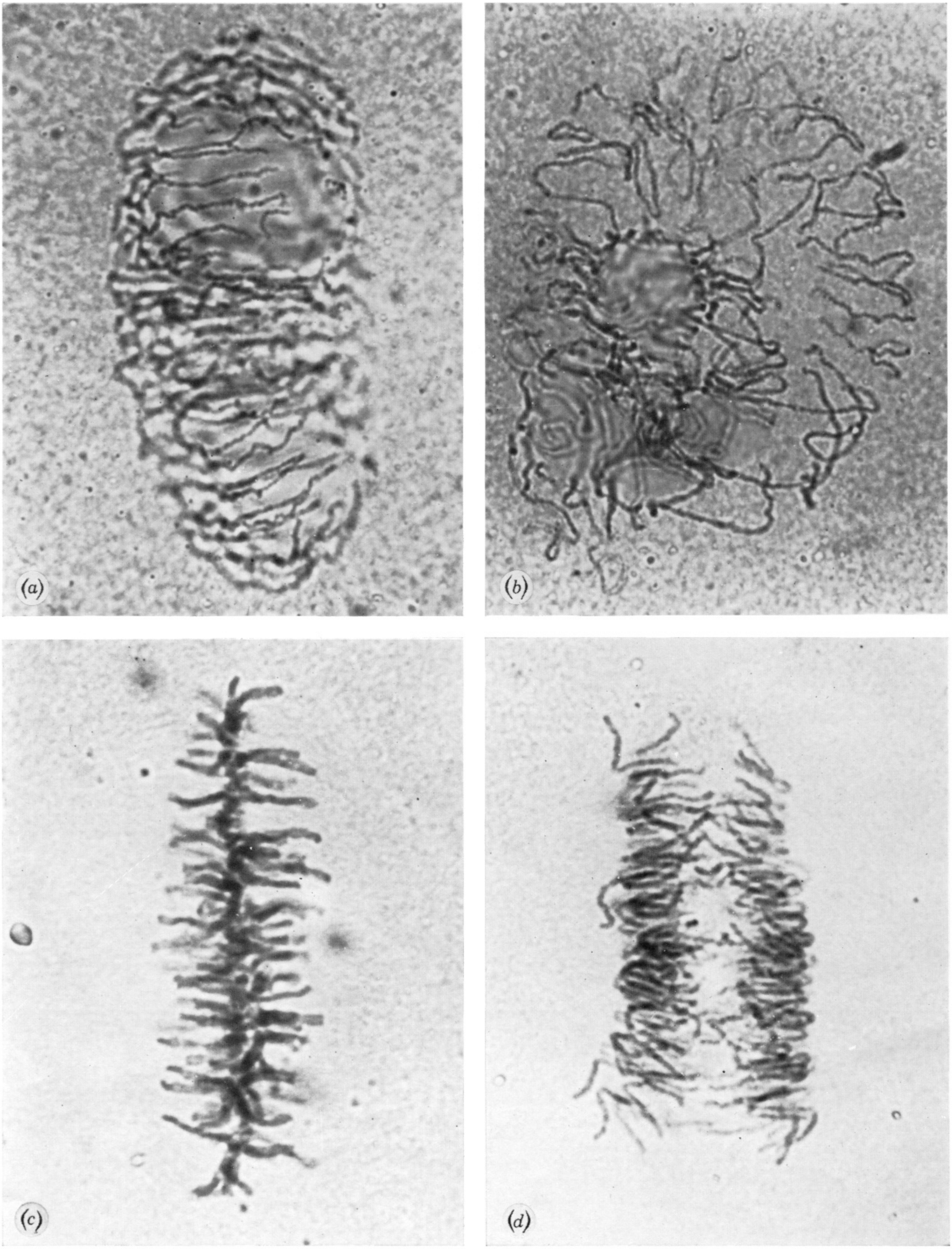

FIGURE 34. The endosperm in Chinese Spring grown at 20 °C showing: (*a*, *b*) two views of nuclei at prophase prior to the formation of a cellular endosperm (note the characteristic organization of the chromosomes and the prominent nucleoli (× 1375)); (*c*) a nucleus at metaphase (× 1705); (*d*) a nucleus at anaphase (× 1705).

FIGURE 35. The endosperm in Chinese Spring grown at 20 °C showing: (*a*, *b*) nuclei at telophase; (*c*) interphase nuclei with several nucleoli (× 330); (*d*) synchronous mitosis in a patch of cells in an endosperm consisting of several thousand cells (× 305).